Simulation of Groundwater Flow and Chloride Transport in the "1,200-Foot" Sand With Scenarios To Mitigate Saltwater Migration in the "2,000-Foot" Sand in the Baton Rouge Area, Louisiana

Scientific Investigations Report 2015–5083
Version 1.1, September 2015

U.S. Department of the Interior
U.S. Geological Survey

Simulation of Groundwater Flow and Chloride Transport in the "1,200-Foot" Sand With Scenarios To Mitigate Saltwater Migration in the "2,000-Foot" Sand in the Baton Rouge Area, Louisiana

By Charles E. Heywood, John K. Lovelace, and Jason M. Griffith

Scientific Investigations Report 2015–5083
Version 1.1, September 2015

U.S. Department of the Interior
U.S. Geological Survey

U.S. Department of the Interior
SALLY JEWELL, Secretary

U.S. Geological Survey
Suzette M. Kimball, Acting Director

For more information on the USGS—the Federal source for science about the Earth, its natural and living resources, natural hazards, and the environment—visit http://www.usgs.gov or call 1–888–ASK–USGS.

For an overview of USGS information products, including maps, imagery, and publications, visit http://www.usgs.gov/pubprod/.

Acknowledgments

Contents

Figures

Tables

Conversion Factors

Inch/Pound to SI

Multiply	By	To obtain
Length		
foot (ft)	0.3048	meter (m)
mile (mi)	1.609	kilometer (km)
Area		
square foot (ft^2)	0.09290	square meter (m^2)
square mile (mi^2)	2.590	square kilometer (km^2)
acre	4,047	square meter (m^2)
Volume		
gallon (gal)	0.003785	cubic meter (m^3)
cubic foot (ft^3)	0.02832	cubic meter (m^3)
Flow rate		
cubic foot per day (ft^3/d)	0.02832	cubic meter per day (m^3/d)
gallon per day (gal/d)	0.003785	cubic meter per day (m^3/d)
million gallons per day (Mgal/d)	0.04381	cubic meter per second (m^3/s)
Density		
pound per cubic foot (lb/ft^3)	16.02	kilogram per cubic meter (kg/m^3)
pound per cubic foot (lb/ft^3)	0.01602	gram per cubic centimeter (g/cm^3)
Hydraulic conductivity		
foot per day (ft/d)	0.3048	meter per day (m/d)

Temperature in degrees Fahrenheit (°F) may be converted to degrees Celsius (°C) as follows: °C=(°F-32)/1.8

Vertical coordinate information is referenced to the National Geodetic Vertical Datum of 1929 (NGVD 29).

Horizontal coordinate information is referenced to the North American Datum of 1983 (NAD 83).

Altitude, as used in this report, refers to distance above the vertical datum.

Concentrations of chemical constituents in water are given in milligrams per liter (mg/L).

Abbreviations

City-Parish	City of Baton Rouge and Parish of East Baton Rouge
Commission	Capital Area Groundwater Conservation Commission
DOTD	Louisiana Department of Transportation and Development
DNR	Louisiana Department of Natural Resources
FHB	Flow and Head Boundary package
GIS	geographic information system
HFB	horizontal flow barrier
HUF	Hydrogeologic-Unit Flow package
IMT	Integrated Mass Transport package
[L]	length dimension
[M]	mass dimension
MNW2	multinode well package
RMSE	root-mean-square error
[T]	time dimension
USGS	U.S. Geological Survey
UTM	Universal Transverse Mercator

Simulation of Groundwater Flow and Chloride Transport in the "1,200-Foot" Sand With Scenarios To Mitigate Saltwater Migration in the "2,000-Foot" Sand in the Baton Rouge Area, Louisiana

By Charles E. Heywood, John K. Lovelace, and Jason M. Griffith

Abstract

Groundwater withdrawals have caused saltwater to encroach into freshwater-bearing aquifers beneath Baton Rouge, Louisiana. The 10 aquifers beneath the Baton Rouge area, which includes East and West Baton Rouge Parishes, Pointe Coupee Parish, and East and West Feliciana Parishes, provided about 184.3 million gallons per day (Mgal/d) for public supply and industrial use in 2012. Groundwater withdrawals from the "1,200-foot" sand in East Baton Rouge Parish have caused water-level drawdown as large as 177 feet (ft) north of the Baton Rouge Fault and limited saltwater encroachment from south of the fault. The recently developed groundwater model for simulating transport in the "2,000-foot" sand was rediscretized to also enable transport simulation within the "1,200-foot" sand and was updated with groundwater withdrawal data through 2012. The model was recalibrated to water-level observation data through 2012 with the parameter-estimation code PEST and calibrated to observed chloride concentrations at observation wells within the "1,200-foot" sand and "2,000-foot" sand. The model is designed to evaluate strategies to control saltwater migration, including changes in the distribution of groundwater withdrawals and installation of scavenger wells to intercept saltwater before it reaches existing production wells.

Seven hypothetical scenarios predict the effects of different groundwater withdrawal options on groundwater levels and the transport of chloride within the "1,200-foot" sand and the "2,000-foot" sand during 2015–2112. The predicted water levels and concentrations for all scenarios are depicted in maps for the years 2047 and 2112. The first scenario is a base case for comparison to the six other scenarios and simulates continuation of 2012 reported groundwater withdrawals through 2112 (100 years). The second scenario that simulates increased withdrawals from industrial wells in the "1,200-foot" sand predicts that water levels will be 12–25 ft lower by 2047 and that there will be a negligible difference in chloride concentrations within the "1,200-foot" sand. The five other scenarios simulate the effects of various withdrawal schemes on water levels and chloride concentrations within the "2,000-foot" sand. Amongst these five other scenarios, three of the scenarios simulate only various withdrawal reductions, whereas the two others also incorporate withdrawals from a scavenger well that is designed to extract salty water from the base of the "2,000-foot" sand. Two alternative pumping rates (2.5 Mgal/d and 1.25 Mgal/d) are simulated in each of the scavenger-well scenarios. For the "2,000-foot" sand scenarios, comparison of the predicted effects of the scenarios is facilitated by graphs of predicted chloride concentrations through time at selected observation wells, plots of salt mass in the aquifer through time, and a summary of the predicted plume area and average concentration. In all scenarios, water levels essentially equilibrate by 2047, after 30 years of simulated constant withdrawal rates. Although predicted water-level recovery within the "2,000-foot" sand is greatest for the scenario with the greatest reduction in groundwater withdrawal from that aquifer, the scavenger-well scenarios are most effective in mitigating the future extent and concentration of the chloride plume. The simulated scavenger-well withdrawal rate has more influence on the plume area and concentration than do differences among the scenarios in industrial and public-supply withdrawal rates.

Introduction

Fresh groundwater is valued for public and industrial supply in southeastern Louisiana and the greater Baton Rouge area (subsequently referred to as the "Baton Rouge area"), which includes East and West Baton Rouge, Pointe Coupee, and East and West Feliciana Parishes. In the Baton Rouge area, fresh groundwater in most aquifers is soft, sodium bicarbonate water with a total dissolved-solids concentration of less than about 200 milligrams per liter (mg/L) (Meyer and Turcan, 1955) and requires little treatment for potable use or industrial purposes (Stuart and others, 1994). Groundwater withdrawals in the Baton Rouge area since the 1940s have lowered water levels and altered groundwater-flow directions in most of the 10 underlying freshwater-bearing

aquifers. During 2010, about 196 million gallons per day (Mgal/d) of groundwater were withdrawn in the Baton Rouge area (Sargent, 2011), mostly in East Baton Rouge Parish. Groundwater usage in 2010 was primarily for public and industrial supply, which consumed about 94 Mgal/d and 73 Mgal/d, respectively. The drawdown of groundwater levels has caused saltwater[1] to encroach into freshwater areas near Baton Rouge. Saltwater encroachment has been detected in seven aquifers, including the "1,200-foot" sand and "2,000-foot" sand in East Baton Rouge Parish (Lovelace, 2007).

Water planners and managers need additional knowledge of the effects of groundwater withdrawals on the rate and pathways of saltwater migration and a tool to assess possible management strategies that could control further saltwater encroachment in the Baton Rouge area. In response to this need, the U.S. Geological Survey (USGS), in cooperation with the Capital Area Groundwater Conservation Commission (Commission), the Louisiana Department of Transportation and Development (DOTD) Public Works and Water Resources Division, and the City of Baton Rouge and Parish of East Baton Rouge (City-Parish), developed the groundwater-flow and saltwater-transport model of the Southern Hills regional aquifer system (Buono, 1983) that is documented in this report. The model simulates the effects of reported groundwater withdrawals on groundwater flow in the regional aquifer system and the movement of saltwater northward from the Baton Rouge Fault in the "1,200-foot" sand and "2,000-foot" sand in East Baton Rouge Parish. The model simulates historical conditions (prior to 2013) and six possible future pumping scenarios. The model provides a tool for evaluation of the effectiveness of modified pumping rates that may affect saltwater encroachment. A digital archive of the groundwater model is on file at the USGS Lower Mississippi-Gulf Water Science Center in Baton Rouge.

Purpose and Scope

This report documents the hydrogeologic framework of the Southern Hills regional aquifer system in southeastern Louisiana and in southwestern Mississippi, the hydraulic properties of the aquifer system, groundwater-withdrawal rates, and a groundwater model that simulates flow in the regional aquifer system and chloride transport in the "1,200-foot" sand and the "2,000-foot" sand in the Baton Rouge area. The simulated effects of groundwater withdrawals on water levels, flow directions, and the movement of saltwater in the "1,200-foot" sand are described. Because the simulated effects of groundwater withdrawals on water levels, flow directions,

and the movement of saltwater in the "2,000-foot" sand were described in a previous report (Heywood and others, 2014), only new scenarios for managing pumpage and saltwater movement within the "2,000-foot" sand are described. Seven hypothetical groundwater-management scenarios that represent the effects of continued groundwater withdrawals at 2012 rates and various modifications to withdrawal rates and (or) installation of a "scavenger well" that could affect saltwater encroachment in the "1,200-foot" sand or "2,000-foot" sand beneath the city of Baton Rouge are simulated and discussed.

The model documented in this report is a modified version of the model previously documented by Heywood and others (2014). Differences from the previous version include refinement of the hydrogeologic framework to represent the "1,000-foot" sand and "1,200-foot" sand as separate aquifers, refinement of the horizontal and vertical finite-difference discretization to provide more detail in the area of transport within the "1,200-foot" sand, specification of reported annual groundwater withdrawals from 2008 through 2012, and recalibration of model parameters to water levels observed through 2012.

The model domain encompasses an area of 6,529 square miles (mi[2]) in southeastern Louisiana and southwestern Mississippi; however, its primary focus is on the "1,200-foot" sand and "2,000-foot" sand in a 48-mi[2] area in the Baton Rouge area (the detailed model area) where large groundwater withdrawals have occurred and where saltwater encroachment is of concern. Simulation of regional groundwater flow through all hydrogeologic units in the Southern Hills regional aquifer system helped ensure reasonable simulated results within the primary area of concern.

Previous Investigations

Several previous reports have included background data on the geologic, hydraulic, and water-quality characteristics of freshwater-bearing aquifers in the Baton Rouge area (Meyer and Turcan, 1955; Morgan, 1961). Morgan and Winner (1964) documented known areas of saltwater in aquifers underlying East and West Baton Rouge Parishes and estimated the rates of saltwater movement toward areas of large groundwater withdrawals in the industrial district and toward public-supply pumping stations. Whiteman (1979) included a detailed discussion of saltwater encroachment in the "600-foot" sand and "1,500-foot" sand and discussions of saltwater in other aquifers. Whiteman (1979) also documented the existence of the east-west trending Baton Rouge Fault as a leaky hydrologic barrier that limits northward movement of saltwater in aquifers in the Baton Rouge area. Buono (1983) described the freshwater-bearing aquifers in the northern parishes of southeastern Louisiana (including those in the Baton Rouge area) and the updip equivalent aquifers in Mississippi as an interdependent system, which he named the "Southern Hills regional aquifer system" (table 1). Griffith (2003) presented hydrogeologic cross sections of

---

[1]For the purposes of this report, saltwater is defined as water containing greater than 250 mg/L chloride. Concentrations of chloride greater than 250 mg/L exceed the Secondary Maximum Contaminant Level (SMCL) for drinking water (U.S. Environmental Protection Agency, 2006). SMCLs are established for contaminants that can adversely affect the aesthetic quality of drinking water. At high concentrations or values, health implications, as well as aesthetic degradation, also may exist. SMCLs are not federally enforceable but are intended as guidelines for the States.

Table 1. Aquifers and aquifer systems in southern Mississippi and southeastern Louisiana and corresponding model layers (modified from Buono, 1975; Stuart and others, 1994; Lovelace and Lovelace, 1995; and Griffith, 2003).

System	Series	Southern Mississippi Aquifer[1] unit	Southeastern Louisiana Aquifer system	Southeastern Louisiana Aquifer[1] unit — Eastern Florida Parishes	Southeastern Louisiana Aquifer[1] unit — Baton Rouge area		Aquifer model layer[2]
Quaternary	Holocene	Alluvium	Near-surface aquifers	No regionally extensive hydrogeologic units	Mississippi River alluvial aquifer		Layer 1
	— ? —		— ? —		Shallow sands		
	Pleistocene	Citronelle formation	Chicot equivalent aquifer system	Upland terrace aquifer Upper Ponchatoula aquifer	Upland terrace aquifer	"400-foot" sand	
						"600-foot" sand	
Tertiary	Pliocene	Graham ferry formation	Evangeline equivalent aquifer system	Lower Ponchatoula aquifer Big Branch aquifer Kentwood aquifer Abita aquifer Covington aquifer Slidell aquifer	"800-foot" sand		
					"1,000-foot" sand		Layer 3
	— ? —	Pascagoula formation			"1,200-foot" sand		Layer 5
					"1,500-foot" sand		Layer 7
					"1,700-foot" sand		Layer 9
	Miocene		Jasper equivalent aquifer system	Tchefuncte aquifer Hammond aquifer Amite aquifer Ramsay aquifer	"2,000-foot" sand		Layers 11–20
		Hattiesburg formation			"2,400-foot" sand		Layer 22
					"2,800-foot" sand		Layer 24
	— ? —	Catahoula formation	Catahoula equivalent aquifer system	Franklinton aquifer	Catahoula aquifer		
	Oligocene						

(Southern Mississippi column spanning note: Southern Hills regional aquifer system)

[1]Aquifers in southern Mississippi and southeastern Louisiana are separated by unnamed discontinuous confining units.

[2]Aquifer model layers are separated by confining model layers except model layers 11–20. Model layer 24 is the bottom model layer.

the freshwater aquifers in southeastern Louisiana, which he described as a sequence of complexly interbedded, interconnected, lenticular (lens shaped), alluvial, freshwater-bearing, clayey, sandy, and graveliferous strata. Morgan and Winner (1964), Whiteman (1979), Tomaszewski (1996), and Lovelace (2007) documented the occurrence of saltwater and increasing chloride concentrations within various aquifers in the Baton Rouge area.

In 1975, the USGS began a cooperative program with the DOTD and the Commission to analyze groundwater flow by using groundwater models of aquifers in the Baton Rouge area, including the "400-foot" sand and "600-foot" sand (Kuniansky, 1989), the "1,200-foot" sand (Halford and Lovelace, 1994), the "1,500-foot" sand and "1,700-foot" sand (Huntzinger and others, 1985), and the "2,000-foot" sand (Torak and Whiteman, 1982) in the Baton Rouge area. Under the USGS regional aquifer-system analysis program, the hydrogeologic framework, groundwater chemistry, and regional flow patterns in the freshwater aquifers along the northern coast of the Gulf of Mexico in Louisiana and parts of Texas and Mississippi were described, and groundwater-flow models were developed to simulate regional flow patterns (Martin and Whiteman, 1990). Heywood and others (2014) developed a groundwater-flow model of the aquifers in the Baton Rouge area, and much of the background information presented herein is from that report.

Study Area Description

The study area encompasses about 6,600 mi^2 in southeastern Louisiana and southwestern Mississippi (fig. 1). The study area extends southward from about 25 miles (mi) north of the Mississippi State line to Gonzales, La., in the south and eastward from Breaux Bridge, La., in the west to Hammond, La., in the east. In southeastern Louisiana, all or parts of Ascension, Avoyelles, Concordia, East and West Baton Rouge, East and West Feliciana, Iberville, Livingston, Pointe Coupee, St. Helena, St. Landry, St. Martin, and Tangipahoa Parishes are in the study area. In Mississippi, all or parts of Adams, Amite, Franklin, Lincoln, Pike, and Wilkinson Counties are in the study area.

The terrain in the study area varies from forested rolling hills in the north to flat lowlands and swamps in the south. The Mississippi River Valley dominates the setting near the western and southern boundaries of the study area. Land-surface altitudes range from zero to more than 450 feet (ft) (Calhoun and Frois, 1997). The climate is subtropical, warm, and temperate, with an average annual temperature of 68 degrees Fahrenheit (°F) (20 degrees Celsius [°C]) and an average annual rainfall of 61 inches (National Oceanic and Atmospheric Administration, 1995).

About 1 million people live within the study area, with the largest population in the Baton Rouge metropolitan area (U.S. Census Bureau, 2010). All of the public water supplied in the Baton Rouge area in 2010 was groundwater (Sargent,

2011). Several industrial facilities, primarily located along the Mississippi River, also utilize the groundwater resources in the study area. In addition, groundwater supplies about 84 percent of agricultural water use in the study area (Sargent, 2011).

Horizontal Datum and Projection Systems

The geographic coordinates of database features, such as well-head locations, and geographic information system (GIS) data used in the model are referenced to the North American Datum of 1983 (NAD 83). To represent model-cell areas accurately, polygon and point GIS coverages of the model finite-difference cells and nodes, created with the program MODELGRID (Kernodle and Philip, 1988), were generated in a Lambert Conformal Conic projection system. The model finite-difference grid columns are oriented north-south in the Lambert Conformal Conic projection system. These GIS coverages were subsequently projected into the Universal Transverse Mercator (UTM) zone 15 coordinate system that was used for GIS coverages of wells, the hydrogeologic framework, and water levels. Consequently, the model finite-difference grid appears slightly rotated in the UTM projection displayed in the map figures in this report. Projection and coordinate system details are included in a file in the digital model archive.

Hydrogeology

Aquifers containing freshwater in the Baton Rouge area are generally part of the Southern Hills regional aquifer system and include the Mississippi River alluvial aquifer, the shallow sands of the Baton Rouge area, and the Upland terrace aquifer; the "400-foot" sand, "600-foot" sand, "800-foot" sand, "1,000-foot" sand, "1,200-foot" sand, "1,500-foot" sand, "1,700-foot" sand, "2,000-foot" sand, "2,400-foot" sand, and "2,800-foot" sand of the Baton Rouge area; and the Catahoula aquifer (Meyer and Turcan, 1955; Morgan, 1961; Buono, 1983; Griffith, 2003). The Mississippi River alluvial aquifer and the shallow sands of the Baton Rouge area are the shallowest aquifers in the Baton Rouge area. Deeper aquifers in the Baton Rouge area include aquifers that are named for their depth of occurrence in the Baton Rouge industrial district (table 1) and the Catahoula aquifer. Aquifers in the Baton Rouge area have been correlated with aquifers in southern Mississippi and in Louisiana parishes east of the study area. The aquifers also have been grouped on the basis of correlative units in southwestern and central Louisiana into the Chicot equivalent, Evangeline equivalent, Jasper equivalent, and Catahoula equivalent aquifer systems (Stuart and others, 1994). Although the Catahoula aquifer contains freshwater in some areas, it is generally too deep and contains too much saltwater to be an economically viable water resource in the Baton Rouge area (Griffith, 2003).
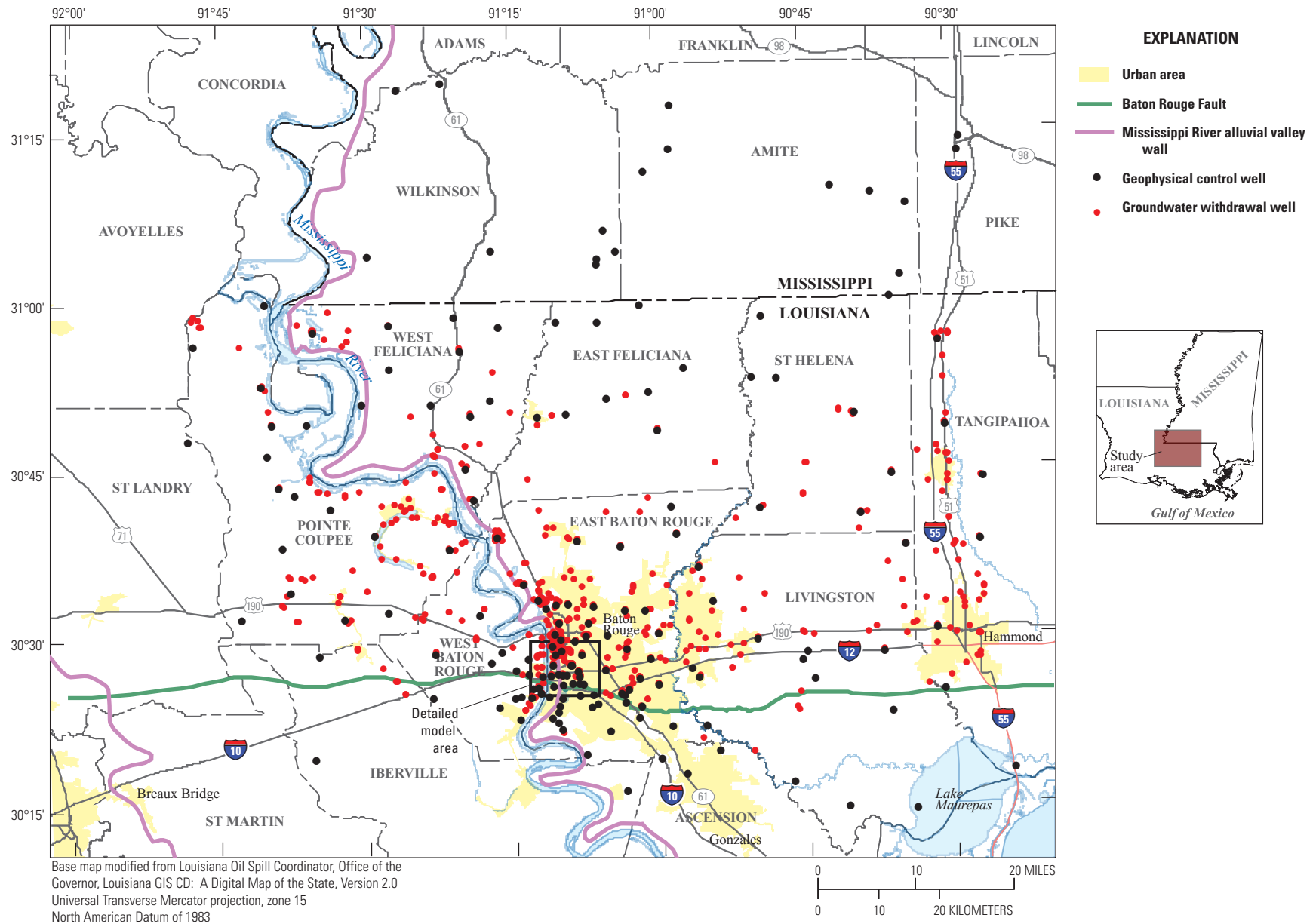
Figure 1. Location of the study area, the Baton Rouge Fault, geophysical control wells, and simulated groundwater-withdrawal wells in southeastern Louisiana and southwestern Mississippi.

Freshwater-bearing aquifers in the Baton Rouge area range in composition from very fine to coarse sand with some pea- to cobble-sized gravel (Griffith, 2003) and are sufficiently permeable to yield economically substantial quantities of water to wells (Bates and Jackson, 1984). The aquifers are separated by confining units composed of materials ranging from solid clay to sandy and silty clay that limit vertical groundwater flow. The freshwater aquifers and intervening confining units in the Baton Rouge area, together with the updip equivalent units in southwestern Mississippi, form a thickening wedge that dips to the south and southwest toward the Gulf of Mexico. The confining units generally pinch out northward, and deeper aquifers coalesce with overlying surficial aquifers.

Precipitation in the northern part of the study area and farther north in Mississippi is the primary source of recharge to the aquifer system. Because the aquifers are interconnected, precipitation that infiltrates the shallow, surficial aquifers located in recharge areas flows southward into deeper aquifers. Kuniansky (1989) estimated a range from 0.2 to 4.6 inches per year (in/yr) for deep regional aquifer recharge in the Baton Rouge area. Groundwater velocities range from a few tens of feet per year to several hundreds of feet per year (Buono, 1983).

The "1,200-foot" sand, like other freshwater aquifers in the study area, generally dips and thickens to the south and consists of single or multiple 65- to 95-ft-thick intervals of fine to medium sand and 100 to 300 ft of medium sand. Where the aquifer contains multiple sand intervals, the sand intervals are separated by clays. The top of the "1,200-foot" sand is about 1,200 ft below land surface north of the Baton Rouge Fault but is displaced downward about 300 ft at the fault (fig. 2). The "1,200-foot" sand is continuous throughout the study area except in parts of Avoyelles, Concordia, and Point Coupee Parishes and in most of Mississippi (fig. 3).

Baton Rouge Fault

The Baton Rouge Fault extends across the southern part of the study area (fig. 1) and is part of a series of east-west trending faults in southern Louisiana (Murray, 1961; Hanor, 1982; Griffith, 2003). The location of the Baton Rouge Fault was documented in the 1960s and 1970s after the importance of the fault as a barrier to groundwater flow in the aquifers in the Baton Rouge area became apparent (Meyer and Rollo, 1965; Whiteman, 1979). McCulloh (1991) mapped the detailed location of the surface expression of faults through East Baton Rouge Parish. Within the study area, the Baton Rouge Fault dips to the south at angles between about 65 and 70 degrees (Durham and Peeples, 1956; Smith and Kazmann,

1978; Whiteman, 1979; Roland and others, 1981; Hanor, 1982; McCulloh, 1991; Griffith, 2003, 2006).

Sediment deformation and displacement of sedimentary layers across the Baton Rouge Fault reduce the hydraulic connections between aquifers, thereby impeding horizontal groundwater flow, which causes substantial changes in both water levels and water quality across the fault. The displacement of aquifers across the fault ranges from about 20 ft near the ground surface to about 300 ft at altitudes of -1,600 to -3,000 ft.

Occurrence and Movement of Saltwater

Groundwater investigations conducted during the 1960s identified a freshwater-saltwater interface located near the Baton Rouge Fault (Morgan and Winner, 1964; Rollo, 1969). Prior to groundwater development in the 1940s, fresh groundwater flowed from recharge areas in Mississippi southward toward the fault and then upward to discharge at springs. This groundwater-flow pattern caused aquifers north of the fault to generally contain freshwater, whereas they may contain saltwater south of the fault. Exceptions exist because freshwater is also found in some areas south of the Baton Rouge Fault, such as West Baton Rouge Parish, where the "2,000-foot" sand contains freshwater areas. In the Baton Rouge area, the base of freshwater is between about 1,100 and 2,600 ft deeper on the north side of the fault than it is on the south side of the fault. The altitude of the base of freshwater ranges between about -1,500 and -3,500 ft north of the fault and between -200 and -1,000 ft south of the fault (Smoot, 1988; Griffith, 2003). Aquifer tests conducted across the fault in the vicinity of Baton Rouge have indicated that the fault impedes groundwater flow (Whiteman, 1979).

Large groundwater withdrawals north of the fault in Baton Rouge, primarily for public supply and industrial use, have lowered water levels and created gradients conducive to the movement of saltwater from the south side of the fault into previously freshwater areas north of the fault (Whiteman, 1979; Tomaszewski, 1996). Groundwater withdrawals from the "2,000-foot" sand have resulted in measured water-level drawdowns as great as 356 ft. Except in the deeper "2,800-foot" sand and Catahoula aquifers, most saltwater currently north of the fault moved there in response to the groundwater withdrawals in the Baton Rouge area. Within the "2,000-foot" sand, saltwater threatens industrial wells located about 3 mi north of the fault. If groundwater withdrawals in the Baton Rouge area continue at rates similar to the historical rates, saltwater encroachment will probably continue to occur (Tomaszewski, 1996).
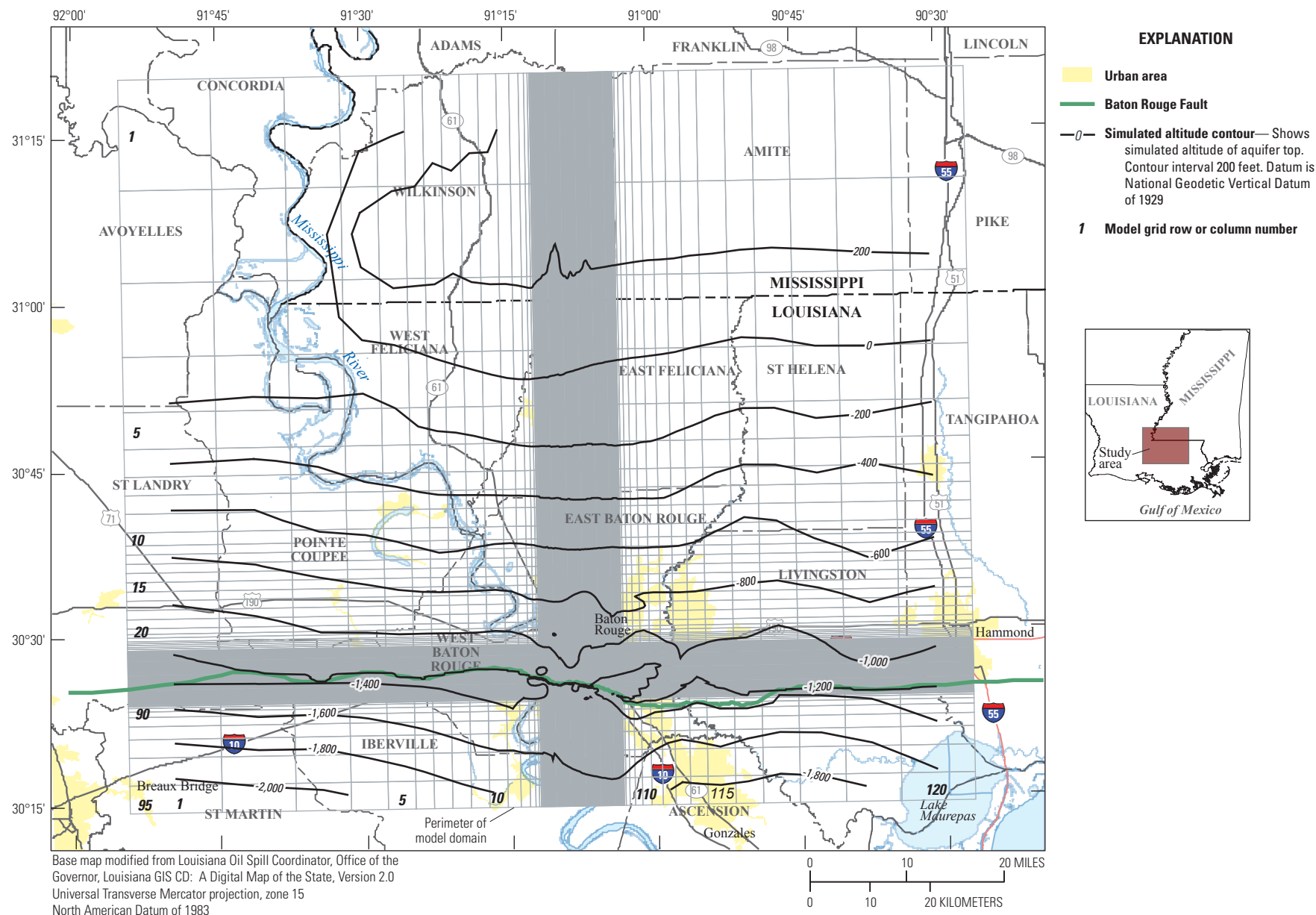
Figure 2. Location of the finite-difference grid and simulated altitude of the top of the "1,200-foot" sand of the Baton Rouge area in southeastern Louisiana and southwestern Mississippi.
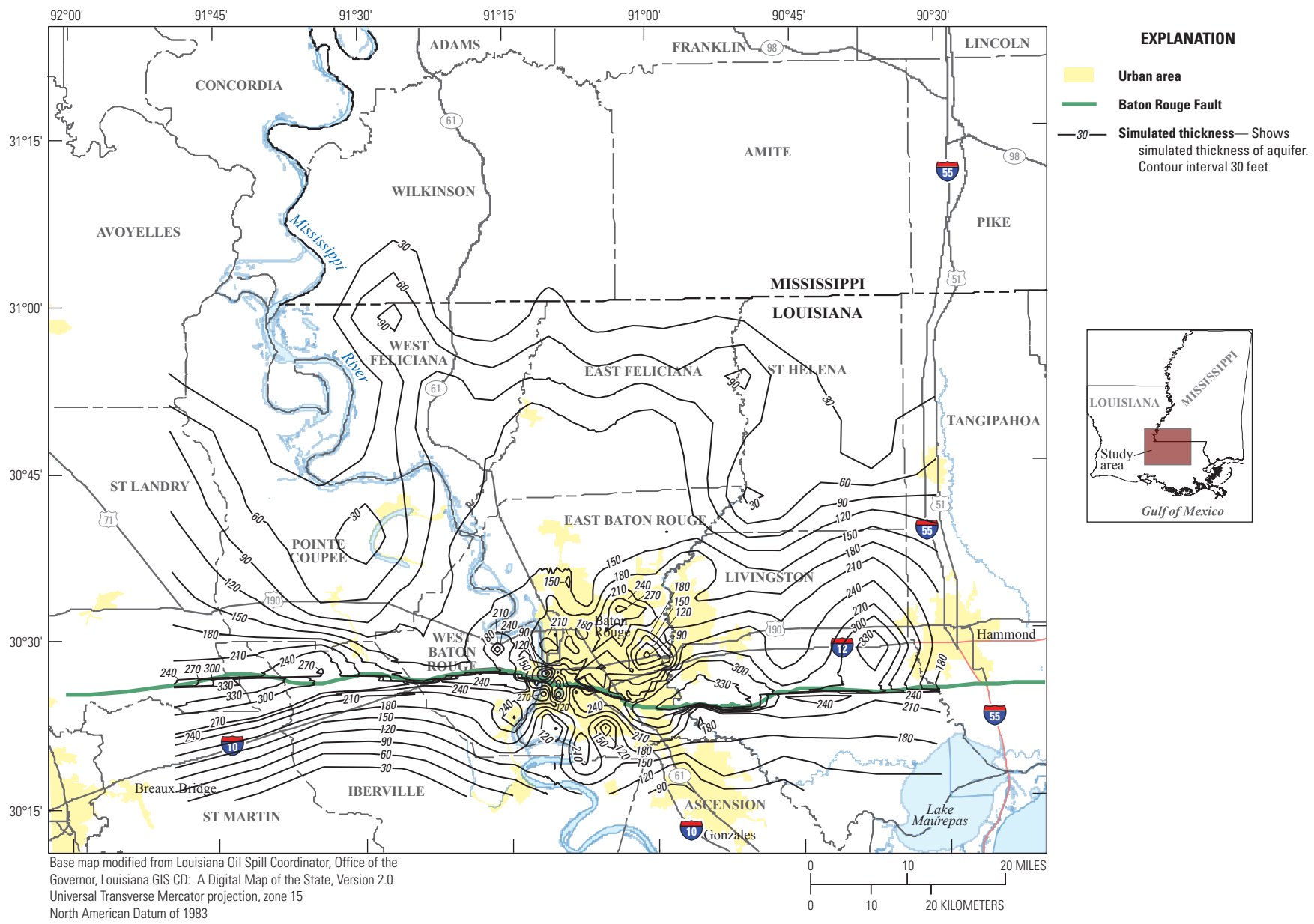
Figure 3. Simulated thickness of the "1,200-foot" sand of the Baton Rouge area in southeastern Louisiana and southwestern Mississippi.

On the basis of geophysical log data and analyses of water samples collected through 2005, saltwater or water containing chloride concentrations above background levels (10 mg/L or less) has been detected north of the Baton Rouge Fault in all 10 sands in the Baton Rouge area (Rollo, 1969; Whiteman, 1979; Tomaszewski, 1996; Lovelace, 2007). Analyses of chloride-concentration measurements collected from wells prior to 1992 indicated that saltwater encroachment had occurred in the "600-foot" sand, "1,000-foot" sand, "1,500-foot" sand, and "2,000-foot" sand (Morgan and Winner, 1964; Whiteman, 1979; Tomaszewski, 1996). Chloride-concentration data collected from 1993 to 2003 indicated that chloride concentrations increased over this period in the "1,000-foot" sand, "1,200-foot" sand, "1,500-foot" sand, "2,000-foot" sand, "2,400-foot" sand, and "2,800-foot" sand (Lovelace, 2007). Chloride concentrations measured during 2004–05 exceeded background levels in one or more water samples from wells in East and West Baton Rouge Parishes north of the fault screened in the "600-foot" sand, "1,000-foot" sand, "1,200-foot" sand, "1,500-foot" sand, "1,700-foot" sand, "2,000-foot" sand, "2,400-foot" sand, and "2,800-foot" sand. Comparison of the 2004–05 data with historical data indicated that chloride concentrations north of the Baton Rouge Fault were increasing in all of those aquifers except the "1,700-foot" sand (Lovelace, 2007). Within the "1,200-foot" sand, chloride concentrations of about 157 mg/L have been measured 6.5 mi east of the Mississippi River and about 300 ft north of the Baton Rouge Fault.

Hydrogeologic Framework

A three-dimensional hydrogeologic framework was constructed to delineate the extents and thicknesses of aquifers and confining units in the study area. The hydrogeologic framework represents the entire sequence of aquifers and confining units in the Southern Hills regional aquifer system above the Catahoula equivalent aquifer system (table 1). The Catahoula equivalent aquifer system was omitted from the framework because in the study area it contains mostly saltwater and is little used and because few geophysical logs were available to delineate the extent and thickness of the aquifers in the system. The hydrogeologic framework defines the top altitudes and thicknesses of the hydrogeologic units simulated in the groundwater model documented in this report. Although the groundwater model documented herein was primarily developed to address concerns about declining groundwater levels and saltwater encroachment in the "1,200-foot" and "2,000-foot" sands, simulating groundwater flow in overlying and underlying aquifers improved the simulation of water levels in the aquifers of concern.

The top of the hydrogeologic framework is the ground surface, and the base is the bottom of the "2,800-foot" sand. The aquifers and confining units are represented by 24 layers, numbered from the top to the bottom (table 1). Layers 1, 3, 5, 7, 9, 11–20, 22, and 24 make up the aquifer layers. Layers

2, 4, 6, 8, 10, 21, and 23 make up confining-unit layers that separate the aquifer layers. Layer 1 represents multiple aquifers that have similar hydraulic characteristics and are likely interconnected, including the Mississippi River alluvial aquifer, shallow sands, Upland terrace aquifer, and the "400-foot" sand, "600-foot" sand, and "800-foot" sand. Layer 5 represents the "1,200-foot" sand.

The location and thickness of aquifer and confining-unit layers in the hydrogeologic framework were specified from lithologic contacts interpreted from 202 borehole resistivity, spontaneous potential, nuclear, and drillers' lithologic logs and the previous work of Griffith (2003). Generally, aquifers and confining units less than 10 ft thick were not represented by discrete layers in the hydrogeologic framework. The location and correlation of hydrogeologic units near the Baton Rouge Fault in the study area are uncertain (Griffith, 2003), and the apparent displacement of units may be due to differences in sediment deposition on either side of the fault (Smith, 1979). By using previous reports (Durham and Peeples, 1956; Murray, 1961; Winner and others, 1968; Rollo, 1969; Smith, 1979; Whiteman, 1979; Hanor, 1982; Smoot, 1988; McCulloh, 1991; Griffith, 2003, 2006) and the lithologic contacts, separate representations of the top altitudes and thicknesses of the hydrogeologic-unit layers were generated for areas north and south of the Baton Rouge Fault. The separate north and south representations for each layer were merged at the fault to form a single representation for each layer so that differences in top altitudes of layers across the Baton Rouge Fault represent the vertical fault displacement.

The top altitudes and thicknesses of all hydrogeologic framework layers were initially constructed with VIEWLOG (Viewlog Systems, 2004) for the entire model domain. Subsequent analysis indicated that the defined top and bottom altitudes of the "1,200-foot" sand were inadequate in a portion of the model domain in the eastern Baton Rouge area. The lithologic contacts were reinterpreted from borehole resistivity logs in this area, and linear interpolation between borehole locations was used to define the top and bottom altitudes of the "1,200-foot" sand. Contour maps depict the top altitude and thickness of the "1,200-foot" sand (figs. 2 and 3) in the groundwater model.

Groundwater Withdrawals

Withdrawal records for 636 wells in Louisiana from the period 1940 through 2012 were compiled from the digital databases and paper records of the USGS and the Commission. Most of these withdrawal records were reported by personnel at public-supply and industrial facilities. Withdrawal rates for wells or facilities inventoried on a 5-year basis from 1960 to 2005 were obtained from USGS water-use records (B. Pierre Sargent, U.S. Geological Survey, written commun., 2013). Sporadic annual withdrawal data from 1940 to 1975 for some facilities in the Baton Rouge area

also were obtained from USGS water-use records (B. Pierre Sargent, U.S. Geological Survey, written commun., 2013). Annual withdrawal rates from wells in East and West Baton Rouge, East and West Feliciana, and Pointe Coupee Parishes from 1975 through 2012 were obtained from the Commission water-use database (Shawn Scallan, Capital Area Groundwater Conservation Commission, written commun., 2013). Annual withdrawal rates from about 1988 through 2012 for facilities that withdrew an average of 1 Mgal/d or greater and were located in other parishes in the study area were obtained from USGS water-use records. Specified groundwater withdrawals from simulated aquifers in the study area (not including the Mississippi River alluvial aquifer, shallow sands, Upland terrace aquifer, "400-foot" sand, "600-foot" sand, and "800-foot" sand represented in layer 1) totaled 171.3 Mgal/d during 2012.

Where only facility-specific withdrawals were available, well-specific rates were typically estimated by evenly distributing the withdrawals reported for each facility among the active wells at that facility. Well registration, construction, and plugging or abandonment data from USGS, DOTD, Commission, and Louisiana Department of Natural Resources (DNR) databases were used to determine when specific wells were in use at the facilities where facility-specific withdrawals were reported. For some wells with intermittent data, annual withdrawals were estimated or interpolated to complete their pumpage records. In some cases, facilities were contacted to verify pumping rates and well activity during different periods.

Well-construction data including the borehole, screen, and casing diameters; screen intervals; pump depth; location; and land-surface altitude were obtained from USGS and State databases. Missing or inadequate information was estimated or adjusted by using ancillary information from topographic maps, well logs, the specifications of nearby wells or wells with identical ownership, well schedules, and thickness data from the hydrogeologic framework. Some wells with inadequate well-construction information and probable withdrawal rates less than 0.01 Mgal/d were omitted. Wells with screen-interval records corresponding to confining-unit intervals in the hydrogeologic framework were assumed to be screened in aquifers and were assigned to the appropriate adjacent aquifer layer.

A graph of the withdrawals from the "400-foot," "600-foot," "800-foot," "1,000-foot," "1,200-foot," "1,500-foot," "1,700-foot," "2,000-foot," "2,400-foot," and "2,800-foot" sands, collectively referred to hereinafter as the "Baton Rouge sands," illustrates both increased total withdrawals and the withdrawal from deeper aquifers through time (fig. 4). Until the early 1950s, groundwater withdrawals were principally from the "400-foot" sand and the "600-foot" sand. Since that time, deeper aquifers such as the "1,200-foot" sand, "1,500-foot" sand, "2,000-foot" sand, "2,400-foot" sand, and "2,800-foot" sand have increasingly supplied most of the groundwater used in the Baton Rouge area. In 2012, an estimated 184.3 Mgal/d were withdrawn from the Baton Rouge sands for public supply

and industrial use, including 24.1 Mgal/d from the "400-foot," "600-foot," and "800-foot" sands that were not specified in the model. Specified withdrawals from aquifers within the study area but outside of the Baton Rouge area that correlate with the Baton Rouge sands totaled 11.1 Mgal/d.

Figures 5 and 6 depict the average daily withdrawal rate during 2012 at wells screened in the "1,200-foot" sand (fig. 5) and the "2,000-foot" sand (fig. 6) and located at or near the Baton Rouge industrial district. Withdrawals from the "1,200-foot" sand in the Baton Rouge area in 2012 (fig. 5) totaled 23.33 Mgal/d, which were split nearly evenly between public supply (11.79 Mgal/d) and industry (11.54 Mgal/d). Withdrawals from the "2,000-foot" sand in the Baton Rouge area in 2012 (fig. 6) totaled 28.5 Mgal/d, and industrial withdrawals, primarily in the Baton Rouge industrial district, accounted for 16.1 Mgal/d, or 57 percent of the total withdrawn.

Simulation of Groundwater Flow and Chloride Transport

The modeling strategy involved an update of the groundwater model previously documented by Heywood and others (2014). The finite-difference grid was rediscretized to separate the "1,000-foot" sand from the "1,200-foot" sand and increase horizontal resolution (with smaller finite-difference cells) in the area where chloride transport within the "1,200-foot" sand is of concern. Specified groundwater withdrawals were updated through 2012, and the model parameters were recalibrated to water levels measured throughout the aquifer system through 2012. Subsequently, saltwater transport was simulated with the variable density groundwater-flow model SEAWAT (Langevin and others, 2003). Calibration of simulated chloride concentrations to chloride concentrations measured in the Baton Rouge area required minor modification of parameters representing the hydraulic characteristics along segments of the Baton Rouge Fault. Estimates of effective porosity and aquifer dispersivities utilized in the previous model documented by Heywood and others (2014) provided a good fit of simulated to measured chloride concentrations in both the "1,200-foot" sand and the "2,000-foot" sand. The highest observed chloride concentration north of the Baton Rouge Fault within the "1,200-foot" sand has been 157 mg/L, implying that groundwater at that location has a density not substantially greater than freshwater. Because the multinode well package, MNW2 (Konikow and others, 2009), of the constant-density groundwater-flow code MODFLOW-2005 (Harbaugh, 2005) can apportion specified pumpage withdrawals among multiple aquifers penetrated by a single well, which is important for simulating transient groundwater flow in the Baton Rouge area, MODFLOW-2005 was used during the groundwater-flow model calibration process. After the groundwater-flow
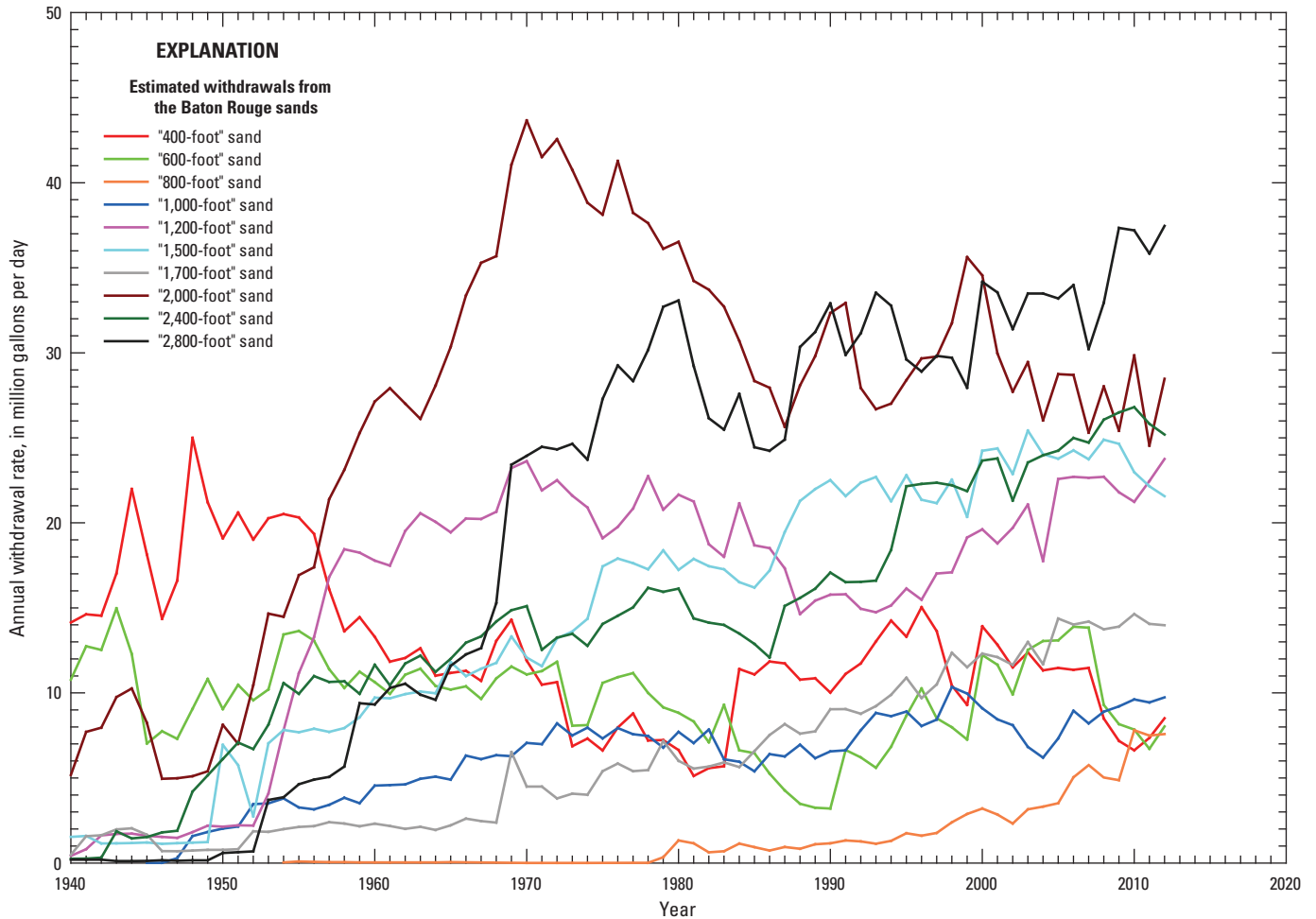
Figure 4. Estimated withdrawals from the Baton Rouge sands, 1940–2012.

model parameters had been estimated, the calibrated set of flow parameters and computed well fluxes were specified in the SEAWAT model, which enabled simulation of saltwater transport. An equivalent Well (WEL) package (Harbaugh and others, 2000) input was generated by the MODFLOW-2005 simulation to specify the layer-variable groundwater fluxes for each withdrawal well in the subsequent SEAWAT simulation.

Conceptual Model for Solute Transport

A simple conceptual model was used for defining initial and boundary conditions within the detailed model area that corresponds to the solute-transport model domain. In this model, groundwater north of the Baton Rouge Fault is assumed to have been fresh prior to groundwater development. Groundwater entering the solute-transport model domain from areas north of the Baton Rouge Fault is simulated to have zero salt concentration. Although the origin of the saltwater

encroaching into the "1,200-foot" sand is unknown, it likely flows through permeable sediments that are adjacent on the south side of the Baton Rouge Fault. Because sediments south of the Baton Rouge Fault are displaced downward, the saltwater may flow from the "1,000-foot" sand south of the Baton Rouge Fault, where its altitude is similar to that of the "1,200-foot" sand north of the fault. Although chloride concentrations south of the Baton Rouge Fault have been observed to vary spatially and some areas of freshwater are known to occur, a simple representation of the saltwater source is preferred to model transport north of the fault. This source was specified within the finite-difference cells adjacent to the south side of the fault that connect to the "1,200-foot" sand on the north side of the fault. As groundwater withdrawals cause water levels to decline in aquifers north of the Baton Rouge Fault, saltwater under higher pressure south of the fault seeps northward across the hydraulically resistive fault.
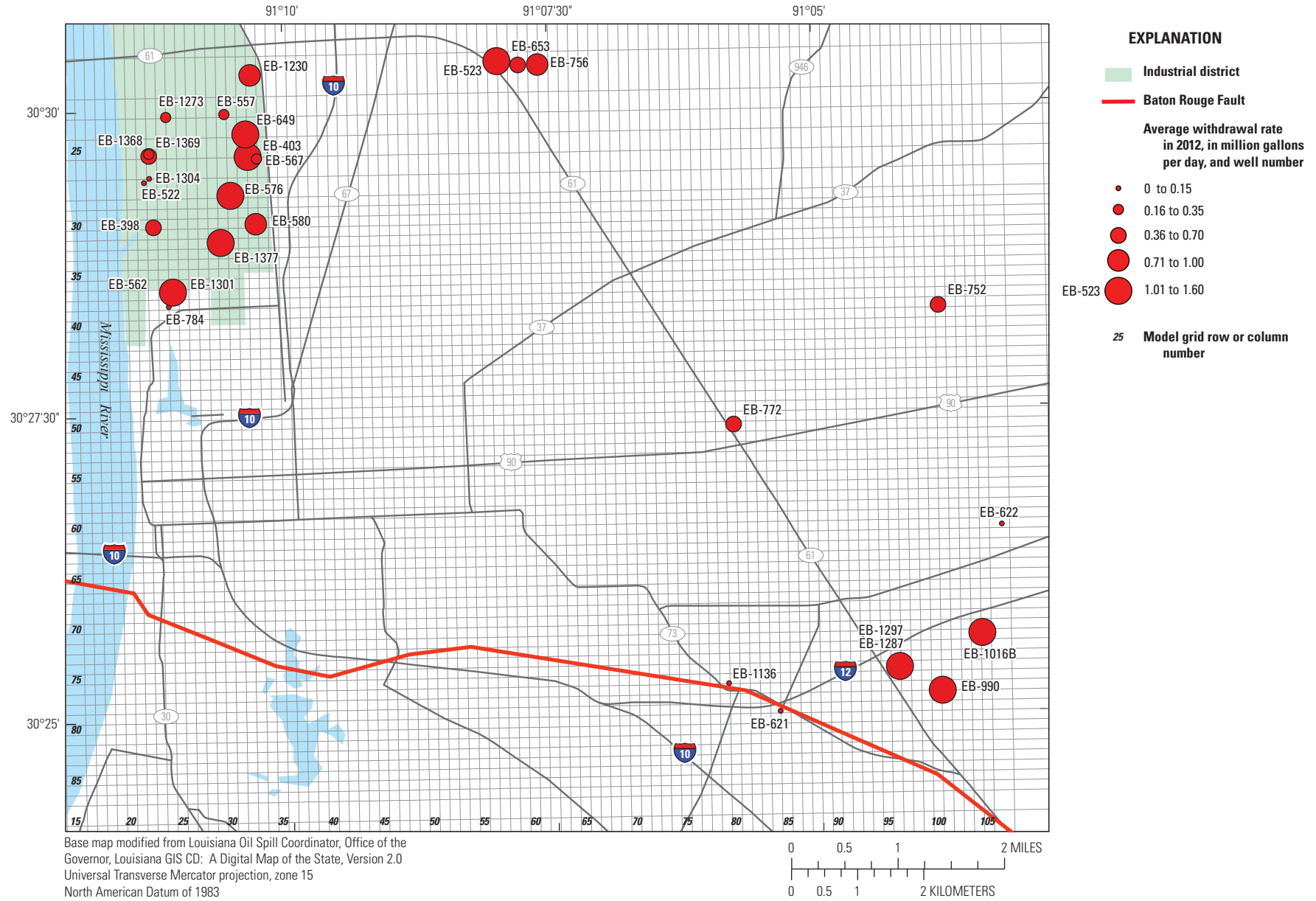
Figure 5. Average daily withdrawal rate during 2012 at wells screened in the "1,200-foot" sand of the Baton Rouge area and located at or near the Baton Rouge industrial district in southeastern Louisiana.
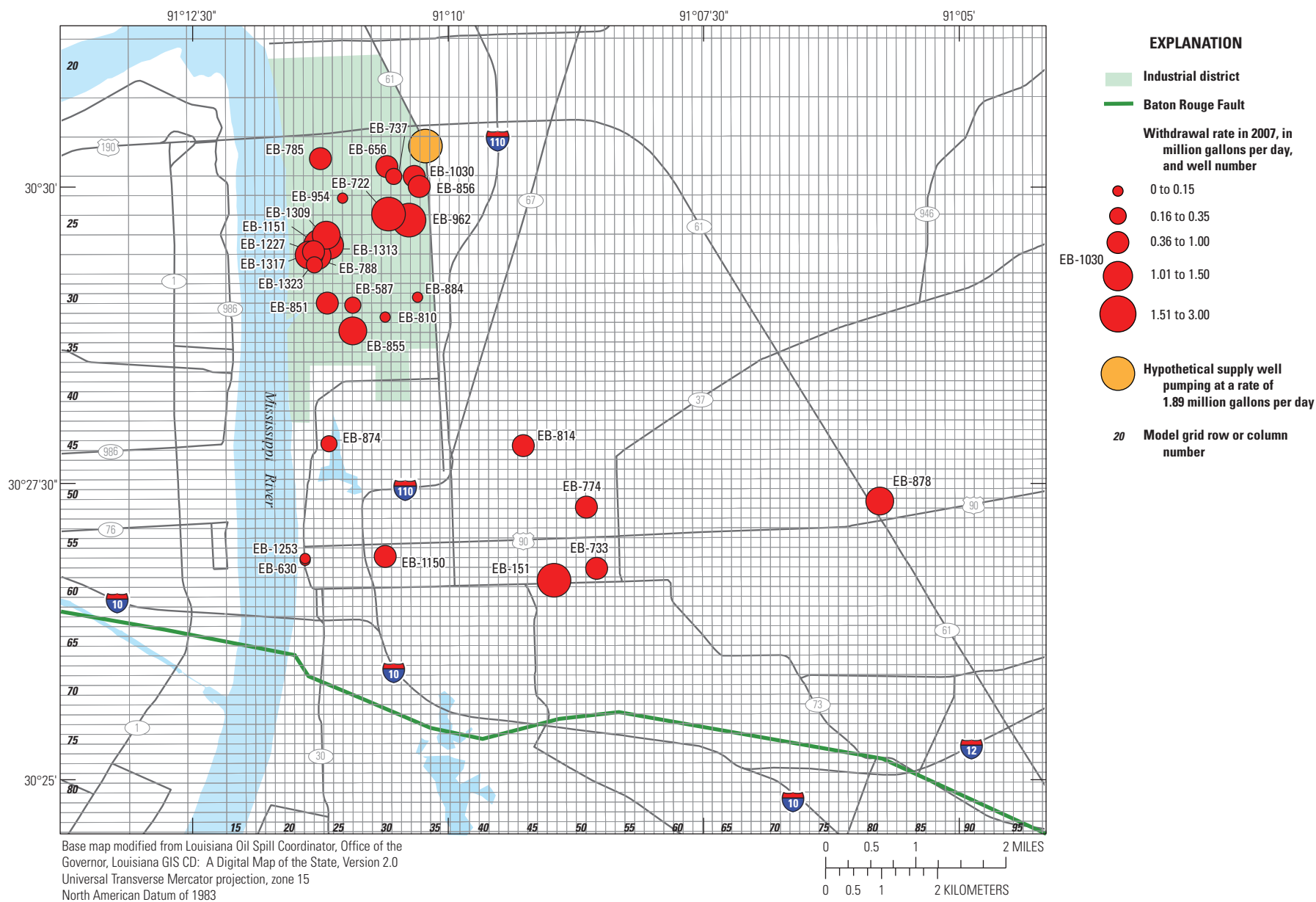
Figure 6. Average daily withdrawal rate during 2012 at wells screened in the "2,000-foot" sand of the Baton Rouge area and located at or near the Baton Rouge industrial district in southeastern Louisiana and location of hypothetical supply well screened in the "2,000-foot" sand.

Equations of Groundwater Flow and Transport

Whereas MODFLOW-2005 solves the constant-density groundwater-flow equation (Harbaugh, 2005), the SEAWAT-2000 (Langevin and others, 2003) code iteratively solves equations that represent variable-density groundwater flow and advective-dispersive mass transport. These equations are succinctly presented below, and the interested reader may refer to the referenced model-code documentation for further details.

Groundwater systems without significant chemical reactions or temperature gradients are governed by equations for variable-density flow,

$$-\nabla \cdot \left(\rho \bar{q}\right) + \bar{\rho} q_s = \rho S_p \frac{\partial P}{\partial t} + \theta \frac{\partial \rho}{\partial C} \frac{\partial C}{\partial t}, \qquad (1)$$

and mass transport,

$$\frac{\partial C}{\partial t} = \nabla \cdot \left(D \nabla C\right) - \nabla \cdot \left(\frac{\bar{q}}{\theta} C\right) - \frac{q_s}{\theta} C_s, \qquad (2)$$

where

∇	is the gradient operator,
ρ	is fluid density [ML^{-3}],
$\bar{q}$	is specific discharge [LT^{-1}],
$\bar{\rho}$	is source or sink fluid density [ML^{-3}],
q_s	is flow rate per unit volume representing sources or sinks [T^{-1}],
S_p	is specific storage in pressure terms [M^{-1}LT^2],
P	is fluid pressure [ML^{-1}T^{-2}],
t	is time [T],
θ	is effective porosity,
C	is solute concentration [ML^{-3}],
D	is the dispersion coefficient [L^{2}T^{-1}], and
C_s	is source or sink solute concentration [ML^{-3}].

These groundwater-flow and mass-transport equations are coupled by the specific discharge ($\bar{q}$) and concentration (C) terms. The dependence of fluid density on concentration can be approximated by a linear equation of state:

$$\rho = \rho_f + \frac{\partial \rho}{\partial C} C, \qquad (3)$$

where

ρ_f is the density of freshwater.

The SEAWAT-2000 (Langevin and others, 2003) code iteratively solves finite-difference versions of these variable-density groundwater-flow and mass-transport equations for every transport time step, thereby coupling the flow and transport equations. Because this solute-transport problem was advection dominated, the mass transport (equation 2) was numerically solved with the third-order total-variation-diminishing (TVD) scheme to reduce numerical dispersion (Zheng and Wang, 1999).

Spatial Discretization

The three-dimensional finite-difference groundwater model grid was designed with variable grid-cell spacing to (1) provide sufficient spatial resolution in a 48-mi^2 area (the detailed model area) (fig. 7) where substantial saltwater migration either has occurred or could occur in the future, (2) locate model boundaries sufficiently far from the detailed model area to minimize the effects of boundary conditions on simulated heads in the area, and (3) limit execution times to enable numerous model simulations to be conducted during calibration through parameter estimation. The total area encompassed by the model domain is 6,529 mi^2 and contains 273,600 active finite-difference cells. The areas encompassed by the finite-difference cells range from 2.5×10^5 square feet (ft^2) (5.74 acres) in the detailed model area to a maximum of 3×10^9 ft^2 (68,870 acres) at the northwest corner of the model domain.

The variable grid spacing creates a large finite-difference-cell aspect ratio, or differences in the north-south versus east-west dimensions, in some areas of the model grid. Although numerical inaccuracies can occur in such areas (Marsily, 1986), cells with large aspect ratios are located in areas of the model grid where high computational accuracy is not required.

The model grid consists of 24 layers of variable thickness, each of which is a rectangular array containing 95 rows and 120 columns of finite-difference cells. For a subset of the model grid, 60 rows by 90 columns, a horizontal grid spacing of 500 ft was specified within the 48-mi^2 detailed model area.

The altitude of the top of each model layer on the north side of the Baton Rouge Fault was assigned the altitude of the top of the hydrogeologic framework unit represented by the layer (table 1). South of the Baton Rouge Fault, the altitudes of the top of each finite-difference layer do not correspond to the hydrogeologic framework units and are constant along columns of finite-difference cells (that is, in the north-south direction). This geometry facilitated simulation of flow across the Baton Rouge Fault and is explained in further detail in the "Internal Flow Package" section of this report. The north-to-south cross-sectional view of the model grid (fig. 8) along column 24 illustrates the variable thickness and "pinching out" of hydrogeologic units north of the Baton Rouge Fault, the offset of hydrogeologic units at the fault, and the discordance between hydrogeologic units and finite-difference cells south of the fault.

In comparison to numerical solution of the transient groundwater-flow equation, numerical solution of the transient solute-transport equation is computationally intensive. It is therefore generally desirable to limit the size of the numerical
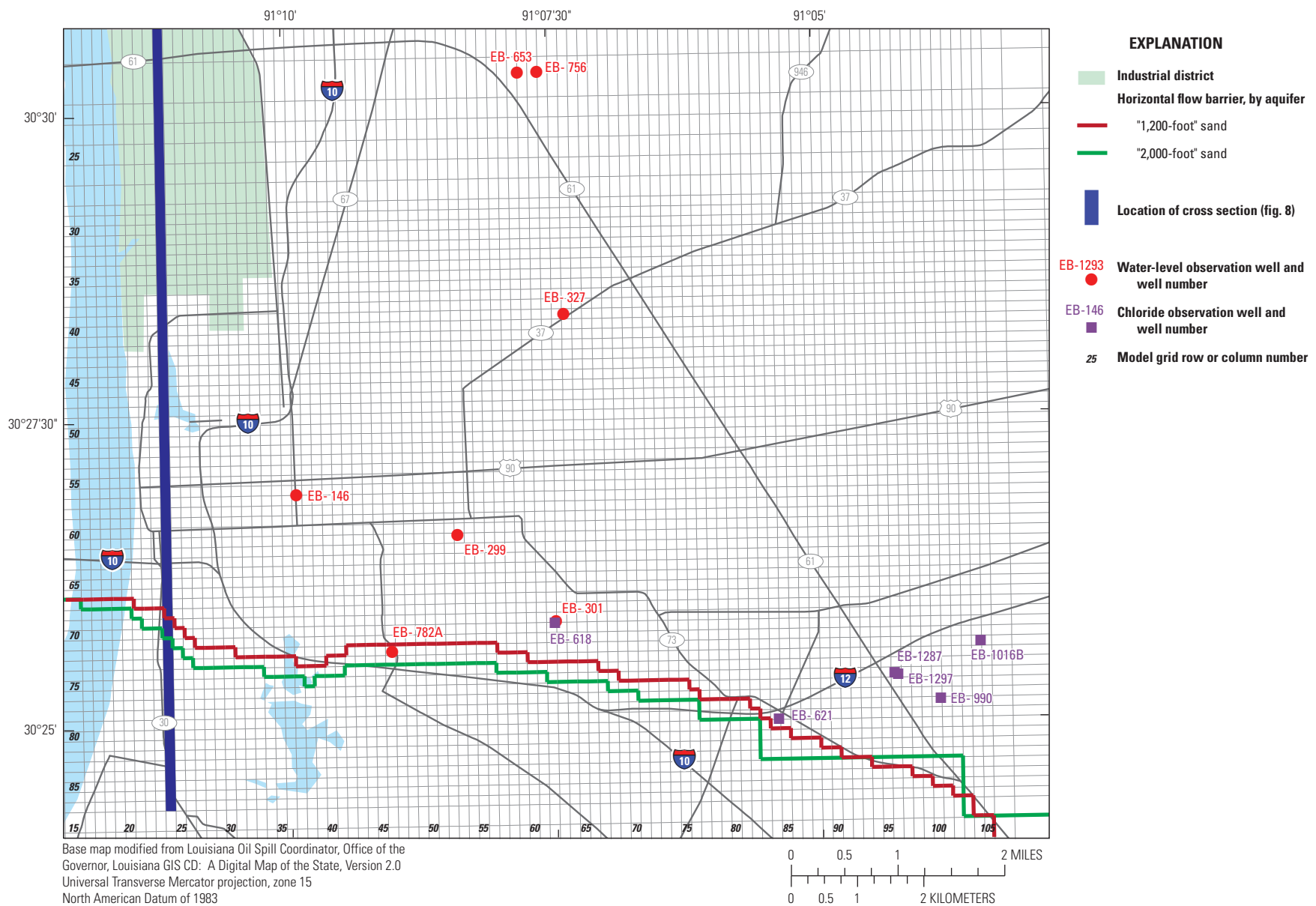
Figure 7. The finite-difference grid, locations of horizontal flow barriers, and selected water-level and chloride observation wells screened in the "1,200-foot" sand of the Baton Rouge area in the detailed model area in southeastern Louisiana.
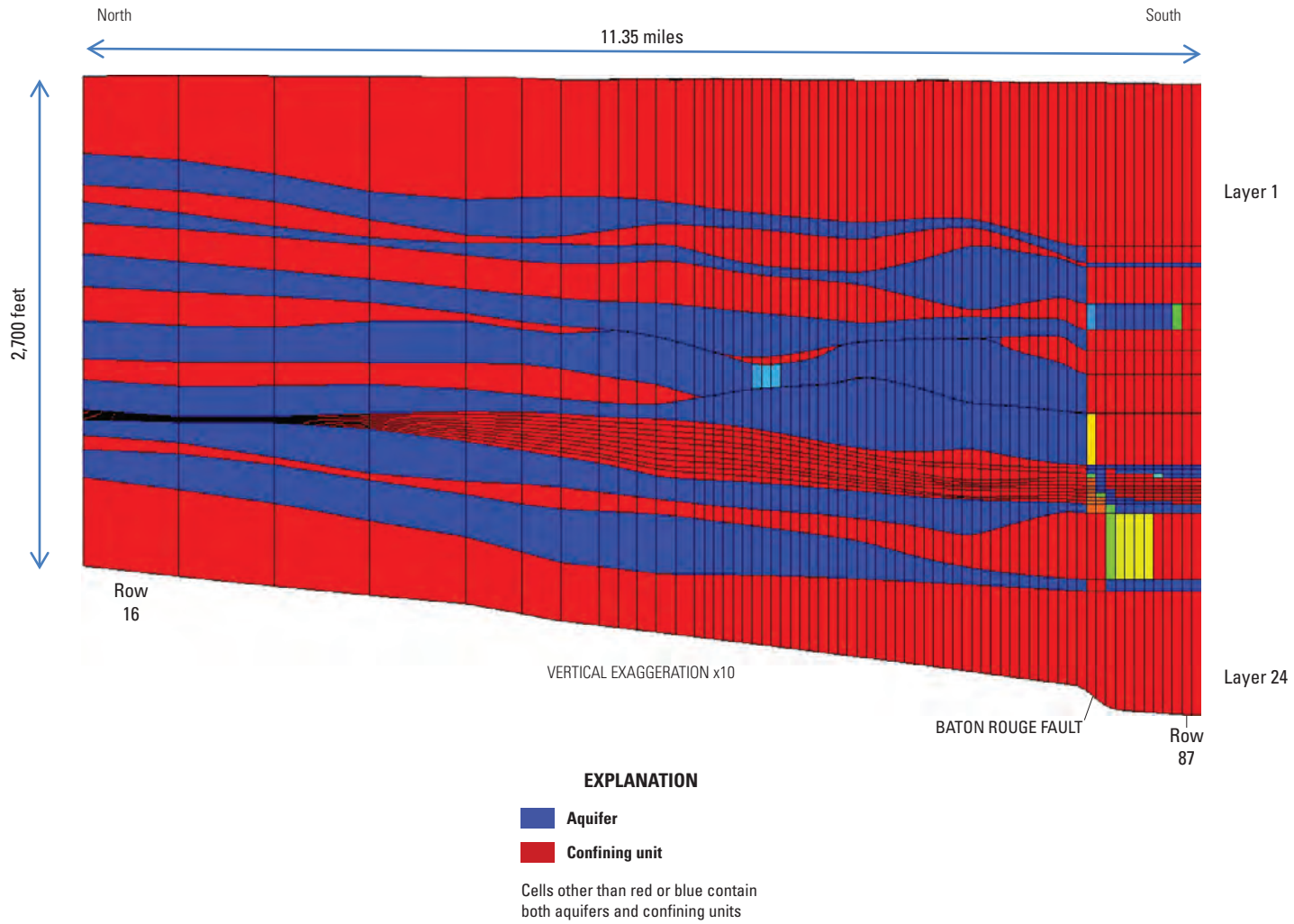
Figure 8.   North-to-south cross section along model column 24 showing aquifers, confining units, and finite-difference discretization.

solute-transport problem when possible. Because simulation of saltwater encroachment is needed in only a small portion of the groundwater-flow model domain, a subset of the groundwater-flow model grid was identified for simulation of solute transport. This solute-transport model domain is the previously described "detailed model area" that has a 500-ft cell spacing (fig. 7). Within this area, the solute-transport equation was numerically solved in all model layers but only calibrated for model layer 5 and model layers 11–20, which correspond to the "1,200-foot" sand and "2,000-foot" sand on the north side of the Baton Rouge Fault, respectively.

Internal Flow Package

Offsets of aquifers at the Baton Rouge Fault may enable flow from stratigraphically younger aquifers south of the fault into stratigraphically older and horizontally juxtaposed aquifers north of the fault. Horizontal flow between juxtaposed hydrogeologic units was enabled by representing the stratigraphy with the Hydrogeologic-Unit Flow package (HUF) (Anderman and Hill, 2000), which represents the thickness of hydrogeologic units independently from that of the finite-difference-grid layers. HUF calculates the storage and intercell conductance terms for each cell from the hydraulic property distributions assigned to individual hydrogeologic units present within that cell. In this model, the altitudes of the finite-difference layers correspond to the tops and bottoms of the aquifers and intervening confining units defined in the hydrogeologic framework for only the portion of the model domain north of the Baton Rouge Fault. South of the Baton Rouge Fault, the altitudes of the finite-difference layers within each model column are flat, with altitudes equal to that at the fault. The finite-difference layers do not correspond to specific hydrogeologic units south of the Baton Rouge Fault. Because of this lack of correspondence, different hydrogeologic units are contained within each finite-difference layer on the north versus south sides of the fault, which allows simulated flow and transport within finite-difference layers between different aquifers that are horizontally juxtaposed at

the fault. For example, the "1,000-foot" sand on the south side of the fault may be connected to the "1,200-foot" sand on the north side of the fault along some portions of the fault.

Horizontal Flow Barriers

The resistance to groundwater flow at the Baton Rouge Fault as a consequence of sediment deformation and displacement of sedimentary layers was simulated with horizontal flow barriers (HFBs) (Hsieh and Freckleton, 1993), which were specified along the vertical faces of cells closest to the fault. The increased resistance between adjacent model cells is specified with a hydraulic characteristic for each HFB that is dimensionally equivalent to the hydraulic conductivity of the fault zone (in the direction perpendicular to the fault plane) divided by the width of the fault zone. HFBs were defined for all model layers that simulated aquifers except model layer 1, for which water levels were specified.

Because the Baton Rouge Fault plane dips to the south between about 65 and 70 degrees, the fault dip was represented by offsetting the fault to the south in deeper framework layers. In layers 3 and 5, the fault is represented 500 ft south of its surface location as indicated in figure 1, whereas in layers 7 through 24, the fault is offset 1,000 ft south of its surface location.

Time Discretization

Because groundwater withdrawals from the Southern Hills regional aquifer system were minor prior to about 1940, a single steady-state stress period was used to simulate predevelopment conditions in the groundwater-flow system (table 2). Seventy-three annual stress periods simulated the time for which annual groundwater-withdrawal data were available between January 1, 1940, and December 31, 2012. Each annual stress period was discretized into five time steps that geometrically increased in duration by a factor of 1.4 such that the first time step of each stress period

Table 2. Discretization of the years 1900–2112 simulated in the model of the Southern Hills regional aquifer system.

Stress period	Groundwater-flow model solution	Years represented	Flow time steps per stress period in groundwater model	Number of transport time steps	Duration of first flow time step
1	Steady state	1900–39	1	2	Not applicable
2–74	Transient	1940–2012	5	*4,785	33.4 days
75	Transient	2013–14	7	239	30.6 days
76	Transient	2015–16	7	**236	30.6 days
77	Transient	2017–47	15	**3,991	29.3 days
78	Transient	2048–2112	15	**8,473	61.4 days

*Total number of transport time steps simulating 1940 through 2012.

**Number of transport time steps differed among scenarios.

simulated 33.4 days. The hypothetical scenarios simulate 100 additional years (2013 through 2112) with four additional stress periods, each divided into either 7 or 15 time steps. A 2-year stress period from 2013 through 2014 utilizes 2012 groundwater-withdrawal rates. Another 2-year stress period encompasses 2015 through 2016, during which groundwater-withdrawal rates were modified for some scenarios. A 31-year stress period that encompasses January 1, 2017, through December 31, 2047, and a final 65-year stress period that encompasses January 1, 2048, through December 31, 2112, simulate identical pumpage stresses but are separated to save simulated results for December 31, 2047. The geometric progression of increasing time-step length provided good temporal discretization for simulation of transient changes in groundwater levels. In the solute-transport simulations, flow time steps are further subdivided into transport time steps. The number of transport time steps was computed internally on the basis of the flow velocity to maintain numerical stability and varied with the specified effective porosity and boundary conditions, such as specified groundwater-withdrawal rates. Smaller transport time steps are required as the flow velocity increases.

Boundary Conditions

Boundary conditions were specified at the boundaries of the groundwater-flow system and within the model domain where they simulate groundwater-withdrawal wells. Three types of boundary conditions were specified for the groundwater-flow model: no flow, specified head, and head-dependent flux. Constant-concentration boundaries were also specified at the lateral boundaries of the solute-transport model.

No-Flow Boundaries

The north, east, and west sides and the top 23 layers of the southern side of the groundwater-flow model domain (fig. 1) are located where negligible groundwater flow is presumed to enter or exit the model domain and were accordingly considered no-flow boundaries. The model-domain perimeter was located sufficiently far from the Baton Rouge area to minimize any effect on simulated water levels in that area from possible inaccuracy of the no-flow boundary-condition specification. The bottom model boundary at the base of layer 24 is also no flow and corresponds to the top of a confining unit located above the Catahoula Formation (table 1), which restricts vertical groundwater flow.

Specified-Head Boundaries

Water levels in the top model layer (layer 1), which represents the "400-foot" sand, "600-foot" sand, and "800-foot" sand, were specified with the Flow and Head Boundary (FHB) package (Leake and Lilly, 1997). Water-level distributions that represent the years 1944, 1980, 1990, 1998, 1999, and 2004 were constructed from existing data. Water levels for times between these years were linearly interpolated for each model cell in the top layer. Steady-state (predevelopment) water levels were specified at the 1944 levels, and water levels for times after 2004 were specified at the 2004 levels. The accuracy of these water-level specifications was verified by calculating the differences between the specified water levels and 1,016 water levels measured in wells screened within the "400-foot" sand, "600-foot" sand, or "800-foot" sand. The mean magnitude of the water-level residuals (measured minus simulated water level) was 8.5 ft, and the standard deviation of the residuals was 13.0 ft.

Water-level maps were digitized from previous reports: predevelopment (1944) (Kuniansky, 1989), 1980–84 (Martin and Whiteman, 1985; Boswell and Arthur, 1988; Kuniansky, 1989), and 1990 (Tomaszewski, 1996). Historical water-level observations were used to enhance the predevelopment water-level map (Kuniansky, 1989) in some areas. Water-level maps for 1998 and 1999 were created through modification of the 1990 and 2004 water-level maps by using water-level data collected at selected wells during 1998 and 1999 to more accurately specify water levels near the Commission's "connector well," which was installed in 1998 and screened in the "800-foot" sand and "1,500-foot" sand (Dial and Cardwell, 1999). The water-level map for 2004 was created by using water-level data collected by the USGS in cooperation with the Commission and the DOTD. Because little water-level change has occurred within the model domain in Mississippi, interpreted water levels in Mississippi during 1982 (Boswell and Arthur, 1988) were incorporated into all of the water-level maps used to specify transient water levels with the FHB package.

The southernmost row of the bottom model layer (row 95 in layer 24) contains a specified-head boundary to simulate groundwater underflow out of the model domain under predevelopment conditions. The water level for this boundary was specified by estimating the value of the associated parameter "bound_head" (table 3) during the model calibration process.

Table 3.   Calibrated parameter values and sensitivities of the groundwater-flow model.

[ft, foot or feet; numbers in parameter names correspond to aquifer name or layer number (see table 2); 2k, "2,000-foot" sand. The fault hydraulic characteristic of the "2,000-foot" sand was specified for three fault segments: fault_2k, fault_2kmid, and fault_2kw]

Parameter type	Units	Parameter name	Calibrated value	Composite sensitivity
Specified head	ft	bound_head	111.3	1.83
Horizontal hydraulic conductivity	ft/day	k_468sand	40.0	fixed
		k_1000sand	10.0	0.15
		k_1200s01	117	0.02
		k_1200s02	6.9	0.03
		k_1200s03	83.6	0.08
		k_1200s04	74.5	0.02
		k_1200s05	15.8	0.02
		k_1200s06	134	0.12
		k_1200s07	46.2	0.03
		k_1200s08	58.3	0.14
		k_1200s09	21.3	0.09
		k_1200s10	5	0.02
		k_1200s11	91.7	0.02
		k_1200s12	36.9	0.07
		k_1200s13	5.28	0.03
		k_1200s14	119	0.10
		k_1200s15	143	0.03
		k_1200s16	163	0.03
		k_1200s17	11.4	0.05
		k_1200s18	183	0.05
		k_1200s19	54.4	0.06
		k_1200s20	88.1	0.07
		k_1200s21	200	0.05
		k_1200s22	5	0.02
		k_1200s23	200	0.11
		k_1500sand	281	0.08
		k_1500neas	53.0	0.48
		k_1500falt	300	0.05
		k_1700sand	7.4	0.36
		k_2000sand[1]	various	various
		k_2400sand	12.1	0.29
		k_2400sand2	13.3	0.19
		k_2800sand	34.0	0.78
		k_clay	2.4×10^{-5}	0.03

Table 3.   Calibrated parameter values and sensitivities of the groundwater-flow model.—Continued

[ft, foot or feet; numbers in parameter names correspond to aquifer name or layer number (see table 2); 2k, "2,000-foot" sand. The fault hydraulic characteristic of the "2,000-foot" sand was specified for three fault segments: fault_2k, fault_2kmid, and fault_2kw]

Parameter type	Units	Parameter name	Calibrated value	Composite sensitivity
Vertical hydraulic conductivity	ft/day	vk_sands	0.1	0.1
		vk_2con	4.5×10^{-5}	0.02
		vk_4con	1.6×10^{-4}	0.09
		vk_6con	1×10^{-5}	0.07
		vk_8con	3.0×10^{-3}	0.30
		vk_19con	6.8×10^{-4}	0.22
		vk_21con	1.2×10^{-5}	0.17
		vk_neocon	3.2×10^{-4}	0.11
		vk_gov	1.5×10^{-3}	0.38
Specific storage	ft^{-1}	ss_sand	2.3×10^{-6}	0.02
		ss_12	1×10^{-6}	0.02
		ss_15	1×10^{-6}	0.02
		ss_17	1.3×10^{-6}	0.02
		ss_24	2.8×10^{-6}	0.03
		ss_28	4.5×10^{-6}	0.10
		ss_neocon	4.4×10^{-6}	0.02
		ss_2ksand	3.1×10^{-6}	0.05
		ss_clay2	1.2×10^{-6}	0.02
		ss_clay4	2.6×10^{-5}	0.22
		ss_clay6	1×10^{-6}	0.03
		ss_clay8	1.5×10^{-5}	0.27
		ss_clay19	1×10^{-6}	0.03
		ss_clay21	1.4×10^{-6}	0.02
Fault hydraulic characteristic	day^{-1}	hfb_1000ft	1.2×10^{-5}	0.02
		hfb_1200ft	1.6×10^{-6}	0.02
		hfb_1500ft	2.3×10^{-5}	0.02
		hfb_1700ft	3.3×10^{-5}	0.02
		fault_2k	5.9×10^{-4}	0.03
		fault_2kmid	1.5×10^{-4}	fixed
		fault_2kw	8.4×10^{-4}	0.03
		fault_24	1×10^{-6}	0.02
		fault_28	1.4×10^{-3}	0.02

[1]This parameter name represents 142 parameter values at pilot points in the "2,000-foot" sand documented in Heywood and others (2014).

Head-Dependent Flux Boundaries

The previously described groundwater withdrawals were simulated with the revised MNW2 of MODFLOW (Konikow and others, 2009) because the screen intervals of many withdrawal wells span multiple model layers. The MNW2 package computes a layer-by-layer distribution of withdrawal for each well on the basis of the hydraulic conductivities and simulated water levels in each finite-difference cell connected to the simulated well-screen interval. For each annual stress period, the average daily withdrawal from each well was specified in cubic feet per day. In some wells, water may flow between model layers when the water level simulated in a connected finite-difference cell is less than that simulated in the well. The effects of turbulent-flow head losses near the well and flow through drilling-damaged formation, gravel pack, or the well screen were not simulated.

Groundwater withdrawals from wells screened in the top model layer (layer 1) corresponding to the Mississippi River alluvial aquifer, shallow sands, Upland terrace aquifer, "400-foot" sand, "600-foot" sand, and "800-foot" sand were not simulated because water levels in this layer were a specified boundary condition. One exception was the cell containing the connector well (EB-1293) (Dial and Cardwell, 1999), where the water level for the top model layer (layer 1) was not specified. At this location, the MNW2 package was used to simulate flow through the connector well, which has screens that intersect the "800-foot" sand (model layer 1) and the "1,500-foot" sand (model layer 7), so that calculated flow through the "connector well" could be compared to that measured by Dial and Cardwell (1999). Exclusion of withdrawals from the "400-foot" sand, "600-foot" sand, and "800-foot" sand, which amounted to about 24 Mgal/d in the Baton Rouge area during 2012, reduced the total withdrawals simulated in the model during 2012 to 171.3 Mgal/d.

Specified-Concentration Boundaries and Initial Conditions

The source of saltwater to the "2,000-foot" sand was simulated on the south side of the Baton Rouge Fault in model columns 16 through 53 (fig. 7), corresponding to a 3.6-mi-long region extending east from the Mississippi River. Within this region, the specified concentration increases linearly from zero above model layer 11 to a maximum of 10,000 mg/L of chloride at the base of layer 20. Constant-concentration cells in the two rows south of the Baton Rouge Fault within each column represent this source.

For the "1,200-foot" sand, the saltwater source is simulated as a constant-concentration boundary of 5,300 mg/L two model rows south of the simulated location of the Baton Rouge Fault in model-grid layer 5, columns 16 through 104, corresponding to an 8.6-mi-long region east of the Mississippi River. Offsetting of the concentration boundary 1,000 ft south of the fault improved calibration to observed concentrations north of the fault by simulating transport during a time period prior to salt crossing the fault. This location approximately corresponds to the simulated location of the Baton Rouge Fault in the underlying "2,000-foot" sand. The 5,300-mg/L chloride concentration and distance south of the fault of this boundary were determined by trial and error calibration of the transport simulation.

Within the solute-transport model domain (the "detailed model area") north of the Baton Rouge Fault, the initial specified concentrations were zero (corresponding to freshwater) and were subsequently calculated by solution of the advective-dispersive equation (2). Model cells south of the Baton Rouge Fault and west of column 16 have zero concentration in all model layers, corresponding to freshwater. Model-grid layers 1 through 4, 6 through 10, and 21 through 24 were specified with zero initial concentration in all areas because simulation of transport in the hydrogeologic units corresponding to those layers is not within the scope of the current modeling effort, and therefore transport was not calibrated in those layers. The concentration of simulated water flowing from surrounding areas to the north, east, and west into the solute-transport model domain is specified as zero, corresponding to freshwater.

Hydraulic-Property Distribution

The simulated horizontal hydraulic conductivities (K_h) within the top specified-head model layer that represents shallow aquifers including the "400-foot" sand, "600-foot" sand, and "800-foot" sand were uniformly fixed at 40 ft per day, the value estimated in the previous model (Heywood and others, 2014). The K_h for aquifer hydrogeologic units representing the "1,000-foot" sand (layer 3), the "1,700-foot" sand (layer 9), and the "2,800-foot" sand (layer 24) were each represented with single parameters that were estimated during model calibration. Because the specified thickness of each of these hydrogeologic units is spatially variable, simulated transmissivity varies spatially within these aquifers. Variability of K_h within the "1,200-foot" sand (layer 5) was simulated with 23 spatial zones within which K_h was uniform. These zones are Thiessen polygons constructed with centroids corresponding to the location of water-level observation wells screened within the "1,200-foot" sand (fig. 9). Variability of K_h within the "1,500-foot" sand (layer 7) was simulated with three zones within which K_h was uniform. Heterogeneity of K_h within the "2,000-foot" sand (layers 11–20) was simulated by estimating values at 142 locations as described by Heywood and others (2014), and the specified values of K_h at those locations were updated. Variability of K_h within the "2,400-foot" sand (layer 22) was simulated with two zones within which K_h was uniform. Areas where the "1,500-foot" sand (layer 7) and "1,700-foot" sand (layer 9) do not exist because those units pinched out were assigned the K_h used for confining-unit layers within their respective hydrogeologic-unit layers. The simulated vertical hydraulic conductivity (K_v) within each hydrogeologic unit that represents a confining unit (model layers 2, 4, 6, 8, 10, 21, and 23 on the north side of the
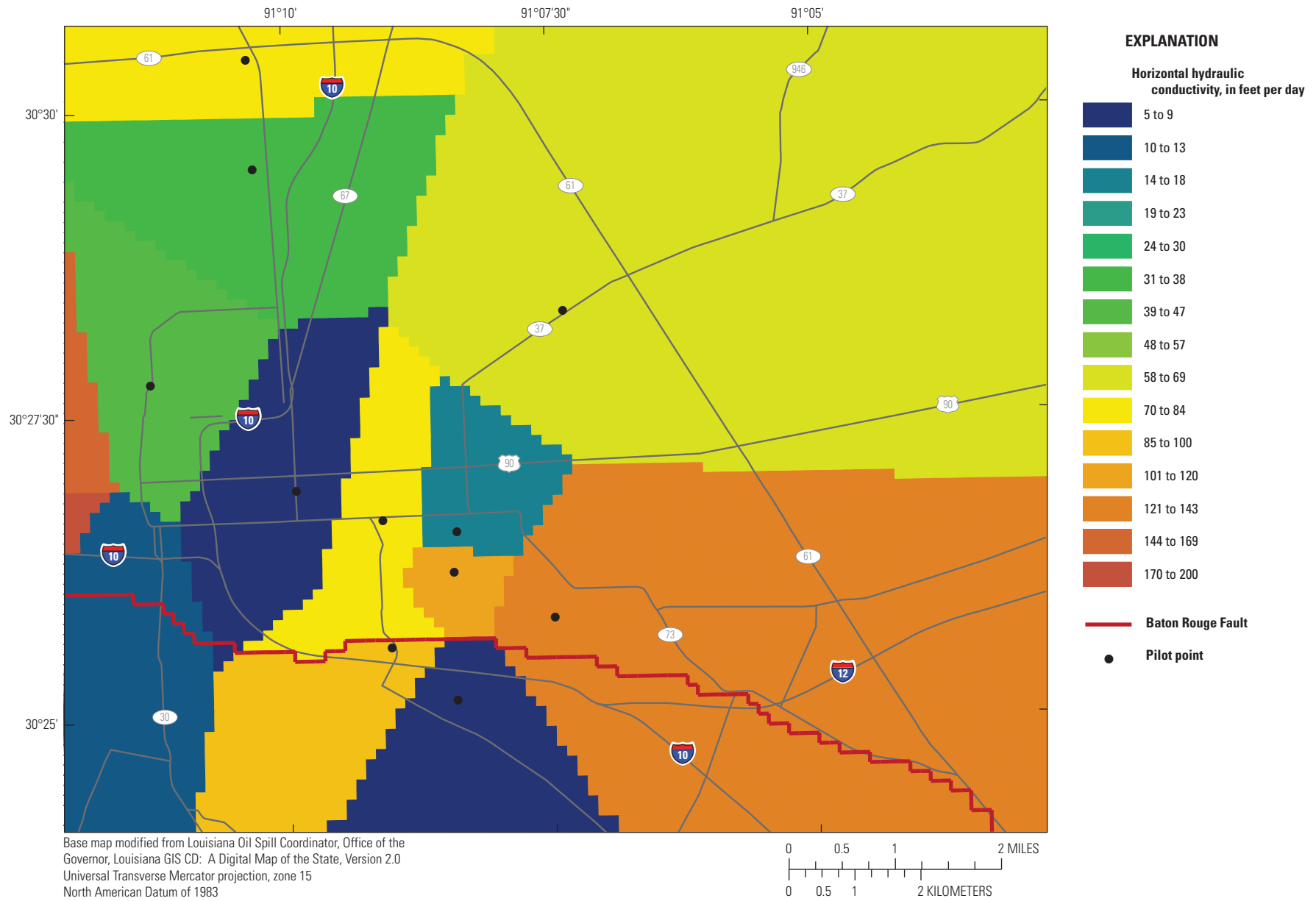
Figure 9.   Pilot point locations and the simulated horizontal hydraulic conductivity distribution within the "1,200-foot" sand of the Baton Rouge area in the detailed model area in southeastern Louisiana.

Baton Rouge Fault, subsequently referred to as "confining-unit layers") was uniform within each confining unit and estimated separately. The K_v of all aquifers and K_h of all confining units were specified with a single parameter for each of these two types of hydrogeologic units (table 3). Separate parameters that represent specific storage (S_s) within each aquifer and confining-unit layer were estimated during model calibration (except for the top specified-head model layer).

Distinct hydraulic characteristics were estimated for three lateral segments of the Baton Rouge Fault within the 10 model layers representing the "2,000-foot" sand north of the fault (layers 11–20). A single hydraulic characteristic was estimated for other model layers that contain aquifers north of the fault (layers 3, 5, 7, 9, 22, and 24). Horizontal flow barriers were simulated for confining-unit layers that separate the "1,000-foot" sand from the "1,200-foot" sand and the "1,200-foot" sand from the "1,500-foot" sand. The calibrated values of the hydraulic properties for the groundwater-flow model are summarized in table 3.

Solution of the advection-dispersion equation with SEAWAT required definition of the spatial distribution of the longitudinal, transverse, and vertical dispersivities, diffusion coefficient, and effective porosity of the aquifer system within the solute-transport model domain. A homogeneous distribution for each of these properties was specified. Because the simulated transport processes are dominated by advection, diffusion is negligible, and the diffusion coefficient was specified equal to zero. The calibrated values of these parameters are summarized in the "Estimated Parameter Values" section of this report and in table 3.

Model Calibration

The groundwater-flow model was calibrated to obtain the best overall agreement between measured heads and their corresponding values simulated with MODFLOW. Although water levels were used as observations in the model-calibration regression, groundwater fluxes were constrained by specification of well withdrawals. By using the parameter-estimation code PEST (Doherty, 2004), the values of 212 parameters, including 142 parameters representing K_h at pilot points in the "2,000-foot" sand, 23 parameters representing K_h within zones of the "1,200-foot" sand, and other parameters summarized in table 3, were adjusted to minimize the objective function:

$$\sum_{k=1}^{4,911} \left(\omega_k H_k - \omega_k H'_k(\mathbf{b}) \right)^2 + \sum_{i=1}^{NPR} \left(\omega_i P_i - \omega_i P'_i(\mathbf{b}) \right)^2 \quad (4)$$

In equation 4, symbols in the first summation are associated with water levels where

4,911	is the number of water-level observations,
ω_k	is the weight applied to water-level observation k,
H_k	is the measured water level for observation k,
H'_k	is the simulated-equivalent water level for observation k, and
$\mathbf{b}$	is the vector of 212 model parameters.

Symbols in the second summation are associated with the "prior information" equations used for the regularization and described by Heywood and others (2014) where

NPR	equals 138, the number of prior equations used to regularize the K_h distributions specified for the "2,000-foot" sand in the regression;
ω_i	is the weight applied to the ith prior estimate;
P_i	is the ith prior estimate; and
P'_i	is the ith simulated value.

Calibration Dataset

The model calibration dataset consisted of groundwater-level observations, connector-well flow, and chloride concentrations. PEST was used to calibrate the water levels simulated with the constant-density MODFLOW model to observed water levels. Observations of chloride concentrations were used to calibrate the solute-transport model parameters. The groundwater-flow model was calibrated through parameter estimation with PEST, whereas the solute-transport model was manually calibrated through trial and error.

Water-Level Observations

A total of 4,911 water levels measured during the period from 1916 through 2012 from 161 wells in Louisiana were utilized in the groundwater-flow model calibration. These measurements were from wells with at least six annual measurements; one measurement per year from any well was incorporated into the calibration database. About 79 percent (3,895) of the measurements made before 2013 in aquifers beneath the "800-foot" sand were used to estimate parameters in the groundwater-flow model calibration. About 21 percent (1,016) were used to evaluate the accuracy of the transient water levels specified for the top model layer from interpolation of historical water-level maps. In locations where multiple observation wells within a single model cell had overlapping periods of record, wells with the longest periods of continuous water-level record were selected for the compilation. Observed water-level altitudes were between 248 and -292 ft. Observed water levels from the wells screened beneath model layer 1 that were used for estimation of groundwater-flow model parameters were between 215 and -292 ft, a range of 507 ft. Within the "1,200-foot" sand, a decrease in water level of 177 ft has been observed in well EB-146 during the years from 1916 through 2011.

Well location and construction information from USGS, DOTD, and DNR records was used to specify the screen intervals and locations of the observation wells. Most

(4,162) water-level observations were measured in wells with screen intervals corresponding to a single model layer, but 749 observations were measured in wells with either long or multiple screens that correspond to more than one model layer. In the latter cases, the measured water levels represent a composite of the actual head conditions in the various aquifer-depth intervals in which the well is screened. The majority of these multilayer observations were measured in wells screened in the "2,000-foot" sand, which is represented by 10 model layers with identical K_h distributions. MODFLOW computed the composite water level for each multilayer well by averaging the water levels simulated in all of the model layers intersected by the well screen.

Chloride-Concentration Observations

Chloride-concentration observations from wells within the "1,200-foot" sand and "2,000-foot" sand were compiled from the USGS National Water Information System (http://waterdata.usgs.gov/nwis/qw). Observed concentrations from five wells located in the area of saltwater encroachment (EB-781, EB-1028, EB-1150, EB-630, and EB-807B) were used as calibration targets for the simulation of transport within the "2,000-foot" sand. Of the four wells useful as transport-calibration targets for the "1,200-foot" sand (EB-618, EB-621, EB-1287, and EB-1297) (fig. 7), only one (EB-621) had a record of chloride concentrations that had risen substantially above background levels. Measured chloride concentrations between 2 and 10 mg/L in the other three observation wells within the "1,200-foot" sand also constrained the extent of the simulated chloride plume.

Observation and Prior-Information Weights

The uncertainties associated with measurement of well-head altitudes and the depth to water in the observation well were described in a previous report (Heywood and others, 2014). The total error for water levels was estimated as the sum of errors in measurement-point altitude and depth to water, which is about 2.5 ft, referred to herein as the "composite variance." The inverse of this composite variance can be used to assign a measurement weight in the model-calibration regression. Because well-head altitude and depth-to-water measurement errors were similar for all observations, observation weights were set equal for water levels measured in aquifers beneath the "800-foot" sand (layer 1). Water-level observations from wells screened within the "400-foot" sand, "600-foot" sand, and "800-foot" sand were assigned zero weight because those aquifers are represented by the specified heads within layer 1. Although effectively removed from the parameter-estimation regression, these observations were retained in the calibration dataset to evaluate the accuracy of the water-level specification within layer 1. PEST automatically adjusts the weight of the set of prior information

equations with respect to the set of observations during the parameter-estimation process.

Calibration Assessment

The quality of the model calibration was evaluated on the basis of the reasonableness of the estimated parameter values, the overall fit of simulated to observed water levels computed by the objective function, the fit of simulated to observed chloride values, and the amount of bias in the distribution of positive and negative water-level residuals. Residuals were calculated by subtracting simulated water-level altitudes from the observed water-level altitudes. A graph of the water-level residuals plotted as a function of the simulated water-level altitudes (fig. 10) indicates that the residuals are randomly distributed around the horizontal (residual=0) abscissa, suggesting a lack of systematic model bias in simulated water levels.

Summary statistics were calculated for the residuals of the 3,895 water-level observations used in the regression. The mean magnitude of the water-level residuals was 11.7 ft. The standard error of the residuals was 15.78 ft. The root-mean-square error (RMSE) was calculated as the square root of the mean of the unweighted squared residuals:

$$RMSE = \sqrt{\frac{\sum_{k=1}^{3,895}\left(H_k - H'_k\right)^2}{3,895}} \qquad (5)$$

where

H_k is the measured water level for observation k, and

H'_k is the simulated-equivalent water level for observation k.

The RMSE and the standard deviation of the residuals were 16.08 and 16.07 ft, respectively. The normalized RMSE was 0.032 and was obtained by dividing the RMSE of the residuals by the 507-ft range of observed water levels. Because the RMSE is only 3 percent of the observed measurement range, the model adequately simulates observed water levels.

Estimated Parameter Values

Parameter values were constrained within reasonable limits on the basis of local knowledge and literature values during the model calibration process with PEST. Several relatively insensitive model parameters drifted toward their respective limiting constraints between successive parameter-estimation iterations but were not allowed to exceed those limits. Consequently, all of the groundwater-model parameters in the "calibrated" MODFLOW-2005 and SEAWAT simulations (table 3) are considered reasonable.
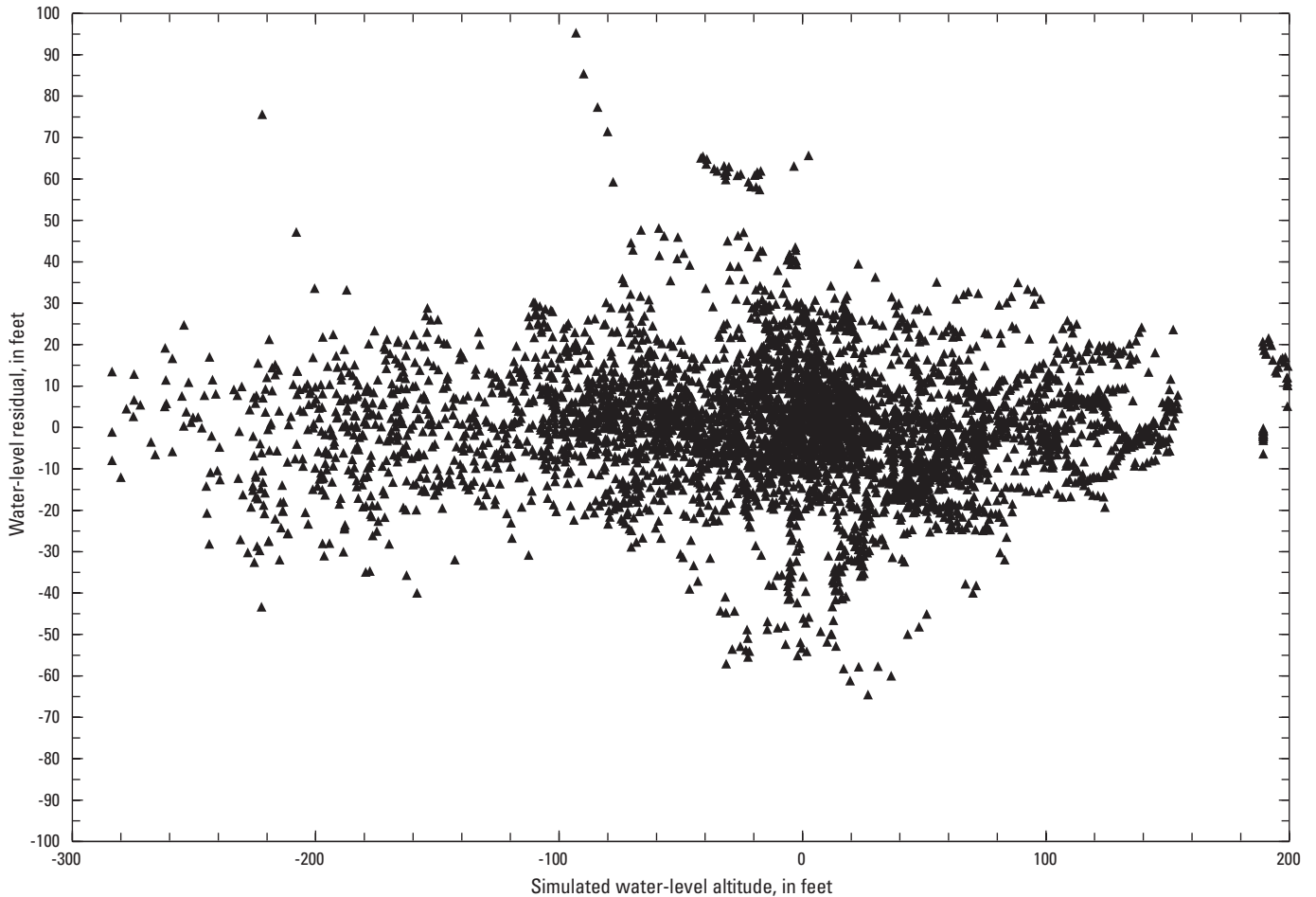
Figure 10.   Water-level residuals as a function of simulated water-level altitudes.

Whereas the groundwater-flow model parameters were formally estimated by minimization of the objective function (equation 4), the values of parameters representing the longitudinal, transverse, and vertical dispersivities and effective porosity that were used in the previously documented version of the model (Heywood and others, 2014) were reevaluated by manual calibration of simulated to observed concentrations, and the previously specified values were retained. The longitudinal component of the aquifer dispersivity was specified homogeneously at 300 ft, the transverse at 30 ft, and the vertical at 3 ft. Effective porosity was homogeneously specified at 15 percent. These values are within the range of reasonable values for these transport parameters (Zheng and Bennett, 1995).

Parameter Sensitivities

The composite parameter sensitivity reflects the total amount of information provided by the water-level observations for the estimation of the model parameter (Hill and Tiedeman, 2007). PEST computes a "composite sensitivity" (Doherty, 2004) of each model parameter with respect to all of the weighted simulated heads (h'_i). The composite sensitivities of parameters included in the regression computed at the final parameter values are summarized in table 3. In general, parameters with sensitivities greater than about 0.1 were well estimated and have correspondingly smaller confidence intervals. Parameters with composite-scaled sensitivities smaller than about 0.1 were more difficult to estimate and (or) have larger confidence intervals. The parameter "bound_head," which controls the specified water level in the bottom row at the south end of the model that represents the groundwater base level (Kafri and Yechieli, 2010) south of the study area, has the highest composite sensitivity, indicating that, in general, simulated water levels are most sensitive to this parameter.

Simulated Groundwater Conditions

In areas where the density of groundwater does not vary spatially, groundwater flows from areas with higher water levels to areas with lower water levels. Because the simulated chloride concentrations and associated groundwater densities are relatively high adjacent to some areas along the Baton Rouge Fault, however, the direction of groundwater flow may not coincide with the gradient of water levels simulated by SEAWAT in this area. The simulated water levels depicted as contour maps in this report represent conditions on December 31 of the indicated year. Comparisons between contour maps generated for different simulated times can be used to quantify water-level changes, and hydrographs of simulated and observed water levels at observation well locations can also be used to visualize water-level changes at various locations and depths in the aquifer system. Hydrographs of simulated water levels presented in this report were computed with the Head Observation Package of MODFLOW, which spatially and temporally interpolates simulated water levels at the location and time of each specified water-level observation. Changes in observed chloride concentration with time (chlorographs) and the corresponding concentrations simulated with SEAWAT are also presented in this report for selected wells.

Simulated Water Levels

Simulated groundwater flow within the "1,200-foot" sand during the predevelopment steady-state period prior to 1940 generally flowed from updip areas near the Louisiana-Mississippi border southward and southwestward toward the Baton Rouge area (fig. 11). Simulated groundwater flow within the "1,200-foot" sand that flows toward the northwest corner of the model domain discharges upward toward the specified-head boundary that represents the surficial aquifers. Because the simulated effects of groundwater withdrawals on water levels and flow directions in the "2,000-foot" sand and on the movement of saltwater in the "2,000-foot" sand were described in a previous report (Heywood and others, 2014), only new scenarios for managing pumpage and saltwater movement within the "2,000-foot" sand are described.

After 73 years of groundwater withdrawals (1940–2012), simulated groundwater levels in much of the study area declined from their predevelopment levels. Groundwater currently flows toward the industrial district in the Baton Rouge area where withdrawals have substantially decreased water levels (fig. 12). Within the "1,200-foot" sand, a simulated "cone of depression" (area of groundwater drawdown) is centered over the industrial district, where the minimum simulated water-level altitude is about -135 ft.

Hydrographs depict the fit of simulated and observed water levels for wells in the detailed model area (see fig. 7 for well locations) and show the history of water-level changes in the "1,200-foot" sand (fig. 13). A spreadsheet and database containing hydrograph information for all observed and simulated water levels are included with the model archive that is available from the USGS Lower Mississippi-Gulf Water Science Center.

Water levels in the "1,200-foot" sand are simulated by model layer 5 north of the fault with a complex hydraulic conductivity distribution (fig. 9). Simulated water levels correspond closely with water levels observed in wells screened in the "1,200-foot" sand, and the 177 ft of drawdown in well EB-146, located about 0.9 mi east of Interstate 10 in Baton Rouge, is accurately simulated (fig. 13*A*). Simulated water levels at two wells (EB-146 and EB-301) are slightly lower than observed water levels during the 1960s and early 1970s, possibly as a result of inaccurate pumpage specified within this layer for those periods.

Simulated Water Budget

Under predevelopment conditions, the simulated steady-state water budget indicates that about 67.46 Mgal/d of water entered and exited the groundwater-flow model domain (table 4). Net inflow of 3.35 Mgal/d from the top specified-head model layer that represents the "400-foot" sand, "600-foot" sand, "800-foot" sand, Mississippi River alluvial aquifer, Upland terrace aquifer, and other shallow sands into the underlying model layer is balanced by net outflow through the constant-head boundary along the southernmost row (row 95) of the deepest model layer (layer 24). By the end of the transient historical simulation (December 31, 2012), substantial net groundwater withdrawals (171.31 Mgal/d during 2012) had caused water-level declines that substantially increased net simulated infiltration from layer 1 to 92.93 Mgal/d. Specified water-level changes in the top model layer account for processes not explicitly simulated by the model, including storage changes in the "400-foot" sand, "600-foot" sand, and "800-foot" sand; evapotranspiration; and recharge. As such, recharge and discharge to the upper aquifers are not represented in the simulated water budget. Inflows from storage simulated in model layers 2–24 represent water from aquifer-matrix compression and water expansion.

A graph of the changes in the contributions from the three major sources and sinks of water during the transient historical groundwater simulation illustrates the effect of groundwater withdrawals on the simulated water budget (fig. 14). After the steady-state stress period that simulates predevelopment conditions (conditions prior to 1940), groundwater withdrawals are initially mostly supplied by the elastic release of water from storage. Over time, vertical hydraulic gradients caused by groundwater withdrawals from the deeper model layers cause increasing downward flow from the top specified-head model layer that represents the upper aquifers. Flow from storage continues to respond to shorter term changes in the pumpage stress. The plot of flow from specified-head boundaries in figure 14 appears relatively smooth through time because it is computed during every time step. In contrast, groundwater withdrawals are specified by stress periods composed of multiple time steps, and flow from storage responds to these specified withdrawals.
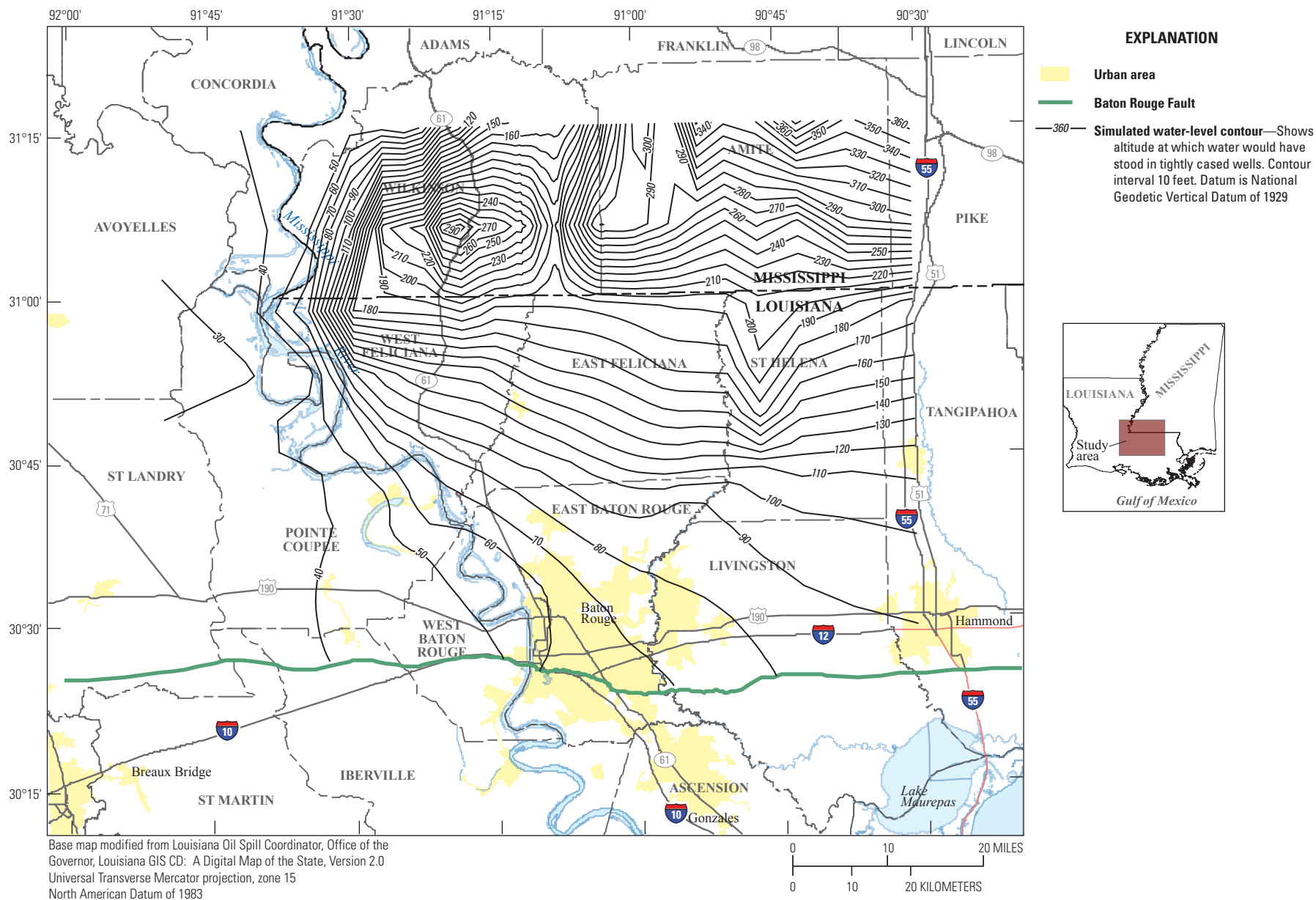
Figure 11. Simulated steady-state water levels within the "1,200-foot" sand of the Baton Rouge area representing predevelopment conditions (before 1940) in southeastern Louisiana and southwestern Mississippi.
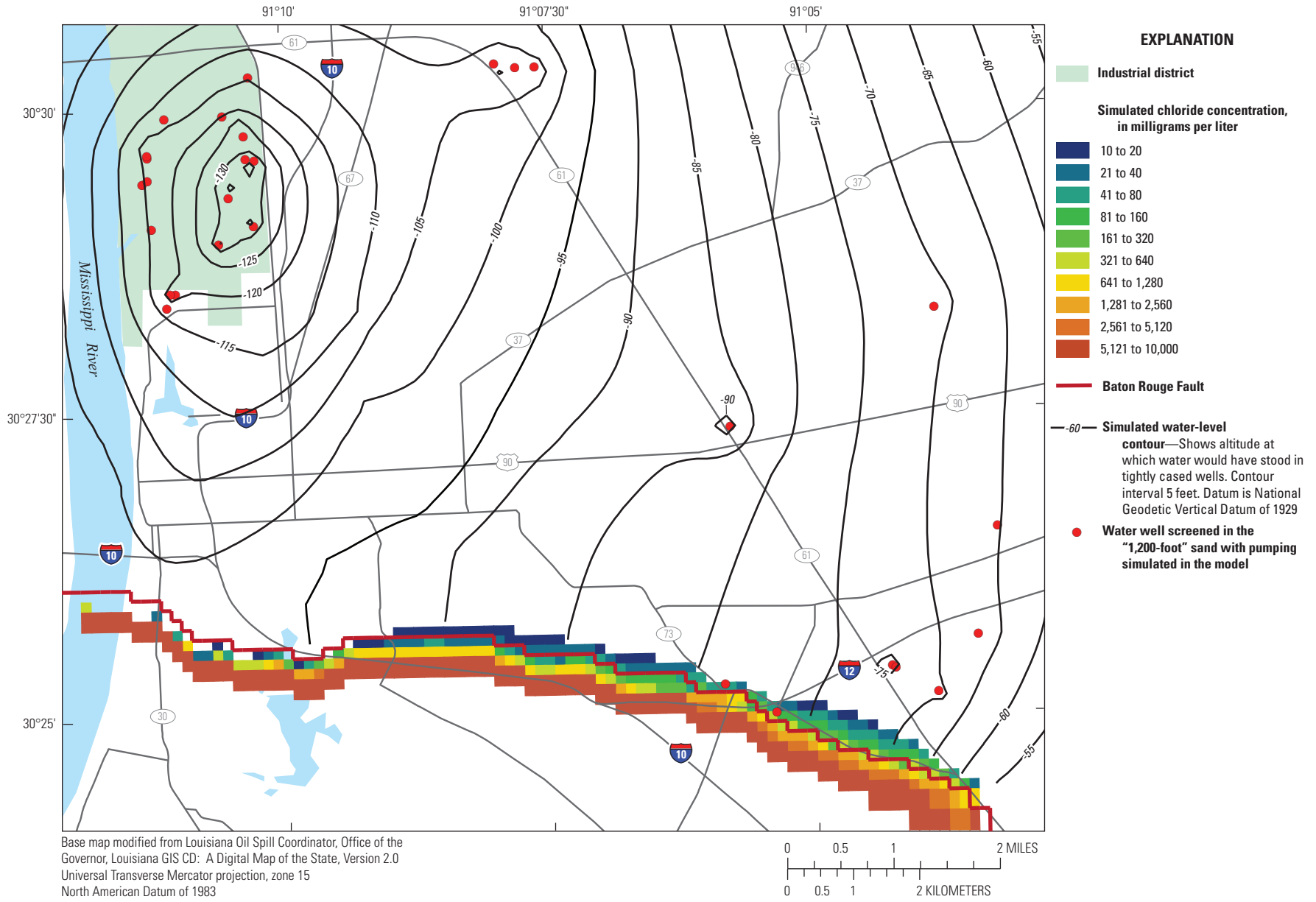
Figure 12.   Simulated 2012 water levels and chloride concentrations in the "1,200-foot" sand of the Baton Rouge area in the detailed model area in southeastern Louisiana.
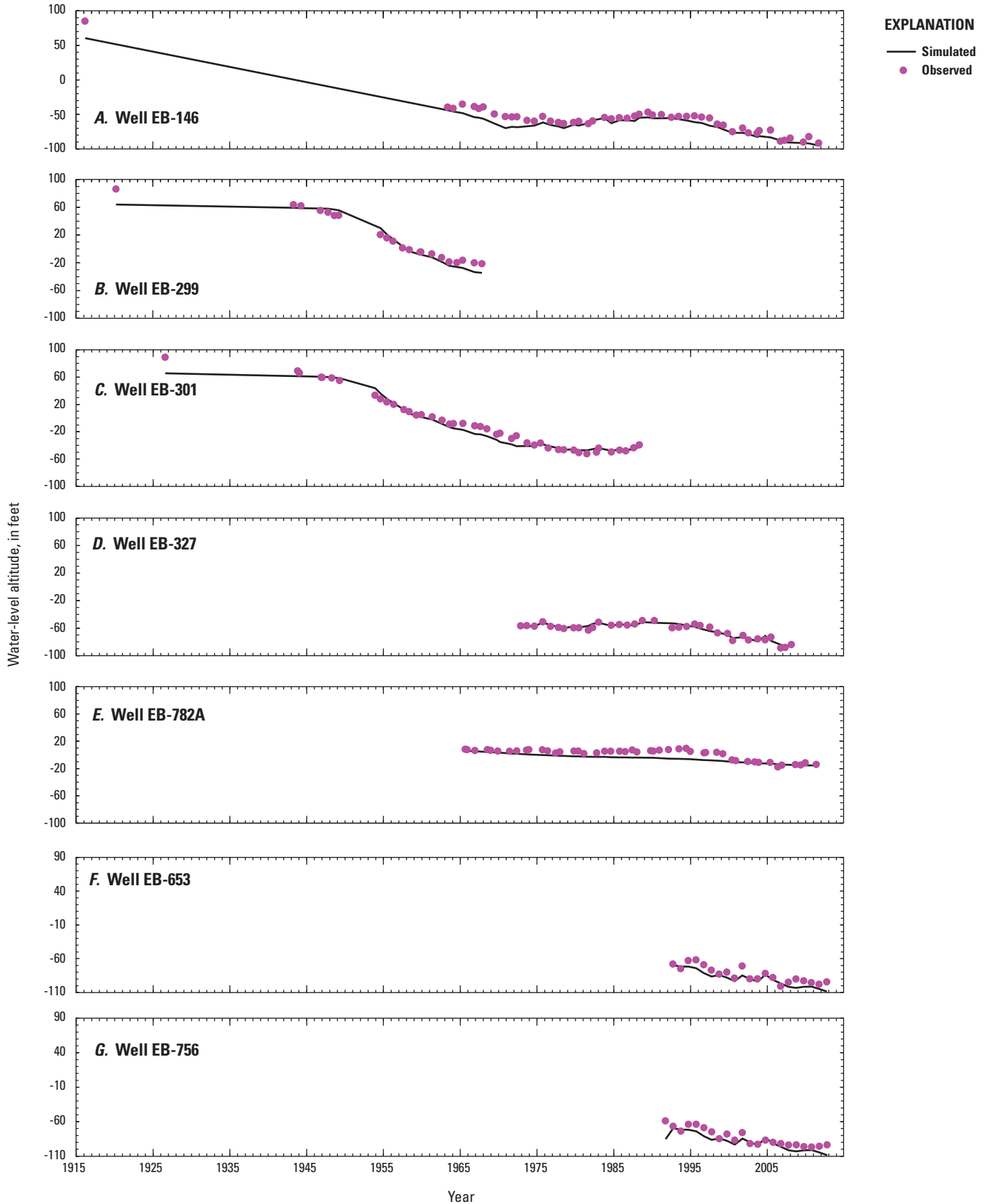
Figure 13. Simulated and observed water-level altitudes within the "1,200-foot" sand of the Baton Rouge area in southeastern Louisiana. *A,* Well EB-146. *B,* Well EB-299. *C,* Well EB-301. *D,* Well EB-327. *E,* Well EB-782A. *F,* Well EB-653. *G,* Well EB-756.

Table 4.   Simulated steady-state and transient water budgets.

[SP, stress period; TS, time step; ft³/d, cubic feet per day; Mgal/d, million gallons per day]

Budget component		Steady-state SP 1 (pre-1940)		Transient SP 74, TS 5 (December 31, 2012)	
		ft³/d	Mgal/d	ft³/d	Mgal/d
In	Specified-head layer 1	8.7647×10^6	65.56	1.4497×10^7	108.45
	South row of layer 24	2.5432×10^5	1.90	8.6547×10^6	64.74
	Storage	0	0	1.8262×10^6	13.66
	Multinode wells	0	0	1.0499×10^5	0.79
Out	Specified-head layer 1	8.3168×10^6	62.21	2.0746×10^6	15.52
	South row of layer 24	7.0176×10^5	5.25	0	0
	Storage	0	0	2.4519×10^3	0.02
	Multinode wells	0	0	2.3006×10^7	172.10
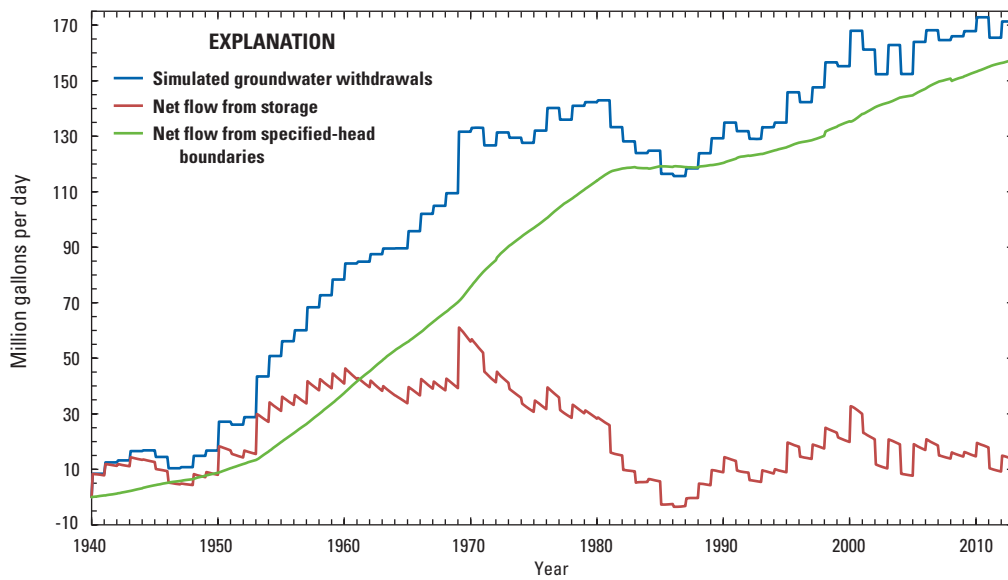
Figure 14.   Simulated groundwater withdrawals and flows from storage and specified-head boundaries.

Simulated Concentrations

The concentration of the chloride source to the "1,200-foot" sand is unknown and was estimated during model calibration. A simulated chloride-source concentration of 5,300 mg/L produced the best overall fit of simulated concentrations to concentrations observed in the "1,200-foot" sand. Simulated chloride concentrations at the centers of model cells containing chloride observation well screens were used to generate the simulated chlorographs (fig. 15). Two factors complicated simulation of the concentrations observed in observation well EB-621 (fig. 15*D*), the screen of which is located about 100 ft north of the Baton Rouge Fault. First, although the precise location of the Baton Rouge Fault at the "1,200-foot" sand depth is somewhat uncertain, it was defined along the finite-difference cell interfaces nearest to its presumed location. Because the finite-difference grid cell spacing is 500 ft in this area, the error inherent in the simulated fault location is likely on the order of 250 ft. Second, the steep, simulated concentration gradient near the north side of the Baton Rouge Fault causes a large difference in simulated concentration among the four model cells surrounding the simulated location of observation well EB-621. Therefore, the concentrations simulated for the four cells around observation well EB-621 were averaged to generate the simulated concentration for this well (fig. 15*D*).

Among the chloride observation wells in the "2,000-foot" sand, EB-1150 and EB-630 are production wells. Well EB-1150 has a screen-interval length of 56 ft, and EB-630 has two screened intervals that are 50 ft and 105 ft in length. The measured chloride-concentration fluctuations over time in both of these wells (fig. 16) are difficult to simulate while maintaining relatively parsimonious initial and boundary conditions and transport-model parameter distributions. The simulated concentrations at these locations were therefore fit in the middle of the range of the observed concentration fluctuations. Although the most recent chloride-concentration observation in well EB-807B, located about 0.7 mi north of well EB-871, was made in 1998, the relatively low concentrations measured before that time provide a useful constraint on model parameters affecting the transport of the saline water in a northerly direction away from source areas near EB-781 and the Baton Rouge Fault. Chloride concentrations immediately north of the fault are as high as 5,120 mg/L and rapidly decline to the north between wells EB-781 and EB-807B (fig. 17).

Limitations and Appropriate Use of the Model

The groundwater model was designed and calibrated primarily to simulate groundwater flow and saltwater transport in the "1,200-foot" sand and "2,000-foot" sand of the Baton Rouge area. Because the model layering was designed to represent the most important hydrogeologic units of the aquifer system and water-level observations from all aquifers in the Baton Rouge area were used for model calibration, groundwater flow within the "1,000-foot" sand, "1,500-foot" sand, "1,700-foot" sand, "2,400-foot" sand, and "2,800-foot" sand is also reasonably well simulated. It is possible to simulate the effects of potential changes in groundwater withdrawals on groundwater levels in each of these sands in the Baton Rouge area. Predictions of changes in water levels in the "1,200-foot" sand and "2,000-foot" sand that might result from changes such as those described in the "Scenarios To Mitigate Saltwater Migration" section of this report are examples of appropriate uses of the model. The predevelopment period (before 1940) was simulated with a steady-state solution of the flow equation, during which transient effects of any minor groundwater withdrawals were not simulated.

Chloride concentrations within the "1,200-foot" sand and "2,000-foot" sand in the Baton Rouge area were used to calibrate the model; consequently, saltwater encroachment in other aquifers in the Baton Rouge area is not simulated. Predictions of changes in chloride concentrations within either the "1,200-foot" sand or the "2,000-foot" sand that might result from changes such as those described in the "Scenarios To Mitigate Saltwater Migration" section of this report are an appropriate use of the model. Predictions of changes in chloride concentrations within other aquifers are not appropriate because the model was not calibrated to chloride-concentration observations within other aquifers.

The variably spaced finite-difference model grid enabled fine discretization with greater numerical accuracy in the Baton Rouge area and coarse and large aspect ratio (long side divided by short side) with less numerical accuracy in the surrounding areas. Water levels predicted for areas with either very coarse or very large aspect-ratio model cells will be less accurate and should be used judiciously.
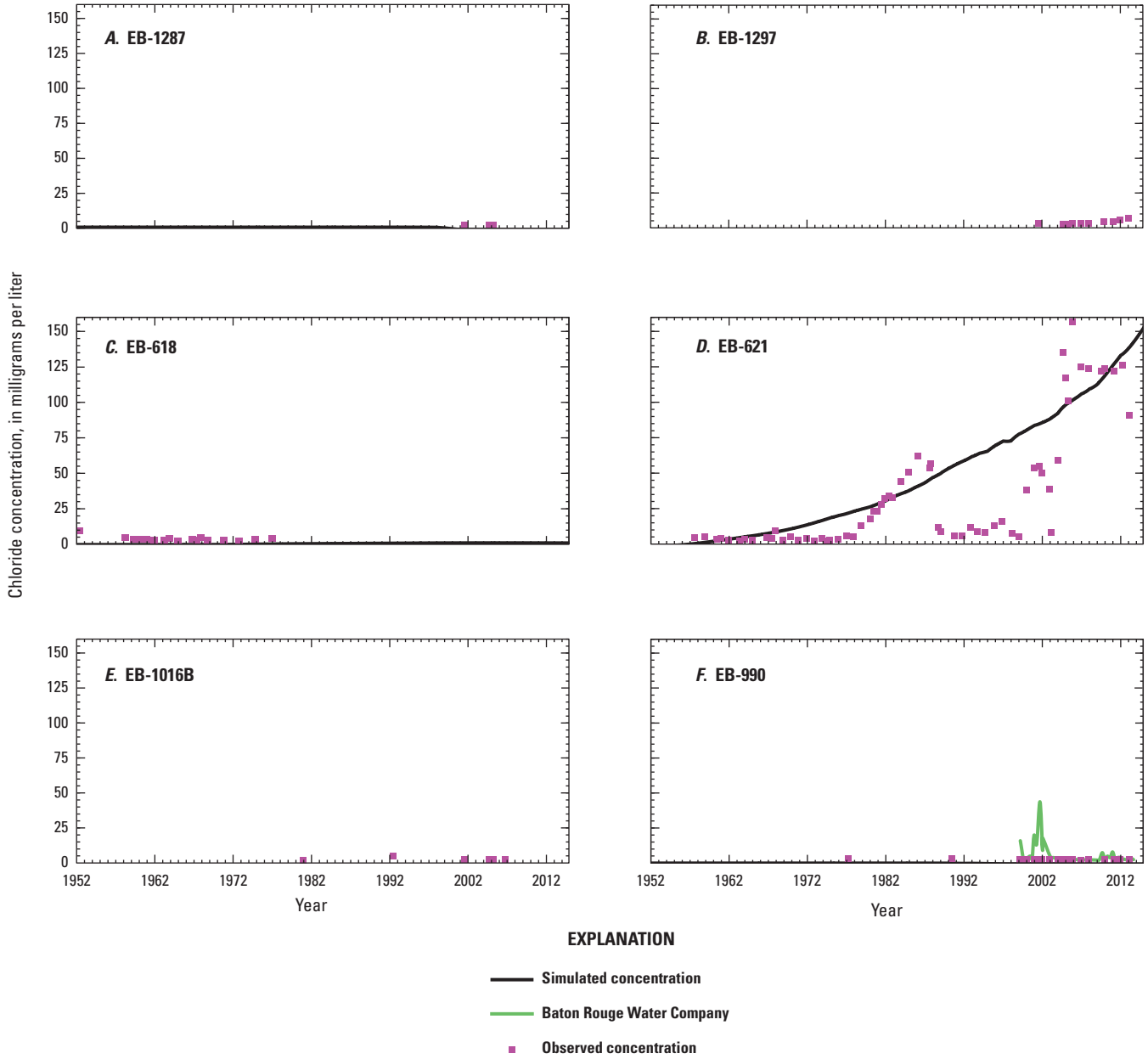
Figure 15.   Simulated and observed chloride concentrations at observation wells within the "1,200-foot" sand of the Baton Rouge area in southeastern Louisiana. *A*, Well EB-1287. *B*, Well EB-1297. *C*, Well EB-618. *D*, Well EB-621. *E*, Well EB-1016B. *F*, Well EB-990.
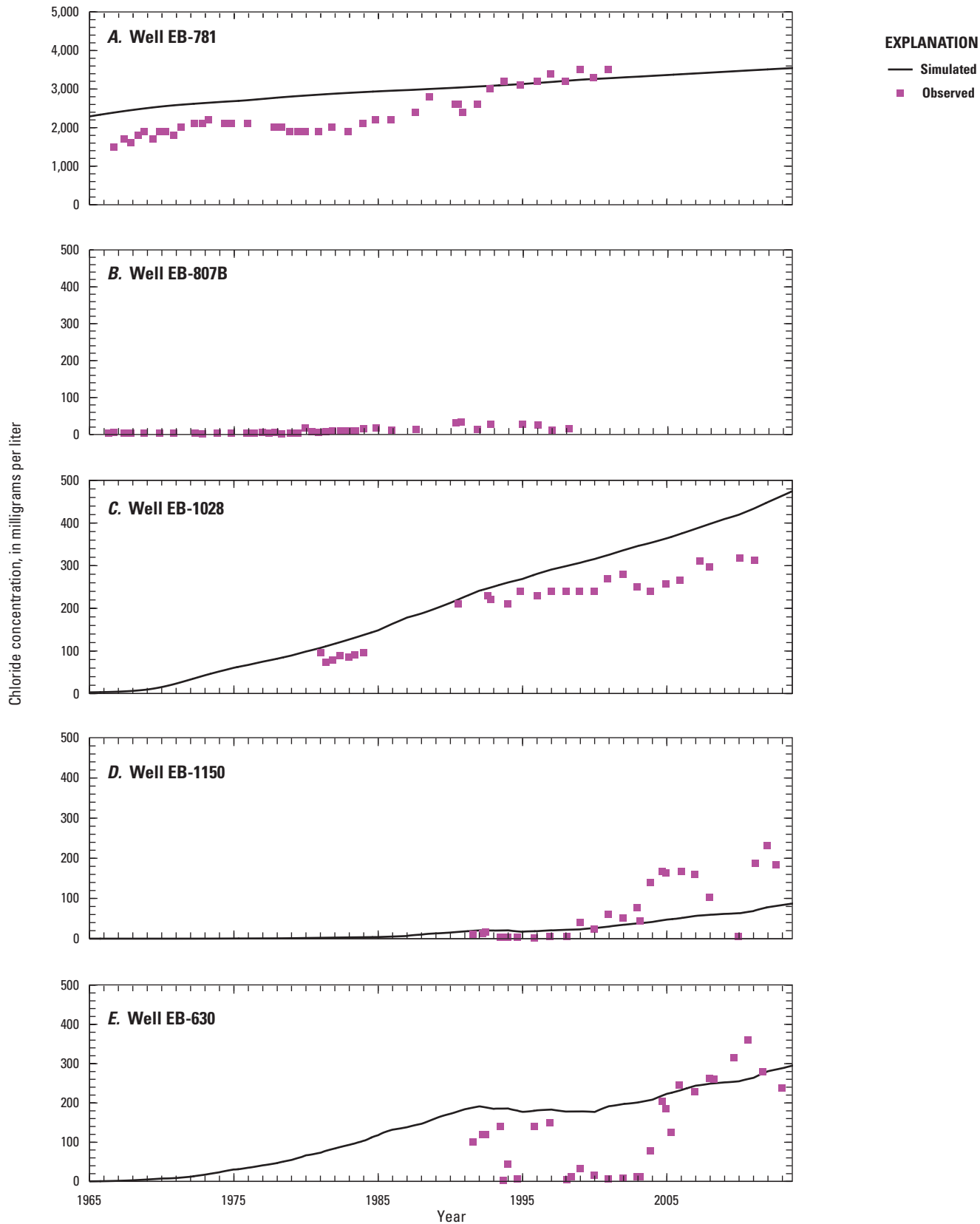
Figure 16.   Simulated and observed chloride concentrations at observation wells within the "2,000-foot" sand of the Baton Rouge area in southeastern Louisiana. *A*, Well EB-781. *B*, Well EB-807B. *C*, Well EB-1028. *D*, Well EB-1150. *E*, Well EB-630.
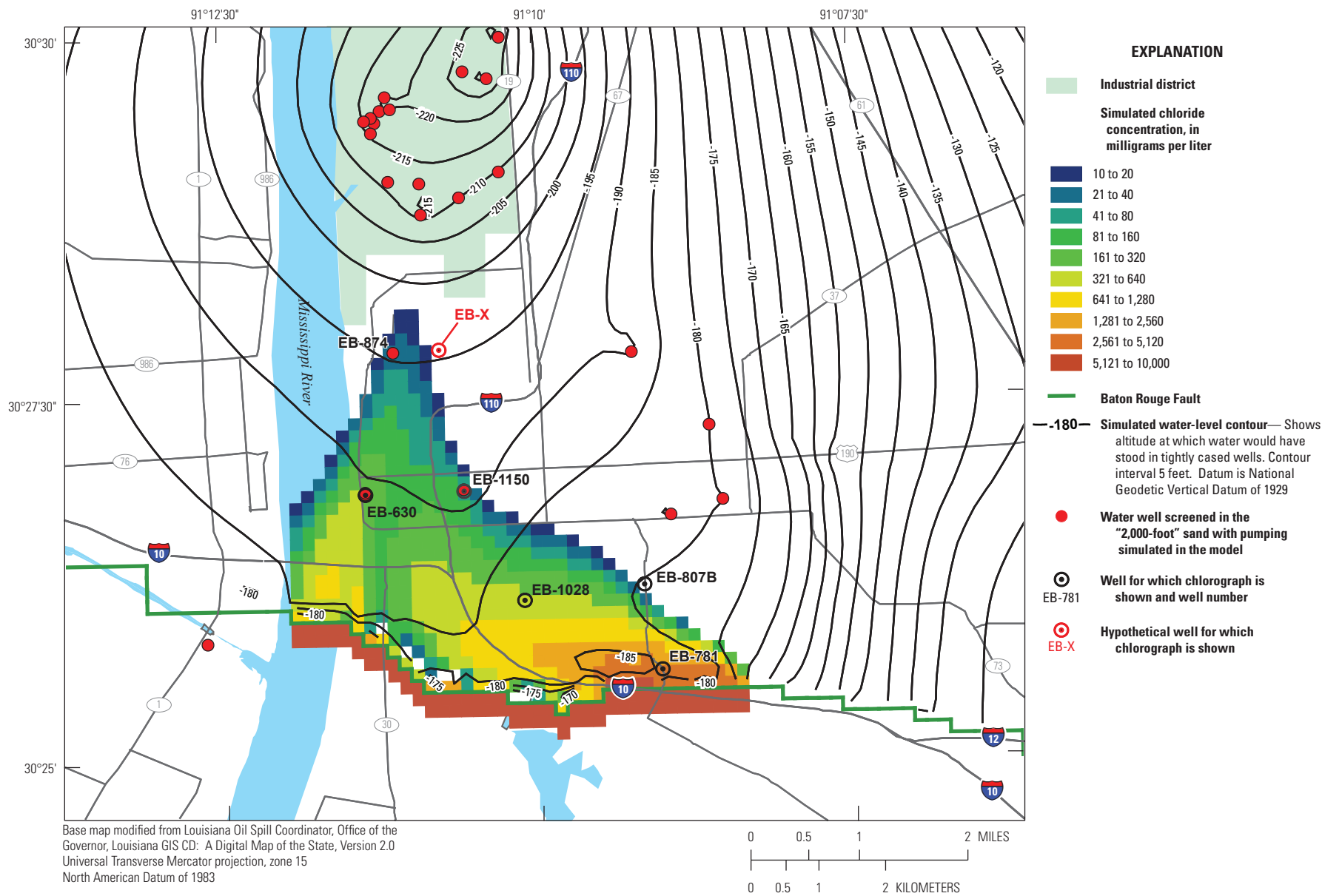
Figure 17. Simulated 2012 water levels and chloride concentrations at the base of the "2,000-foot" sand of the Baton Rouge area in the detailed model area in southeastern Louisiana.

Scenarios To Mitigate Saltwater Migration

Seven hypothetical groundwater-management scenarios were formulated to evaluate the effects of modifying groundwater withdrawals on future groundwater levels and saltwater concentrations from 2013 through 2112. Maps showing predicted water levels and chloride concentrations in 2047 and 2112 are presented for each scenario. The first (scenario 1) represents the effects of continued, or "status quo," groundwater withdrawals at 2012 rates and serves as a base case for comparison with the other scenarios in which various changes were simulated. Scenario 2 predicts the effects of increased withdrawals from selected wells screened in the "1,200-foot" sand on future groundwater levels and chloride concentrations in that sand. The remaining five scenarios, 3 through 7, simulate the effects of various pumping schemes on future groundwater levels and chloride concentrations in the "2,000-foot" sand and incorporate a hypothetical new public-supply well within the industrial district withdrawing 1.9 Mgal/d. In all of the scenarios, 2012 groundwater-withdrawal rates are specified for the 2-year period from 2013 through 2014. All modifications to simulated pumping rates begin in 2015, with the exception of withdrawals simulated to begin in 2017 from the "scavenger well" that is designed to extract salty water from the base of the "2,000-foot" sand. Two alternative pumping rates from the scavenger well are simulated in scenarios 4 and 7, which are denoted with the suffix "a" or "b" in their respective scenario descriptions and associated figures. Water levels at specified-head boundaries in the top model layer remained at the 2004 levels until 2112 in all of the scenarios.

Scenario 1: Continued Groundwater Withdrawals at 2012 Rates

Continuation of the "status quo" groundwater withdrawals was simulated by using the 2012 withdrawal rates for an additional 100 years (2013–2112). Contours of predicted water levels within the "1,200-foot" sand for 2047 (fig. 18) are similar to those simulated for 2012 (fig. 12) but are about 10 ft lower in the industrial district and about 5 ft lower in other parts of the detailed model area. The leading edge of the saltwater plume is predicted to migrate a maximum of about 1 mi north of the Baton Rouge Fault in 35 years.

By 2112, predicted water levels within the "1,200-foot" sand (fig. 19) are almost identical to the 2047 levels (fig. 18), indicating that the simulated groundwater system was close to hydraulic equilibrium by 2047. Between 2047 and 2112, the plume of saltwater continued to migrate northward toward the cone of depression in the industrial area, and the leading edge reached a distance of about 2 mi north of the Baton Rouge Fault.

In the "2,000-foot" sand, water levels for 2047 (fig. 20) are generally about 8 ft lower than during 2012 (fig. 17) in the detailed model area. The lowest water-level altitudes, about -240 ft, are predicted in the industrial district for 2047 compared to about -235 in the 2012 simulation. Comparison of the predicted chloride-concentration distributions in layer 20 for years 2047 (fig. 20) and 2012 (fig. 17) indicates that the portion of the saltwater plume containing chloride concentration in the 161- to 320-mg/L range at the base of the "2,000-foot" sand would migrate approximately 0.6 mi northward toward the industrial district. The area of the plume containing concentrations above background levels (10 mg/L) at the base of the "2,000-foot" sand north of the Baton Rouge Fault would increase by about 20 percent (table 5).

By 2112, predicted water levels within the "2,000-foot" sand (fig. 21) are within about a foot of the 2047 levels (fig. 20), indicating that the simulated groundwater system was close to hydraulic equilibrium by 2047. Between 2047 and 2112, the saltwater plume continues to migrate northward toward the cone of depression in the industrial area, and chloride concentrations increase at most observation wells (fig. 22), except possibly near well EB-807B.

EXPLANATION

Industrial district

Predicted chloride concentration, in milligrams per liter
- 10 to 20
- 21 to 40
- 41 to 80
- 81 to 160
- 161 to 320
- 321 to 640
- 641 to 1,280
- 1,281 to 2,560
- 2,561 to 5,120
- 5,121 to 10,000

Baton Rouge Fault

—-60— **Predicted water-level contour**—Shows altitude at which water would have stood in tightly cased wells. Contour interval 5 feet. Datum is National Geodetic Vertical Datum of 1929

● **Water well screened in the "1,200-foot" sand with pumping simulated in the model**

Base map modified from Louisiana Oil Spill Coordinator, Office of the Governor, Louisiana GIS CD: A Digital Map of the State, Version 2.0
Universal Transverse Mercator projection, zone 15
North American Datum of 1983

Figure 18. Predicted 2047 water levels and chloride concentrations in the "1,200-foot" sand of the Baton Rouge area in the detailed model area in southeastern Louisiana after continued pumping at 2012 rates (scenario 1).
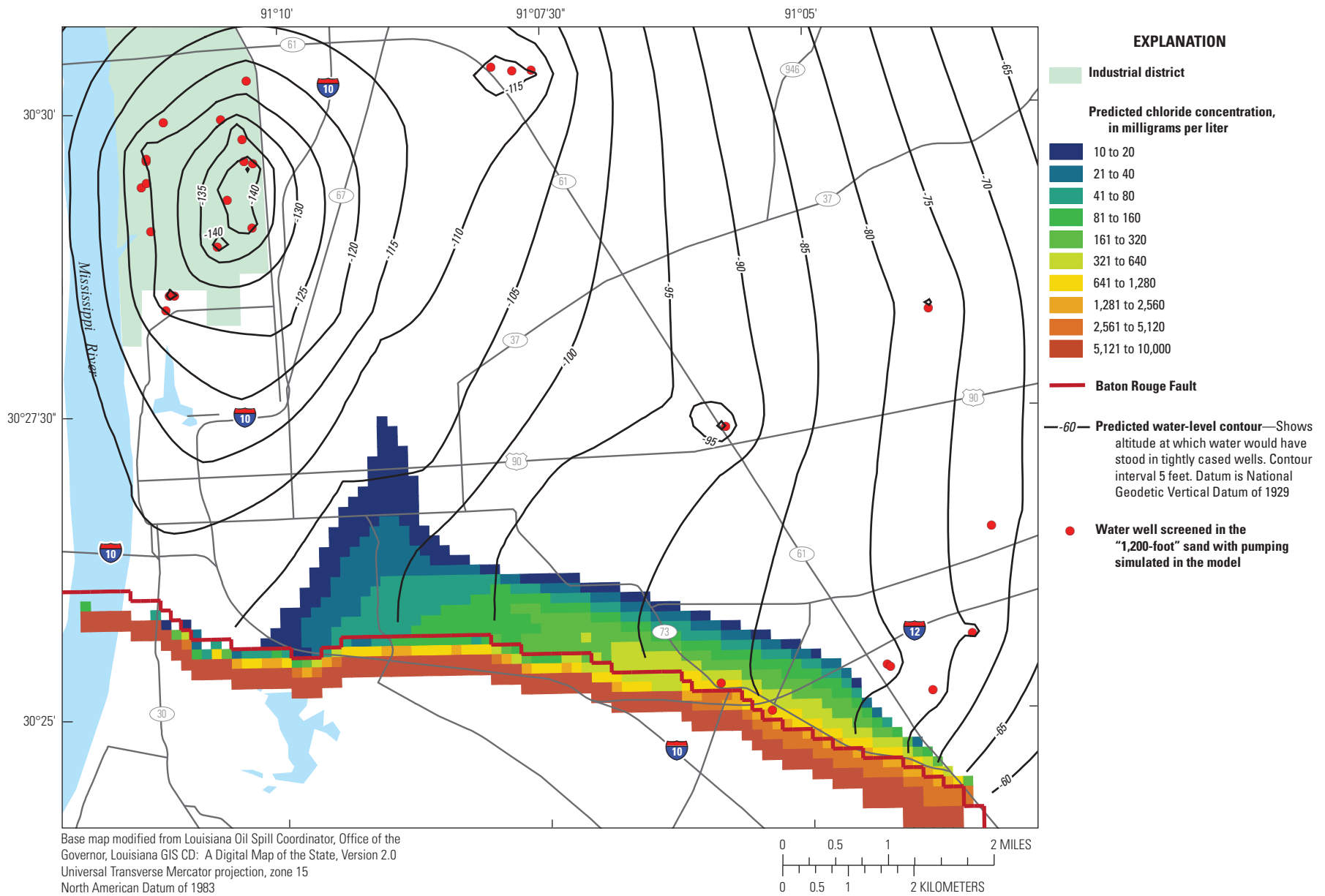
Figure 19. Predicted 2112 water levels and chloride concentrations in the "1,200-foot" sand of the Baton Rouge area in the detailed model area in southeastern Louisiana after continued pumping at 2012 rates (scenario 1).
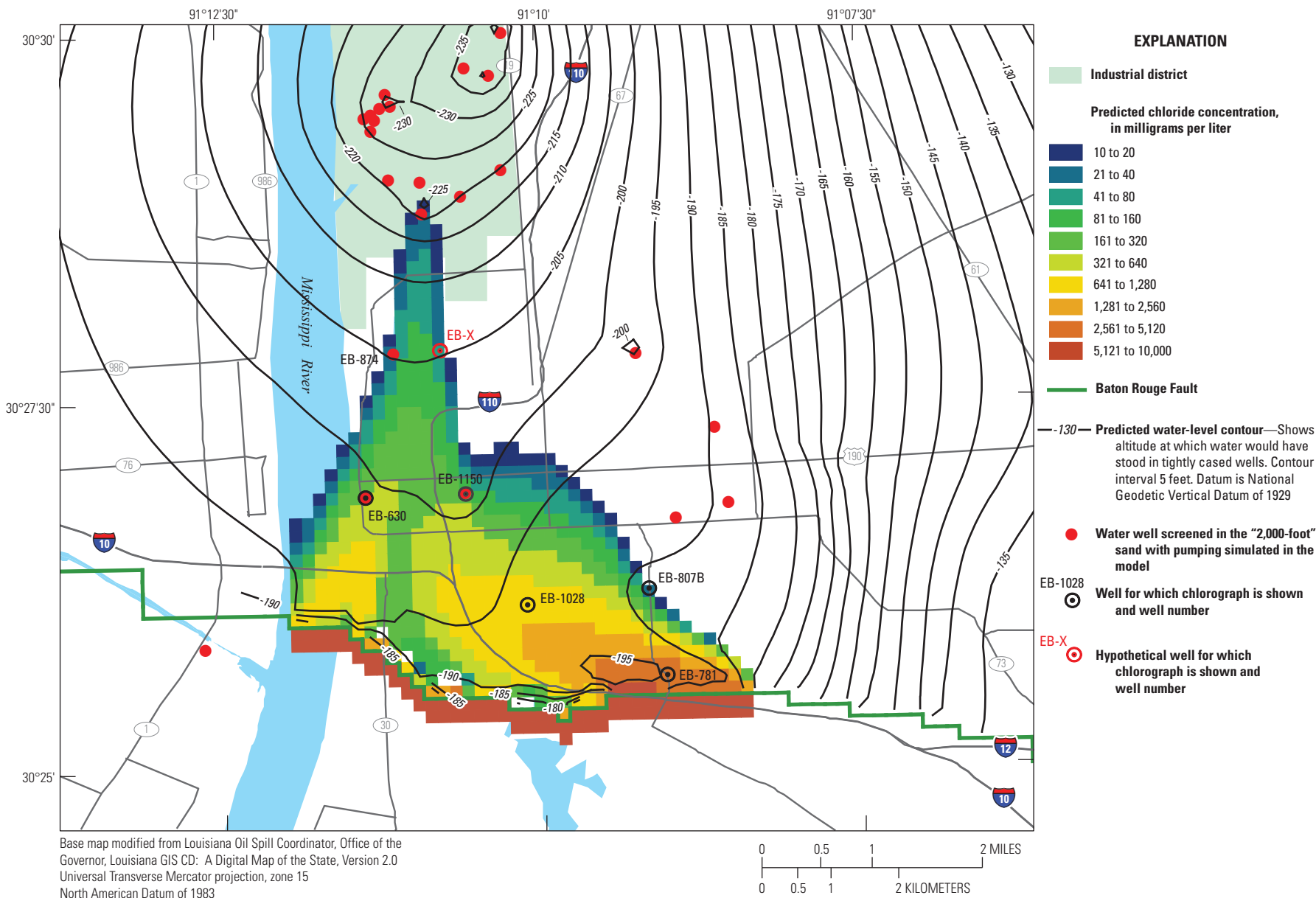
Figure 20. Predicted 2047 water levels and chloride concentrations at the base of the "2,000-foot" sand of the Baton Rouge area in the detailed model area in southeastern Louisiana after continued pumping at 2012 rates (scenario 1).

Table 5. Plume area and average chloride concentrations simulated for 2012 and predicted for 2047 at the base of the "2,000-foot" sand (layer 20).

[mi², square miles; mg/L, milligrams per liter]

Date and (or) scenario	Plume area (mi²)	Mean layer 20 cell chloride concentration (mg/L)	Median layer 20 cell chloride concentration (mg/L)
2012	4.84	575	253
2047: Scenario 1	5.84	626	302
2047: Scenario 3	5.26	656	357
2047: Scenario 4a	4.32	600	178
2047: Scenario 4b	4.65	637	296
2047: Scenario 5	5.19	663	348
2047: Scenario 6	5.19	675	325
2047: Scenario 7a	4.29	597	109
2047: Scenario 7b	4.62	631	189

Figure 21.   Predicted 2112 water levels and chloride concentrations at the base of the "2,000-foot" sand of the Baton Rouge area in the detailed model area in southeastern Louisiana after continued pumping at 2012 rates.
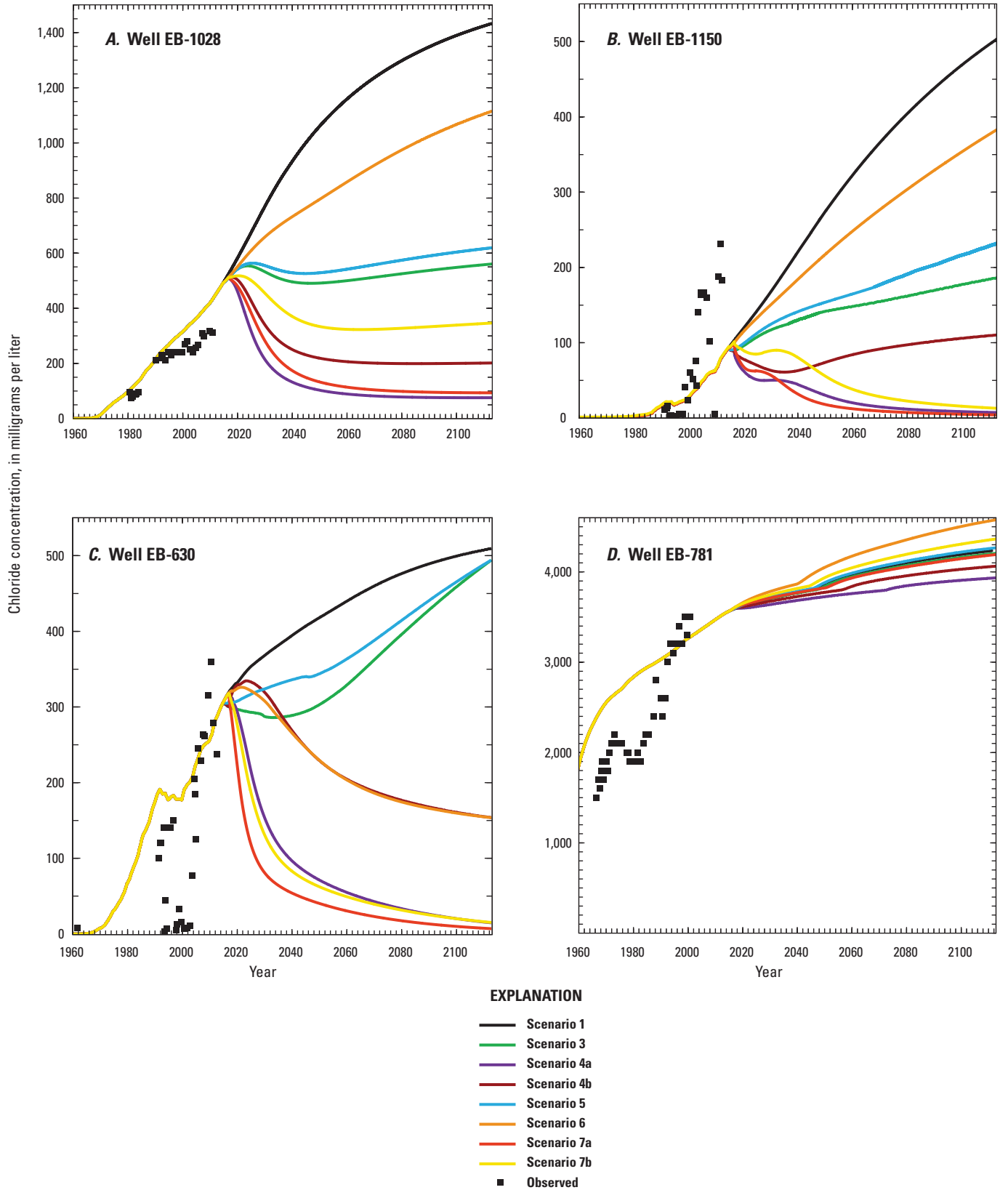
Figure 22.   Observed and predicted chloride concentrations at the base of the "2,000-foot" sand resulting from pumping rates specified for scenarios 1, 3, 4a, 4b, 5, 6, 7a, and 7b for observation wells and a scavenger well in the detailed model area in the Baton Rouge area in southeastern Louisiana. *A*, Well EB-1028. *B*, Well EB-1150. *C*, Well EB-630. *D*, Well EB-781. *E*, Well EB-807B. *F*, Well EB-X. *G*, Scavenger well.
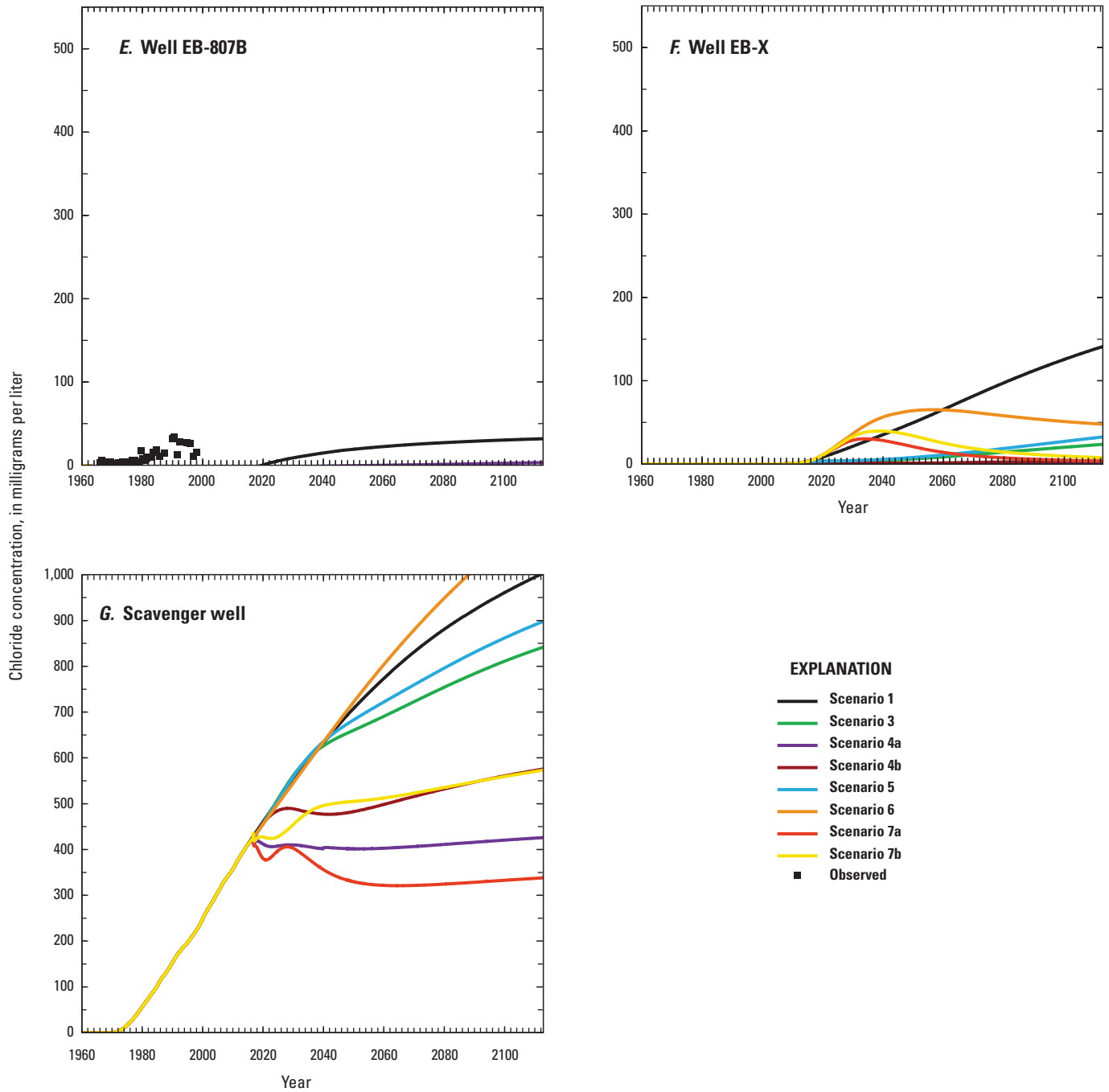
Figure 22. Observed and predicted chloride concentrations at the base of the "2,000-foot" sand resulting from pumping rates specified for scenarios 1, 3, 4a, 4b, 5, 6, 7a, and 7b for observation wells and a scavenger well in the detailed model area in the Baton Rouge area in southeastern Louisiana. *A*, Well EB-1028. *B*, Well EB-1150. *C*, Well EB-630. *D*, Well EB-781. *E*, Well EB-807B. *F*, Well EB-X. *G*, Scavenger well.—Continued

Scenario 2: Increased Groundwater Withdrawals From the "1,200-Foot" Sand

A net increase of 2.0 Mgal/d in groundwater withdrawals from the "1,200-foot" sand within the industrial district was simulated by increasing pumpage from two industrial-area wells (EB-567 and EB-1304) (see fig. 5 for well locations) by 1.0 Mgal/d, each beginning in 2015 while maintaining all other well withdrawals at the 2012 rates. Referenced to 2012 water levels (fig. 12), simulated water levels within the "1,200-foot" sand decline about 25 ft in the industrial district and about 10–15 ft elsewhere by 2047 (fig. 23). The migration of saltwater north of the Baton Rouge Fault within the "1,200-foot" sand is essentially the same as that predicted under scenario 1 for 2047 (fig. 18).

By 2112, predicted water levels within the "1,200-foot" sand (fig. 24) remain approximately equal to the 2047 levels (fig. 23), indicating that the groundwater system approached hydraulic equilibrium by 2047 under scenario 2. Between 2047 and 2112, the northward migration of the saltwater plume toward the cone of depression in the industrial area is similar to that of scenario 1 (fig. 19).

Scenario 3: Modification of Groundwater Withdrawals From the "2,000-Foot" Sand

A net decrease of 0.696 Mgal/d in groundwater withdrawals from the "2,000-foot" sand was simulated by discontinuing 1.889 Mgal/d of withdrawals from two public-supply wells (EB-151 and EB-733), commencing equivalent withdrawals from the "2,000-foot" sand at a hypothetical new public-supply well located north of the detailed model area in row 22 and column 34, discontinuing 0.696 Mgal/d of withdrawals from three industrial wells (EB-810, EB-851, and EB-884) (see fig. 6 for well locations), and keeping all other well withdrawals at the 2012 rates. Despite these withdrawal reductions, water levels are predicted to decline about 10 ft in the industrial district from 2012 levels (fig. 17) and about 5 ft in other parts of the detailed model area by 2047 (fig. 25). The predicted concentration of the chloride plume generally increases and continues to migrate northward, with concentrations up to about 80 mg/L predicted in the industrial district by 2047. The eastern edge of the chloride plume recedes about 0.2 mi westward, away from the location of the discontinued public-supply withdrawals. The predicted area of the plume for 2047 with a concentration above background levels (10 mg/L) is about 10 percent less than in scenario 1, and the median and mean cell concentrations within that area are slightly greater than those in scenario 1 (table 5).

By 2112, predicted water levels are less than 1 ft lower than the 2047 levels (figs. 25 and 26). The predicted concentration within the chloride plume increases, and the leading edge of the plume migrates about 1 mi further north into industrial district. The predicted chloride concentration is between 80 and 160 mg/L near the southernmost industrial wells.
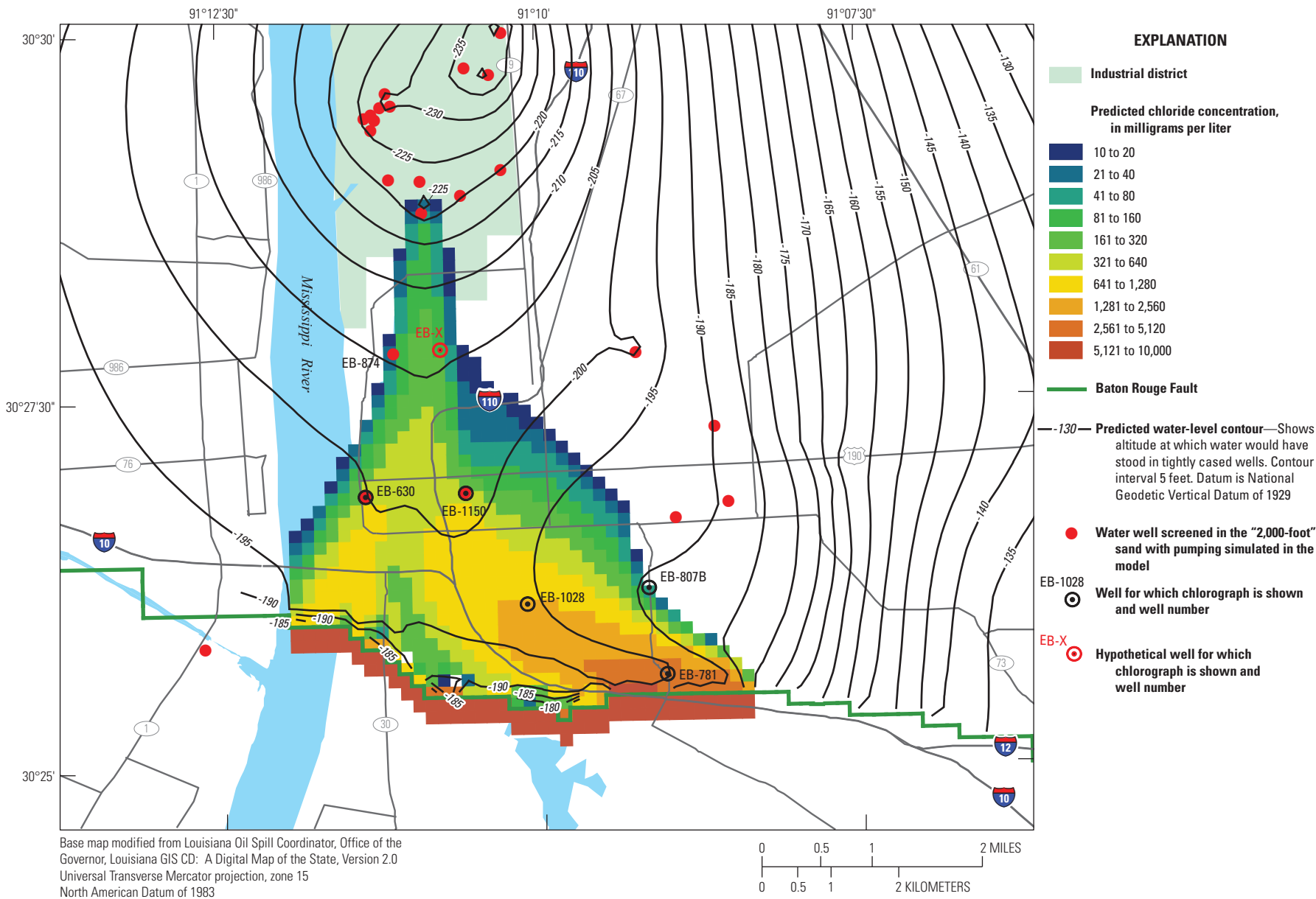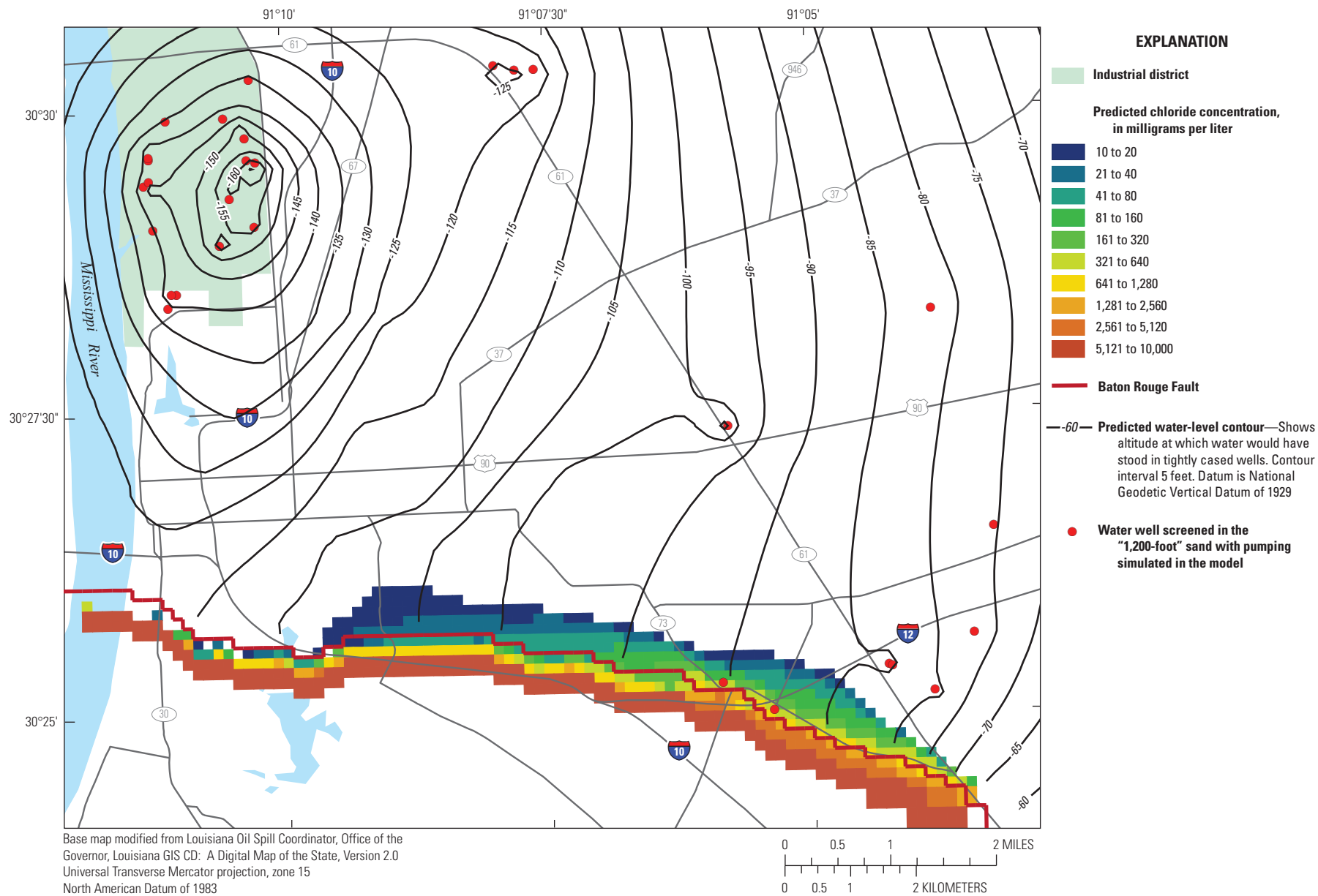
Figure 23. Predicted 2047 water levels and chloride concentrations in the "1,200-foot" sand of the Baton Rouge area in the detailed model area in southeastern Louisiana after a pumping increase (from 2012 rates) of 2 million gallons per day at selected wells in the Baton Rouge industrial district beginning in 2015 (scenario 2).
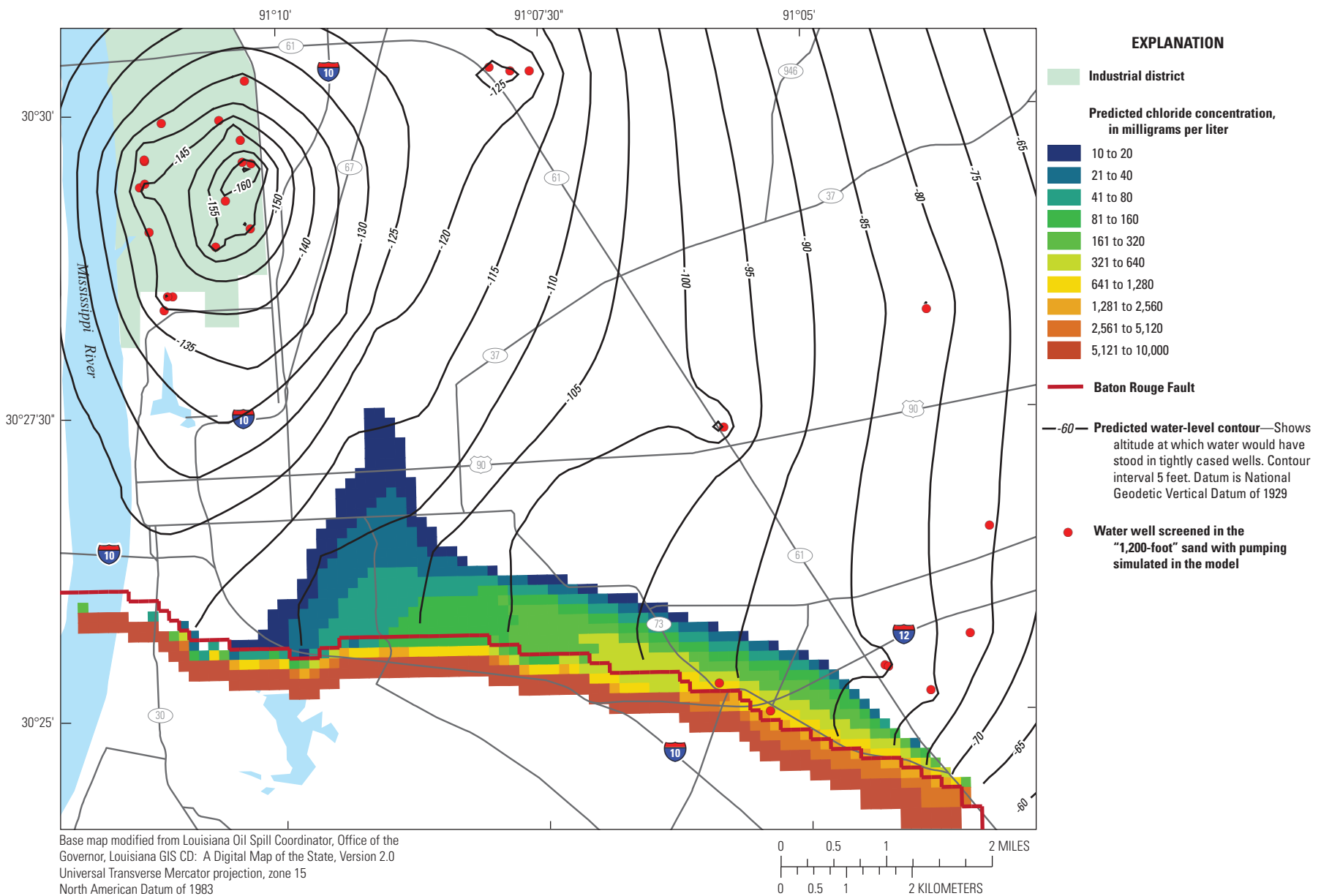
Figure 24. Predicted 2112 water levels and chloride concentrations in the "1,200-foot" sand of the Baton Rouge area in the detailed model area in southeastern Louisiana after a pumping increase (from 2012 rates) of 2 million gallons per day at selected wells in the Baton Rouge industrial district beginning in 2015 (scenario 2).
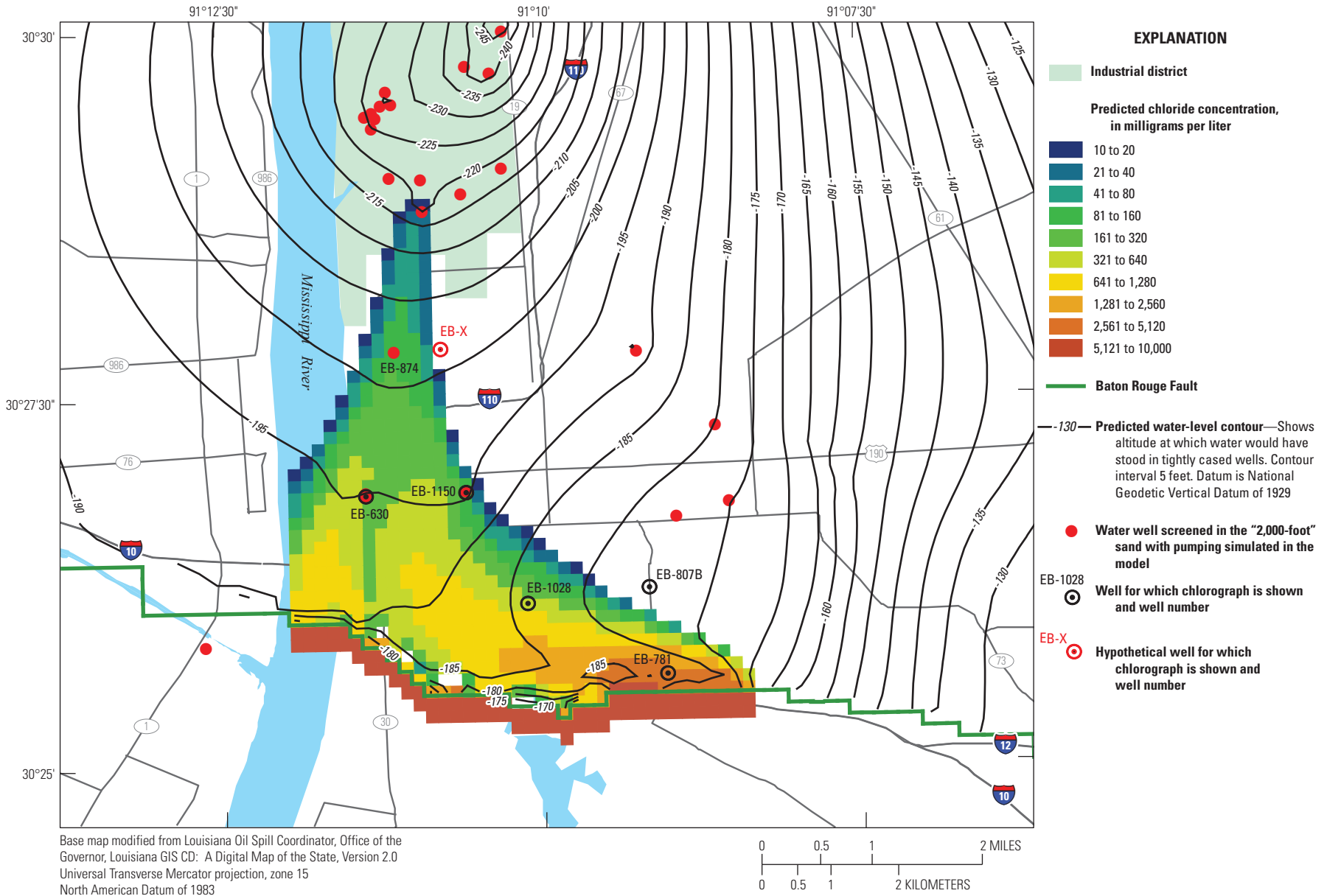
Figure 25. Predicted 2047 water levels and chloride concentrations at the base of the "2,000-foot" sand of the Baton Rouge area in the detailed model area in southeastern Louisiana after pumping is turned off at selected industrial and public-supply wells and a hypothetical public-supply well located north of the detailed model area in model row 22 and column 34 (see fig. 6) is turned on starting in 2015 (scenario 3).

Figure 26. Predicted 2112 water levels and chloride concentrations at the base of the "2,000-foot" sand of the Baton Rouge area in the detailed model area in southeastern Louisiana after pumping is turned off at selected industrial and public-supply wells and a hypothetical public-supply well located north of the detailed model area in model row 22 and column 34 (see fig. 6) is turned on starting in 2015 (scenario 3).

Scenario 4: Modification of Groundwater Withdrawals With Installation of a Scavenger Well in the "2,000-Foot" Sand

The installation of a scavenger well couplet was simulated in model row 64 and column 29 (fig. 6) with two wells: one screened in the upper portion and one screened in the bottom of the "2,000-foot" sand. The bottom well (screened in model layer 20) of the scavenger-well couplet is screened at the base of the "2,000-foot" sand where the saltier, denser water is simulated, and the upper well (screened in model layers 11–13) is screened toward the top of the aquifer where it may extract better quality water. Simultaneous withdrawals from both of these aquifer intervals preserve horizontal flow toward the scavenger-well couplet, thereby maintaining separation of the saltier and fresher fractions of water in that area of the aquifer. Two alternative total pumping rates from the scavenger-well couplet were simulated: 2.5 Mgal/d (scenario 4a) and 1.25 Mgal/d (scenario 4b). In scenario 4a, the withdrawals from the upper and lower wells were specified at 1.5 Mgal/d and 1.0 Mgal/d, respectively. The scavenger-well withdrawal rates were reduced by 50 percent for scenario 4b; withdrawals from the upper and lower wells were specified at 0.75 Mgal/d and 0.5 Mgal/d, respectively. The withdrawal rates from other industrial and public-supply wells were identical to those of scenario 3.

By 2047, the scavenger well had pumped at 2.5 Mgal/d for 31 years, and water levels are predicted to decline 20–25 ft in the industrial district and 15–20 ft (fig. 27) in other parts of the detailed model area compared to 2012 (fig. 20), except near the scavenger well, where a distinct cone of depression forms. Predicted chloride concentrations decrease in the plume north of the scavenger well, but the leading edge of the plume continues to migrate northward into the industrial district. In comparison to scenario 1, the plume recedes westward about 0.5 mi away from the area where public-supply withdrawals were reduced. Chloride concentrations increase within the plume between the scavenger well and the Baton Rouge Fault because the increased hydraulic gradient created by the scavenger-well pumping stress increases simulated advective

transport of chloride. Overall, the plume area decreases about 10 percent in comparison to its 2012 extent, causing the mean plume concentration to rise about 4 percent, yet the median cell concentration decreases by almost 30 percent (table 5).

By 2112, water levels remain at 2047 levels (figs. 27 and 28). The leading edge of the plume recedes southward more than 1 mi, and concentrations north of the scavenger well continue to decline compared to 2047 (fig. 27). Concentrations between the scavenger well and the Baton Rouge Fault remain similar to the concentrations predicted for 2047.

The rate of salt mass transport across the Baton Rouge Fault into the "2,000-foot" sand, the rate of extraction of salt mass through wells screened in this aquifer, and the net change of salt mass in the aquifer are affected by withdrawals from public-supply wells and the scavenger well (fig. 29). Beginning around 1980, some salt is withdrawn by wells pumping from the "2,000-foot" sand. The increased hydraulic gradient caused by commencement of scavenger-well withdrawals in 2017 initially increases the rate of salt transport across the fault; both the hydraulic gradient and transport rate decrease in subsequent years as hydraulic equilibrium is approached. The simulated scavenger well effectively withdraws salt from the aquifer and causes an order of magnitude decrease in the rate of salt accumulation in the aquifer.

For scenario 4b, the withdrawals from the scavenger well were one-half that of scenario 4a (1.25 Mgal/d). By 2047, predicted water levels within the "2,000-foot" sand are generally about 10 ft higher (fig. 30) than under scenario 4a (fig. 27) in the Baton Rouge area. The plume area remains about 8 percent larger than under scenario 4a for 2047 (table 5), within which the mean and median predicted chloride concentrations are also higher.

By 2112, predicted water levels have declined an additional 2 ft near the scavenger well but elsewhere are very close to their 2047 levels (figs. 30 and 31). In comparison to the effect of the higher scavenger-well pumping of scenario 4a, predicted water levels are about 10 ft higher in the Baton Rouge area, but higher chloride concentrations remain in the aquifer north of the scavenger well.
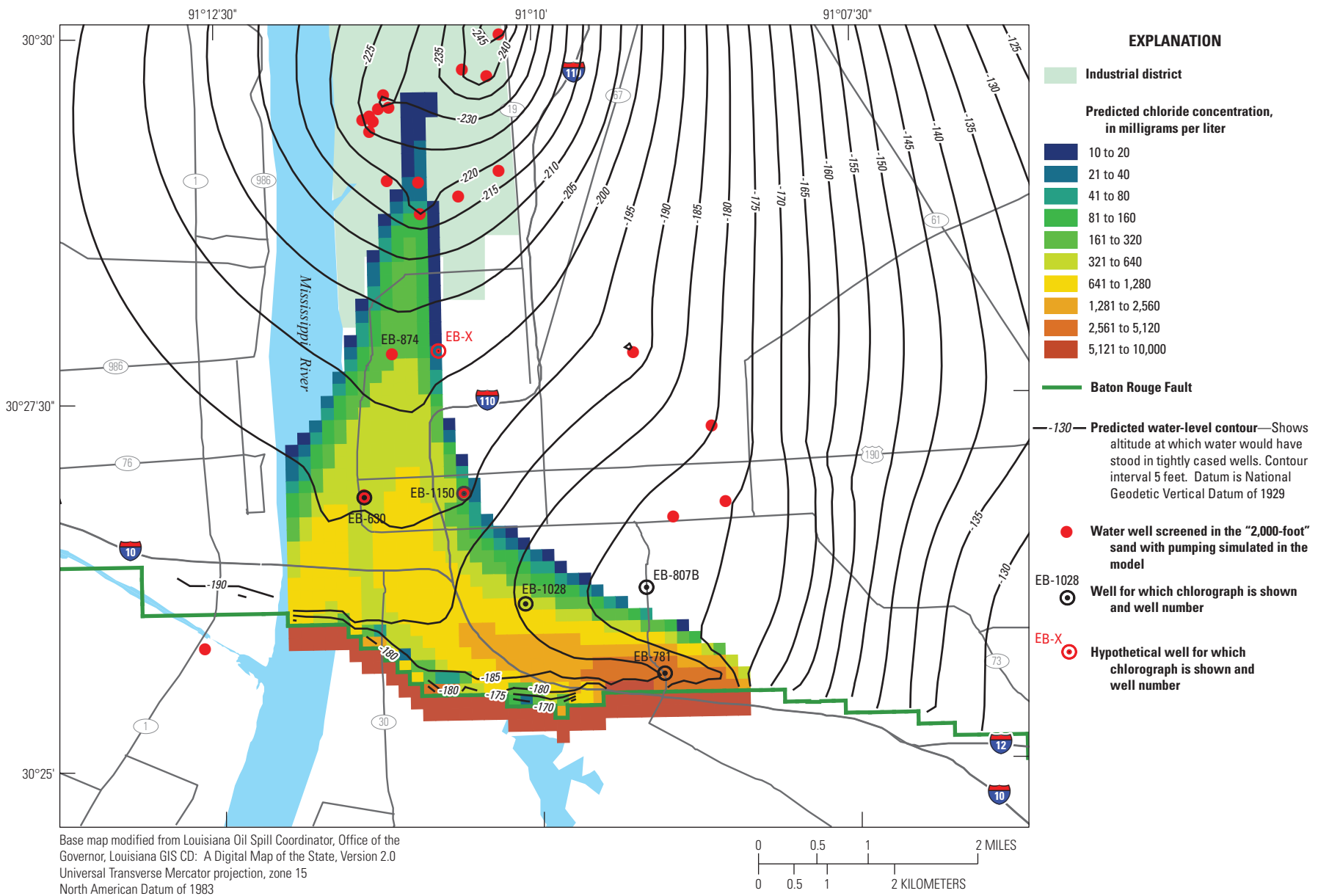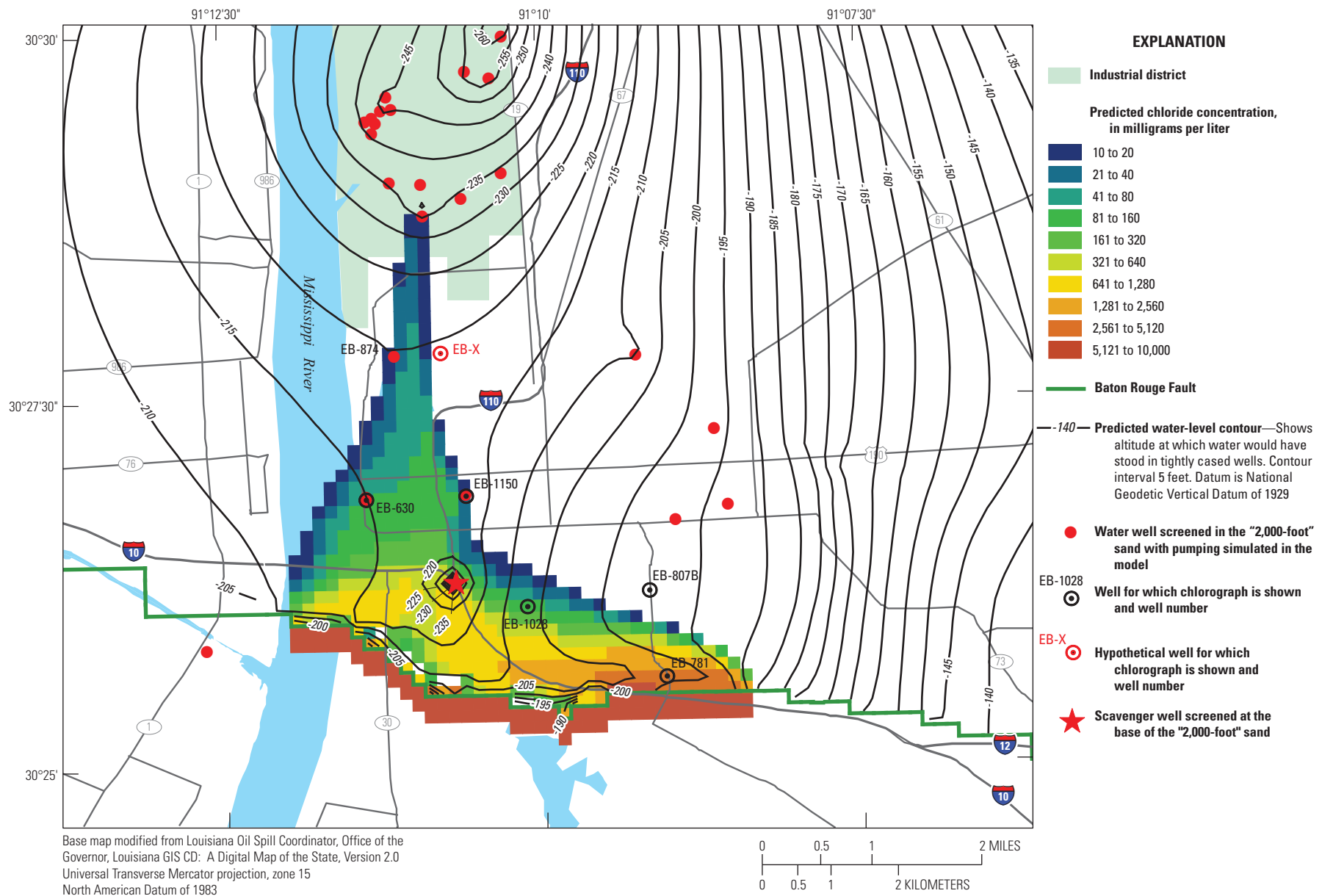
Figure 27. Predicted 2047 water levels and chloride concentrations at the base of the "2,000-foot" sand of the Baton Rouge area in the detailed model area in southeastern Louisiana after pumping is turned off at selected industrial and public-supply wells, a hypothetical public-supply well located north of the detailed model area in model row 22 and column 34 (see fig. 6) is turned on in 2015, and a scavenger well located in row 64 and column 29 pumps at 2.5 million gallons per day beginning in 2017 (scenario 4).
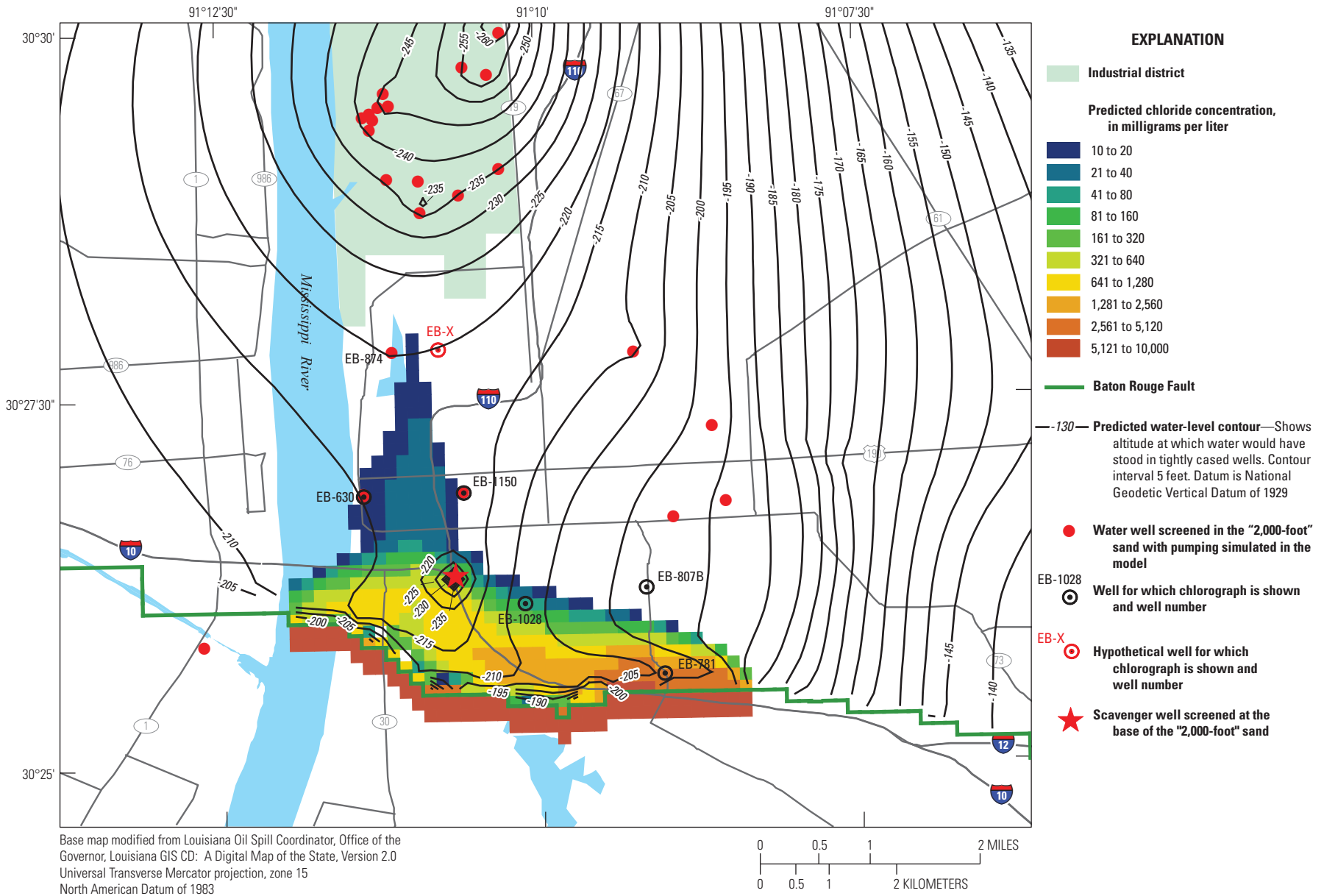
Figure 28. Predicted 2112 water levels and chloride concentrations at the base of the "2,000-foot" sand of the Baton Rouge area in the detailed model area in southeastern Louisiana after pumping is turned off at selected industrial and public-supply wells, a hypothetical public-supply well located north of the detailed model area in model row 22 and column 34 (see fig. 6) is turned on in 2015, and a scavenger well located in row 64 and column 29 pumps at 2.5 million gallons per day beginning in 2017 (scenario 4).
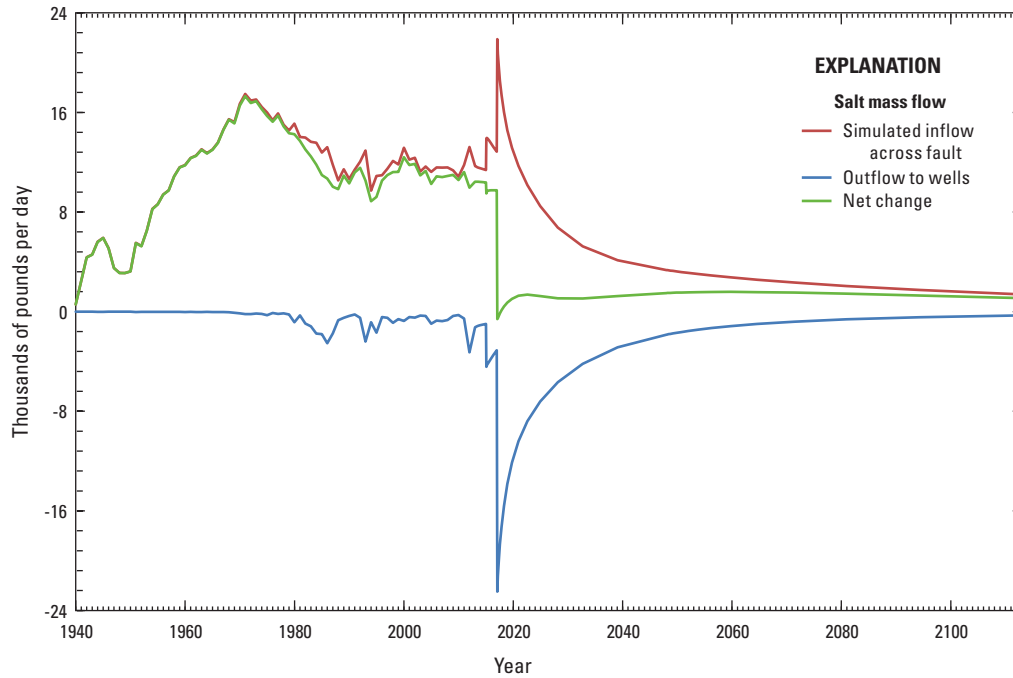
Figure 29.   Simulated inflow across fault, outflow to wells, and net change of salt mass in the "2,000-foot" sand of the Baton Rouge area north of the Baton Rouge Fault, 1940–2012, and predicted changes in salt mass, 2013–2112, after pumping changes are made at selected industrial and public-supply wells in 2015 and pumping at a rate of 2.5 million gallons per day from a simulated scavenger well begins in 2017 (scenario 4a).

EXPLANATION

Industrial district

Predicted chloride concentration, in milligrams per liter

- 10 to 20
- 21 to 40
- 41 to 80
- 81 to 160
- 161 to 320
- 321 to 640
- 641 to 1,280
- 1,281 to 2,560
- 2,561 to 5,120
- 5,121 to 10,000

Baton Rouge Fault

-130 — Predicted water-level contour—Shows altitude at which water would have stood in tightly cased wells. Contour interval 5 feet. Datum is National Geodetic Vertical Datum of 1929

Water well screened in the "2,000-foot" sand with pumping simulated in the model

EB-1028 Well for which chlorograph is shown and well number

EB-X Hypothetical well for which chlorograph is shown and well number

Scavenger well screened at the base of the "2,000-foot" sand

Base map modified from Louisiana Oil Spill Coordinator, Office of the Governor, Louisiana GIS CD: A Digital Map of the State, Version 2.0
Universal Transverse Mercator projection, zone 15
North American Datum of 1983

0   0.5   1   2 MILES

0   0.5   1   2 KILOMETERS

Figure 30. Predicted 2047 water levels and chloride concentrations at the base of the "2,000-foot" sand of the Baton Rouge area in the detailed model area in southeastern Louisiana after pumping is turned off at selected industrial and public-supply wells, a hypothetical public-supply well located north of the detailed model area in model row 22 and column 34 (see fig. 6) is turned on in 2015, and a scavenger well located in row 64 and column 29 pumps at 1.25 million gallons per day beginning in 2017 (scenario 4b).

Figure 31. Predicted 2112 water levels and chloride concentrations at the base of the "2,000-foot" sand of the Baton Rouge area in the detailed model area in southeastern Louisiana after pumping is turned off at selected industrial and public-supply wells, a hypothetical public-supply well located in model row 22 and column 34 is turned on in 2015, and a scavenger well located in row 64 and column 29 begins pumping at 1.25 million gallons per day in 2017 (scenario 4b).

Scenario 5: Reduction of Industrial Withdrawals From the "2,000-Foot" Sand

For scenario 5, the changes to groundwater withdrawals are similar to scenario 3, but an additional 1.678 Mgal/d of withdrawal reductions were specified from industrial wells by discontinuing withdrawals from three wells (EB-722, EB-856, and EB-587) while maintaining withdrawal from EB-851 at the 2012 rate (see fig. 6 for well locations), resulting in a net decrease of 2.222 Mgal/d from the total 2012 withdrawal rate. Overall, the predicted conditions are similar to those predicted under scenario 3. By 2047, predicted water levels increase about 15 ft throughout much of the detailed model area (fig. 32) compared to scenario 1 (fig. 20). The leading edge of the plume continues to migrate northward and reaches the southernmost industrial well but at a slower rate than in scenario 1, resulting in a plume area that is 11 percent smaller than scenario 1 in 2047 (table 5).

By 2112, water levels remain near 2047 levels (figs. 32 and 33). The chloride plume continues to migrate northward, but at a slightly lower rate than predicted in scenario 3 (fig. 25).

Scenario 6: Extensive Reduction of Industrial and Public-Supply Withdrawals From the "2,000-Foot" Sand

A net reduction of 7.344 Mgal/d in groundwater withdrawals from the "2,000-foot" sand with respect to 2012 rates was predicted by discontinuing withdrawals from two public-supply wells (EB-151 and EB-733) and seven industrial wells (EB-1317, EB-1323, EB-1313, EB-1309, EB-1151, EB-788, and EB-1227) and by commencing 1.889 Mgal/d of withdrawal from a hypothetical public-supply well located north of the detailed model area in model row 22 and column 34 (see fig. 6 for well locations).

By 2047, predicted water levels recover from 2012 levels (fig. 17) and are about 50 ft higher (fig. 34) in the industrial district and 35–40 ft higher in other parts of the detailed model area. Nevertheless, the leading edge of the plume continues to migrate northward, and low chloride concentrations (less than 40 mg/L) are predicted near the southernmost industrial wells. The area and average concentration of the predicted plume are similar to those in scenario 5 (table 5).

By 2112, predicted water levels remain very close to the predicted 2047 levels (figs. 34 and 35), indicating that the simulated system approached hydraulic equilibrium by 2047. Chloride concentrations do not change substantially near the industrial district, though concentrations closer to the Baton Rouge Fault continue to increase.
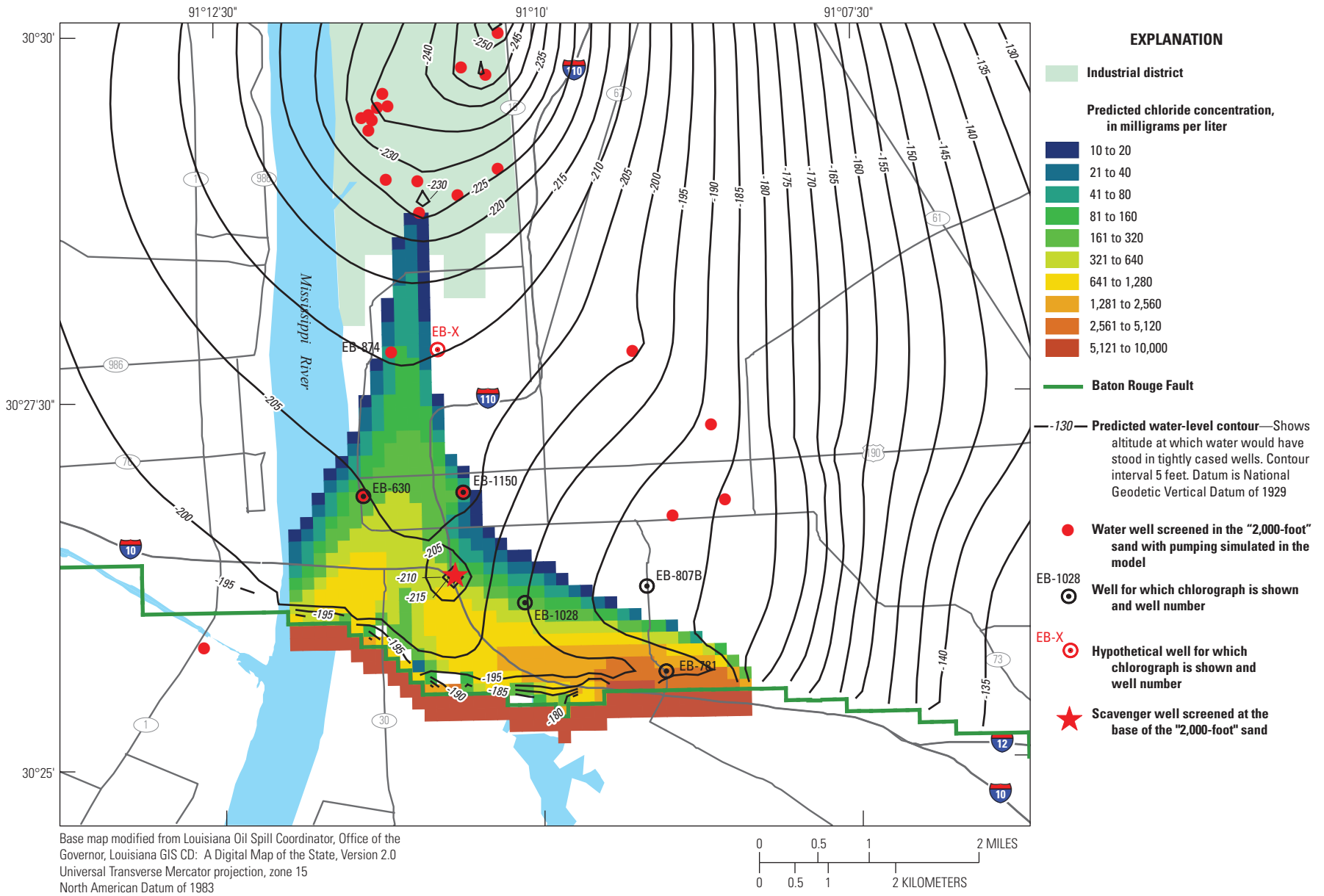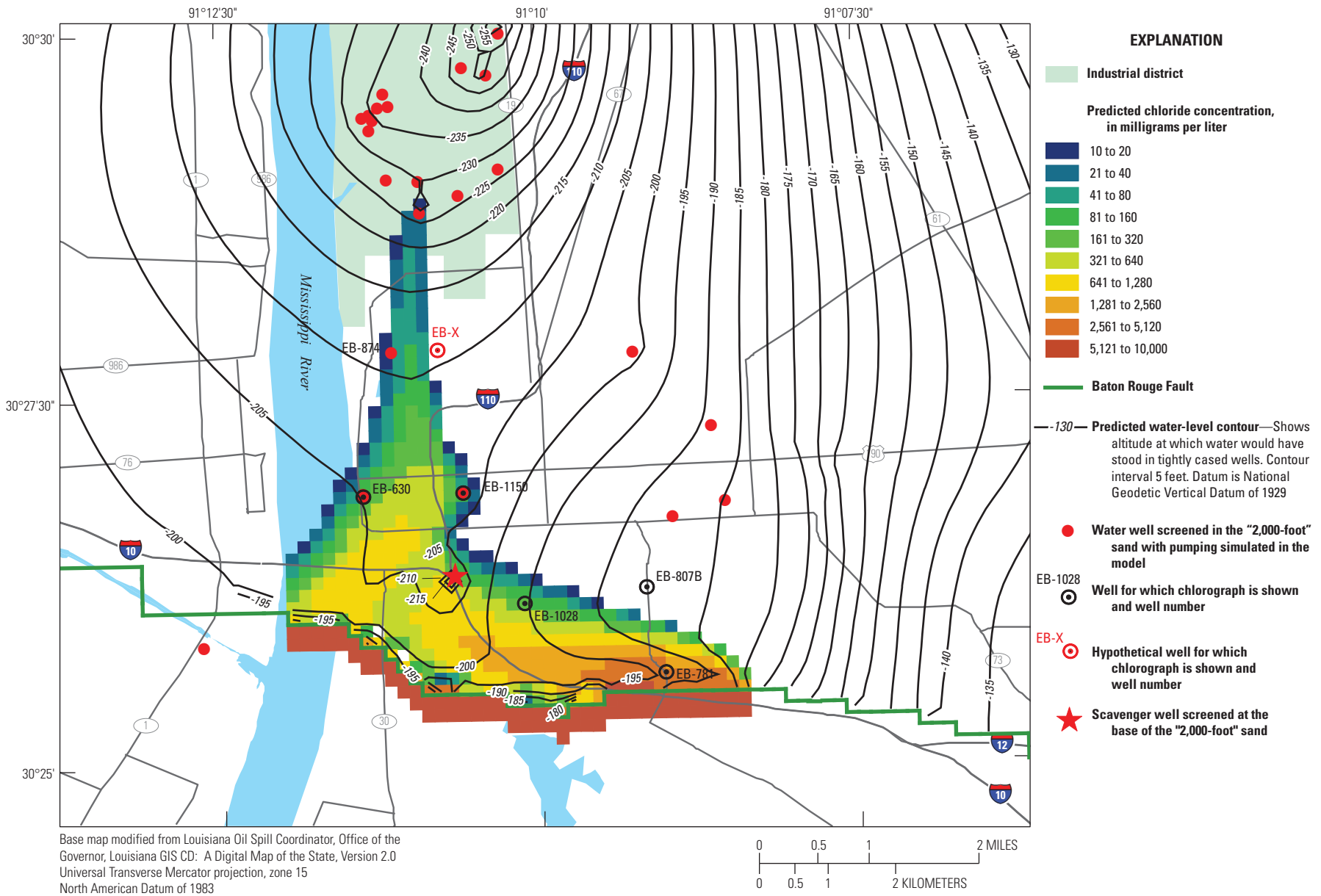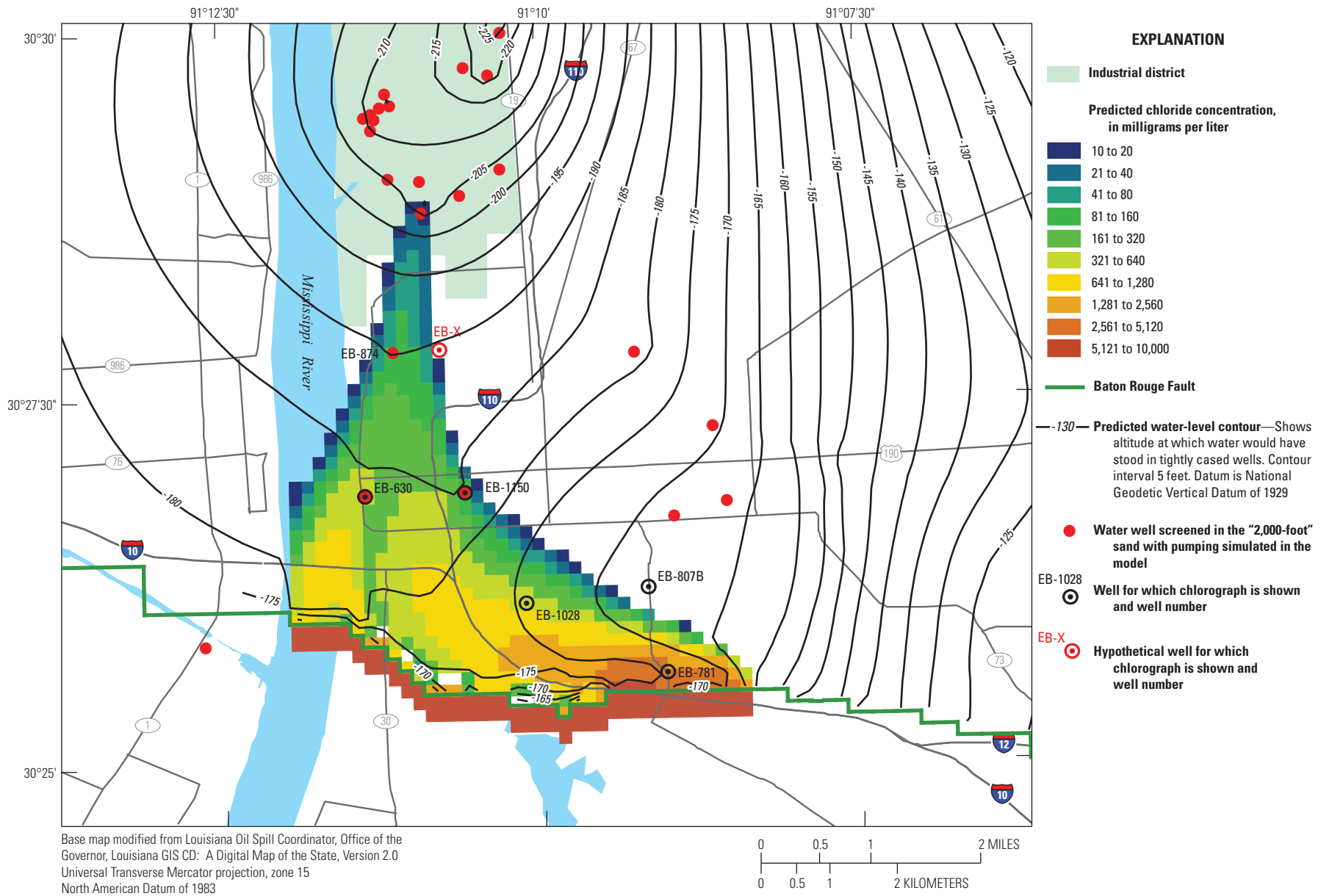
Figure 32. Predicted 2047 water levels and chloride concentrations at the base of the "2,000-foot" sand of the Baton Rouge area in the detailed model area in southeastern Louisiana after pumping is turned off at selected industrial and public-supply wells and a hypothetical public-supply well located north of the detailed model area in model row 22 and column 34 (see fig. 6) is turned on starting in 2015 (scenario 5).
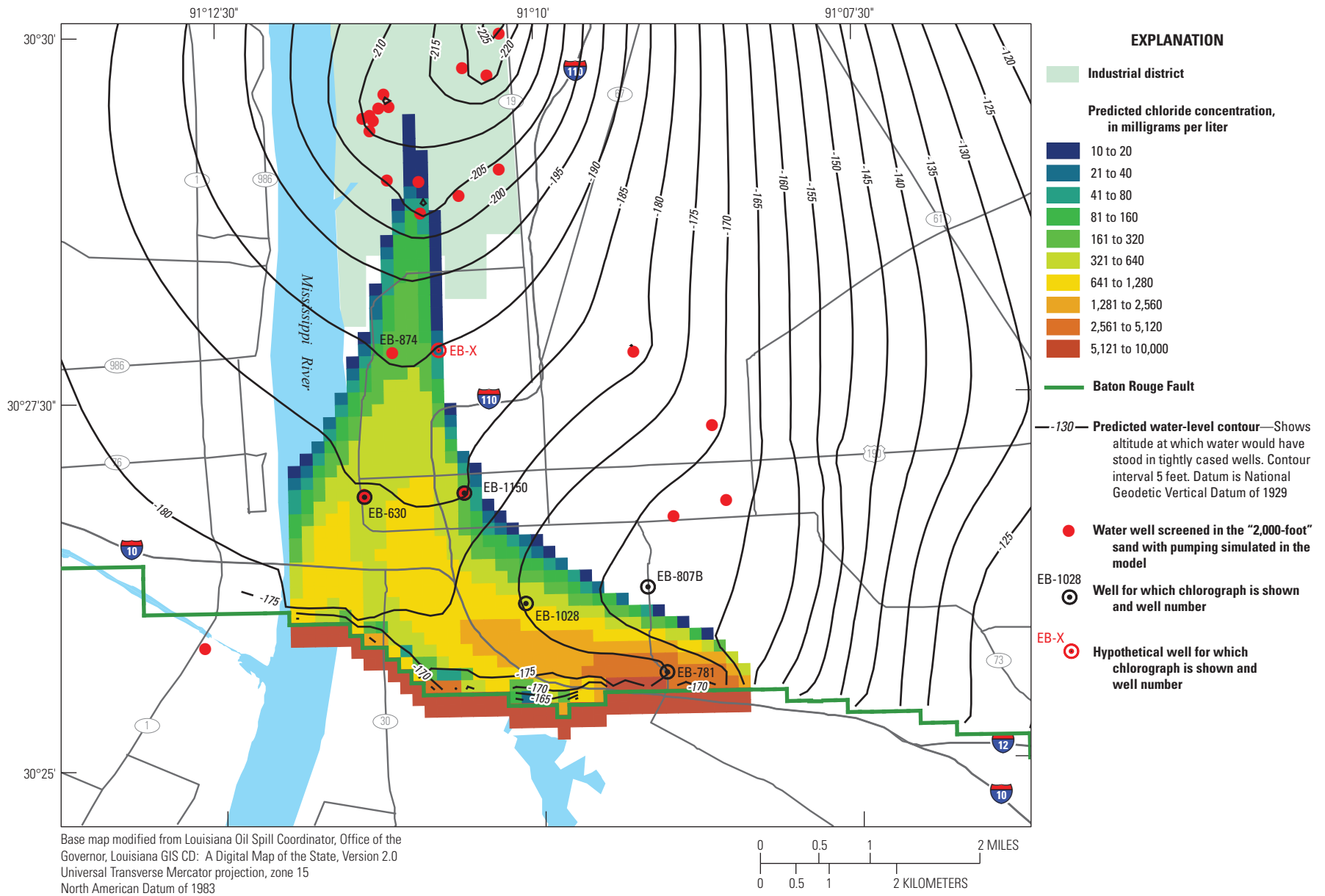
Figure 33. Predicted 2112 water levels and chloride concentrations at the base of the "2,000-foot" sand of the Baton Rouge area in the detailed model area in southeastern Louisiana after pumping is turned off at selected industrial and public-supply wells and a hypothetical public-supply well located north of the detailed model area in model row 22 and column 34 (see fig. 6) is turned on starting in 2015 (scenario 5).
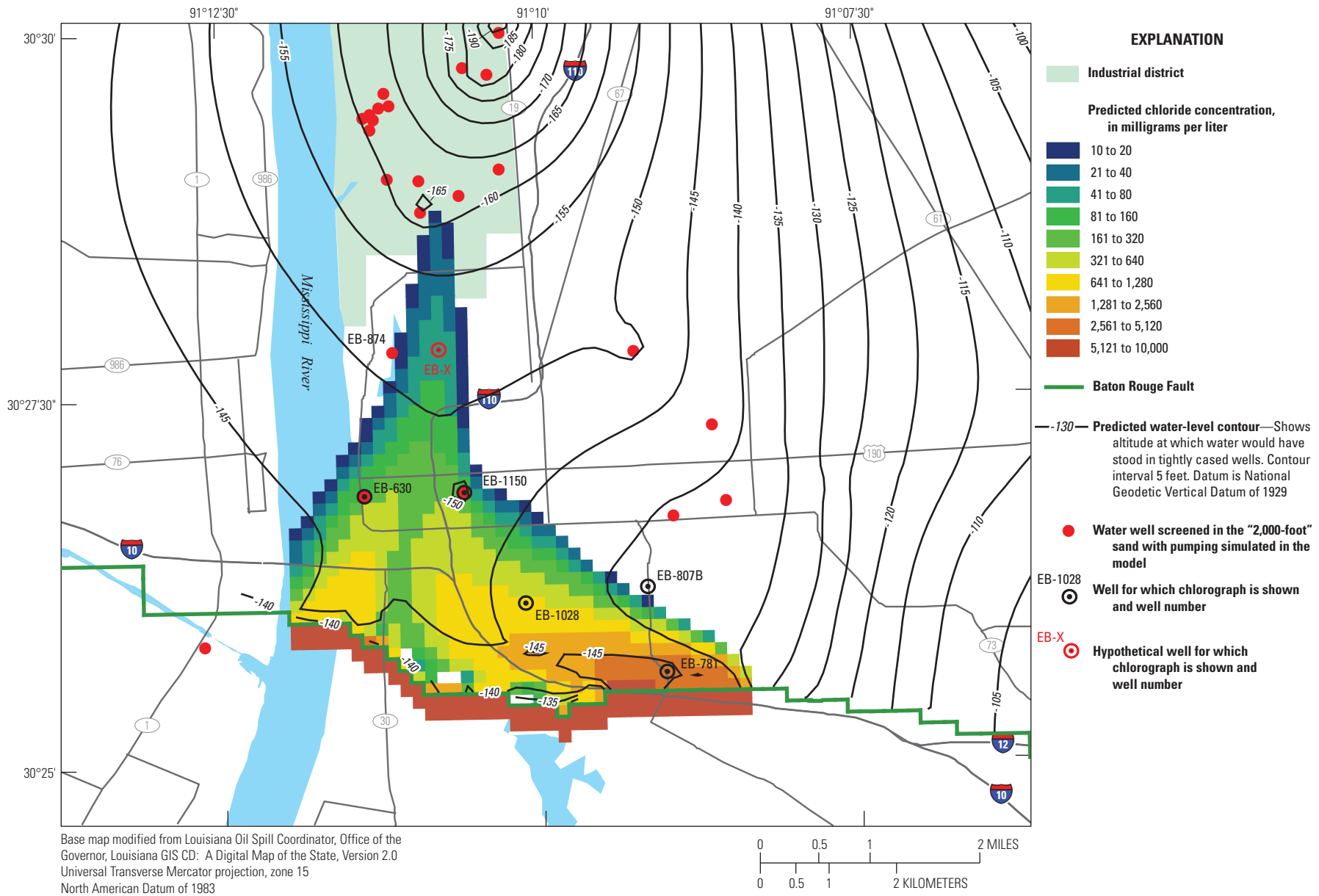
Figure 34. Predicted 2047 water levels and chloride concentrations at the base of the "2,000-foot" sand of the Baton Rouge area in the detailed model area in southeastern Louisiana after pumping is turned off at selected industrial and public-supply wells and a hypothetical public-supply well located north of the detailed model area in model row 22 and column 34 (see fig. 6) is turned on starting in 2015 (scenario 6).

Figure 35. Predicted 2112 water levels and chloride concentrations at the base of the "2,000-foot" sand of the Baton Rouge area in the detailed model area in southeastern Louisiana after pumping is turned off at selected industrial and public-supply wells and a hypothetical public-supply well located north of the detailed model area in model row 22 and column 34 (see fig. 6) is turned on starting in 2015 (scenario 6).

Scenario 7: Extensive Reduction of Industrial and Public-Supply Withdrawals With Installation of a Scavenger Well in the "2,000-Foot" Sand

In scenarios 7a and 7b, the reductions to groundwater withdrawals from the "2,000-foot" sand are identical to those in scenario 6, but installation of a scavenger well was also predicted in model row 64, column 29 (the same location as scenario 4). Two alternative total pumping rates from the scavenger-well couplet were predicted: 2.5 Mgal/d (scenario 7a) and 1.25 Mgal/d (scenario 7b). In scenario 7a, the withdrawals from the upper and lower wells were specified at 1.5 Mgal/d and 1.0 Mgal/d, respectively. In scenario 7b, withdrawals from the upper and lower wells were specified at 0.75 Mgal/d and 0.5 Mgal/d, respectively. The withdrawal rates from other industrial and public-supply wells were identical to those of scenario 6.

With the scavenger-well couplet withdrawing 2.5 Mgal/d, predicted water levels in the "2,000-foot" sand recover from their 2012 levels and are about 40 ft higher in the industrial district and about 20 ft higher in other parts of the detailed model area than they were in 2012 (figs. 17 and 36). A groundwater divide formed at latitude 30 degrees 27 minutes 30 seconds, approximately beneath the east-west portion of Interstate 110. This groundwater divide is the northern extent of the scavenger well's capture zone, which prevents continued migration of the chloride plume toward the industrial district. By 2047, the plume area decreases and is 27 percent smaller than that predicted for scenario 1 (table 5). The median cell concentration is substantially lower than in 2012 or scenario 1, though the mean cell concentration remains slightly higher than it was in 2012 because of higher chloride concentrations between the scavenger well and the Baton Rouge Fault.

By 2112, predicted water levels remain at the 2047 levels (figs. 36 and 37). The size of the plume is dramatically reduced in extent, and the plume has been diluted to freshwater in areas it previously occupied to the north of the scavenger well within the "2,000-foot" sand.

In scenario 7b, with the scavenger-well couplet withdrawing only 1.25 Mgal/d, predicted water levels in the "2,000-foot" sand make a greater recovery than in scenario 7a and by 2047 are simulated to be about 45 ft higher in the industrial district and about 30 ft higher in other parts of the detailed model area than they were during 2012 (figs. 17, 37, and 38). Because the scavenger-well withdrawals are half those in scenario 7a, the chloride plume area remains larger, and average concentrations remain somewhat higher than they were in scenario 7a (table 5).

By 2112, predicted water levels remain at the levels predicted for 2047 under scenario 7b (figs. 38 and 39).

The predicted extent of the chloride plume has reduced from its 2047 extent but not as dramatically as it had with the greater withdrawal rate simulated in scenario 7a (figs. 37, 38, and 39).

Scenario Comparison

In all scenarios, water levels essentially equilibrate by 2047, after 31 years of simulated constant withdrawal rates. Table 5 provides a quantitative comparison of the relative effectiveness of the various groundwater-withdrawal scenarios in mitigating the areal extent and average concentration of the chloride plume in the "2,000-foot" sand. Comparison of the total salt mass in the "2,000-foot" sand provides an additional metric of the effectiveness of the scenarios. Although the total mass indicated in figure 40 is uncertain because of uncertainty in the concentration and extent of the salt source near the Baton Rouge Fault, the relative magnitudes of the curves provide a useful comparison among the scenarios. As a group, the scavenger-well scenarios (4a, 4b, 7a, and 7b) simulate the lowest total salt mass, plume area, and median cell concentration, with the higher scavenger-well withdrawal-rate scenarios (4a and 7a) being most effective by these metrics. The simulated scavenger-well withdrawal rate is likely more influential in chloride plume mitigation than other differences among the scenarios in industrial and public-supply withdrawal rates. The relatively minor withdrawal reduction in scenario 3 predicts a greater total salt mass and average concentrations than scenario 1, though the smaller area and distribution of the chloride plume may be advantageous over that predicted by continuation of the 2012 pumping rates. Scenarios 5 and 6, which predict the effects of greater withdrawal-rate reductions and redistributions, are somewhat more effective in plume area and concentration reduction but are not as effective as the scavenger-well scenarios.

Differences among the scenarios in the rates of salt mass accumulation in the "2,000-foot" sand are more evident in figure 41, which is similar to figure 29 discussed under scenario 4, but depicts only the net mass for each scenario. The slope of the scenario curves after 2015 could be used to evaluate the rapidity with which various scenarios affect aquifer remediation. By this metric, scenarios 3 and 5 may be least effective in reducing salt accumulation. Scenarios 3 and 5 also predict increasing concentrations in the central portion of the plume, near public-supply well EB-630 (fig. 22*C*).

The chlorographs are useful for discerning differences among predictions of the scenarios in specific areas that are not readily apparent from the summary statistics or aquifer-mass plots. For example, among the scavenger-well scenarios, scenario 4a, which simulates greater groundwater withdrawals than scenario 7a, predicts slightly greater reduction in chloride concentration in the vicinity of well EB-1028 (fig. 22*A*).
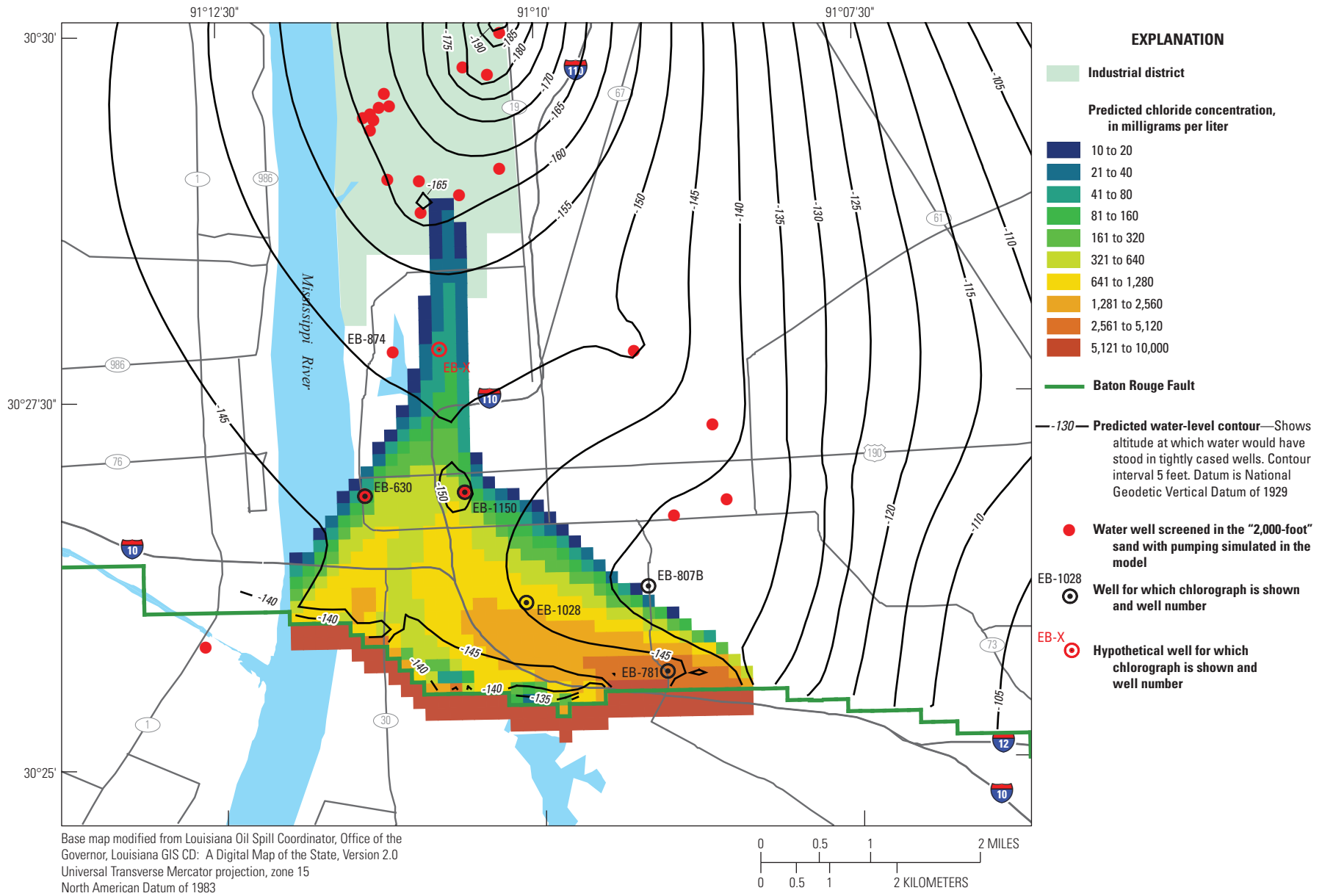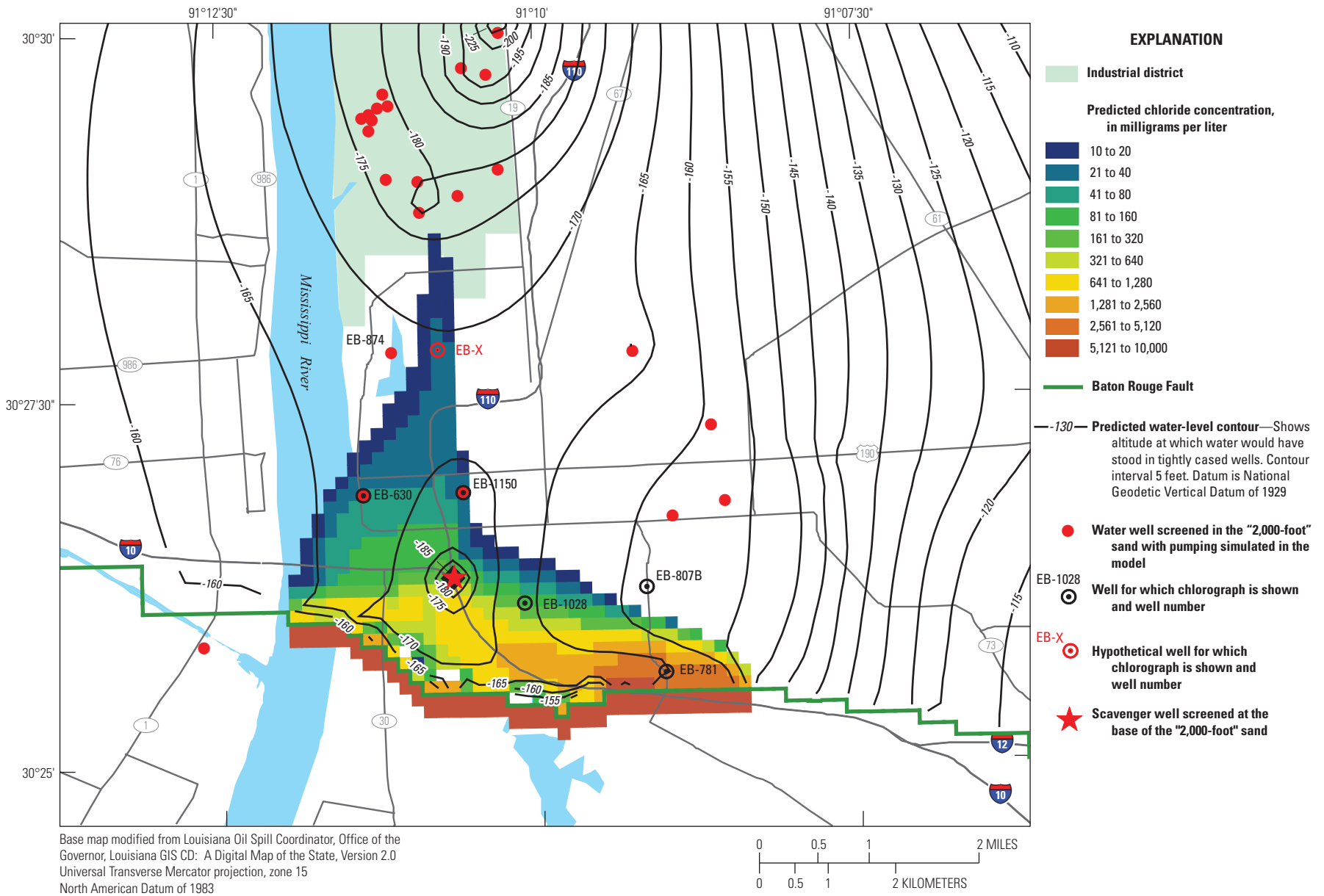
Figure 36.   Predicted 2047 water levels and chloride concentrations at the base of the "2,000-foot" sand of the Baton Rouge area in the detailed model area in southeastern Louisiana after pumping is turned off at selected industrial and public-supply wells, a hypothetical public-supply well located north of the detailed model area in model row 22 and column 34 (see fig. 6) is turned on in 2015, and a scavenger well located in row 64 and column 29 pumps at 2.5 million gallons per day beginning in 2017 (scenario 7a).
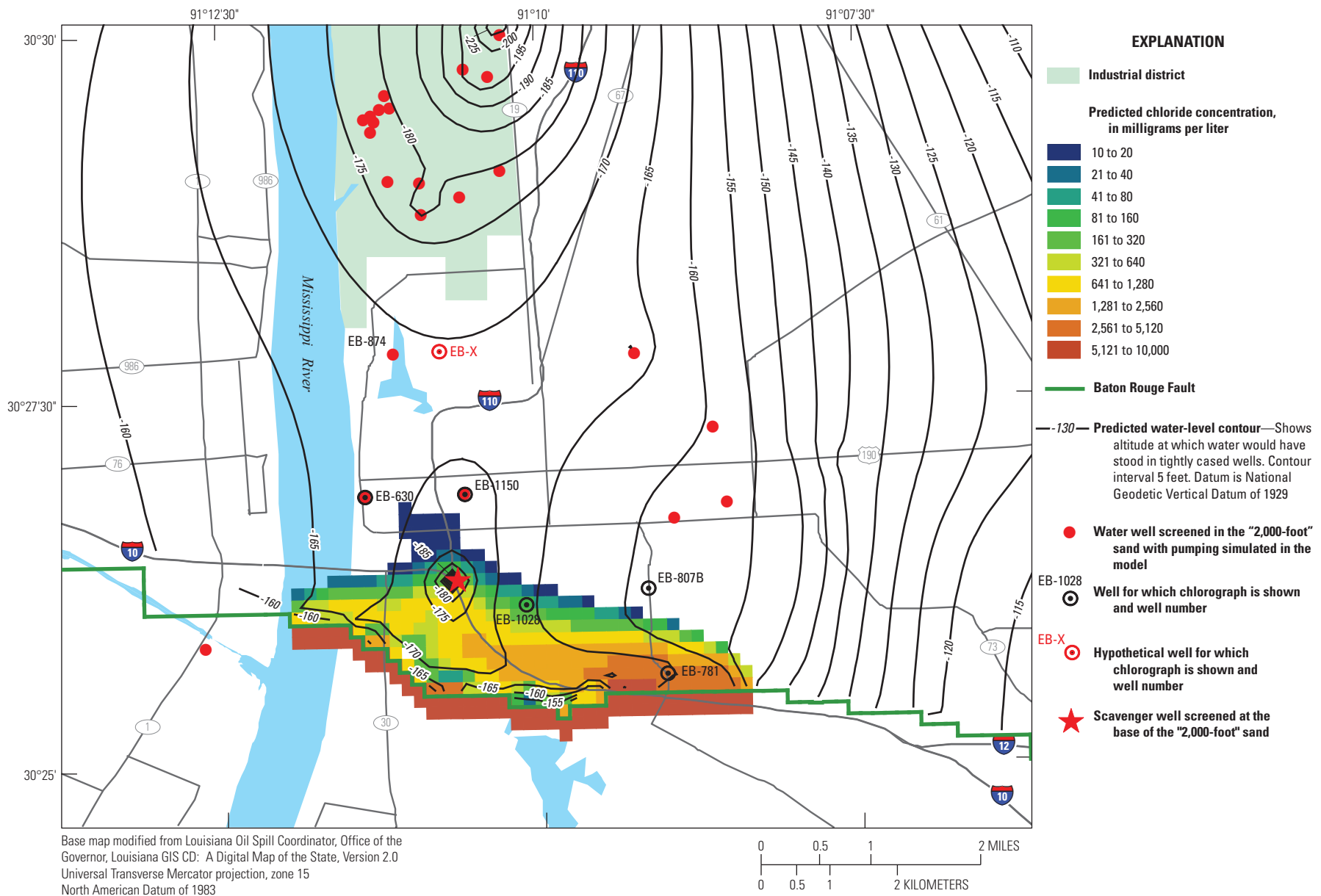
Figure 37. Predicted 2112 water levels and chloride concentrations at the base of the "2,000-foot" sand of the Baton Rouge area in the detailed model area in southeastern Louisiana after pumping is turned off at selected industrial and public-supply wells, a hypothetical public-supply well located north of the detailed model area in model row 22 and column 34 is turned on in 2015, and a scavenger well located in row 64 and column 29 (see fig. 6) pumps at 2.5 million gallons per day beginning in 2017 (scenario 7a).
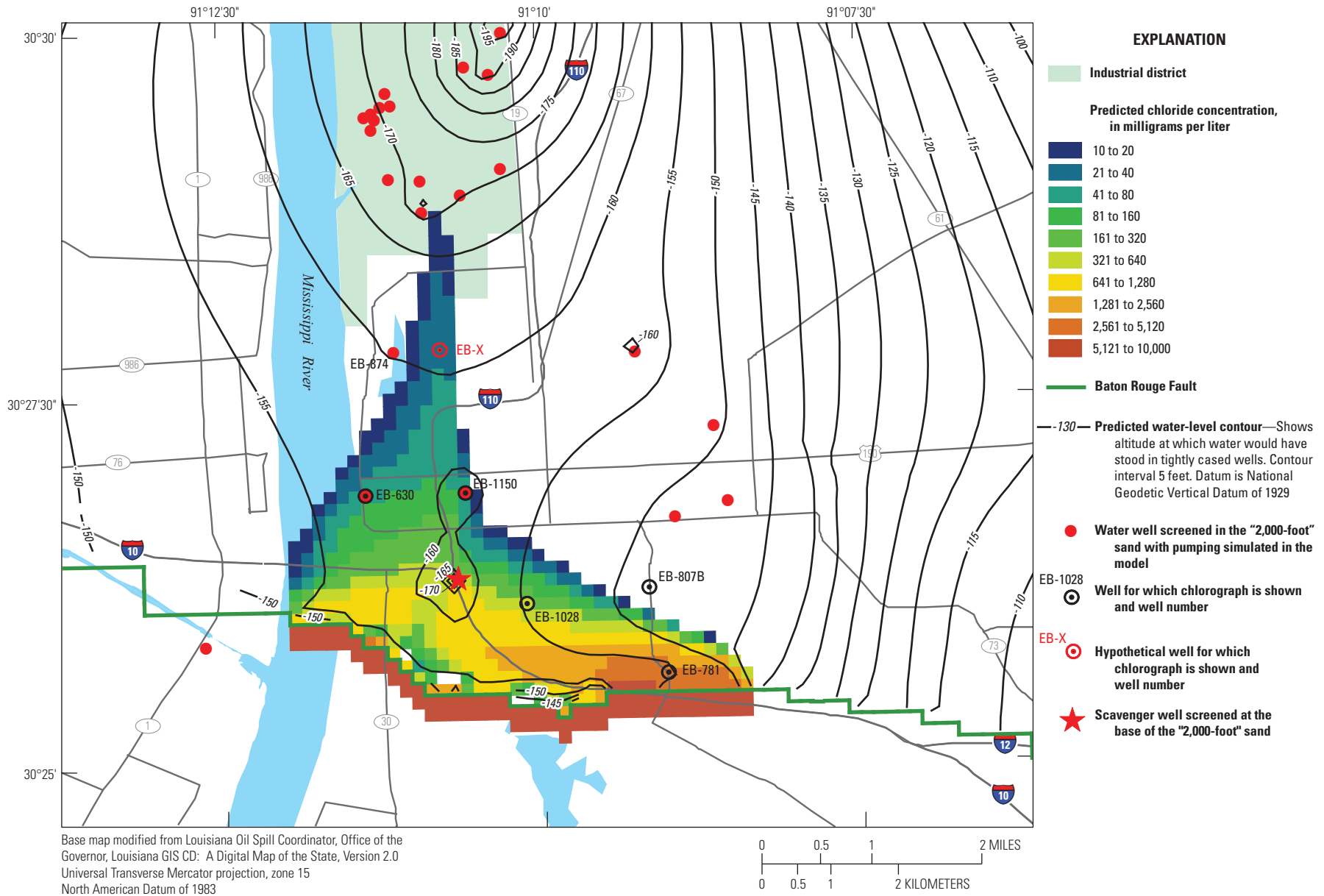
Figure 38. Predicted 2047 water levels and chloride concentrations at the base of the "2,000-foot" sand of the Baton Rouge area in the detailed model area in southeastern Louisiana after pumping is turned off at selected industrial and public-supply wells, a hypothetical public-supply well located north of the detailed model area in model row 22 and column 34 is turned on in 2015, and a scavenger well located in row 64 and column 29 (see fig. 6) pumps at 1.25 million gallons per day beginning in 2017 (scenario 7b).
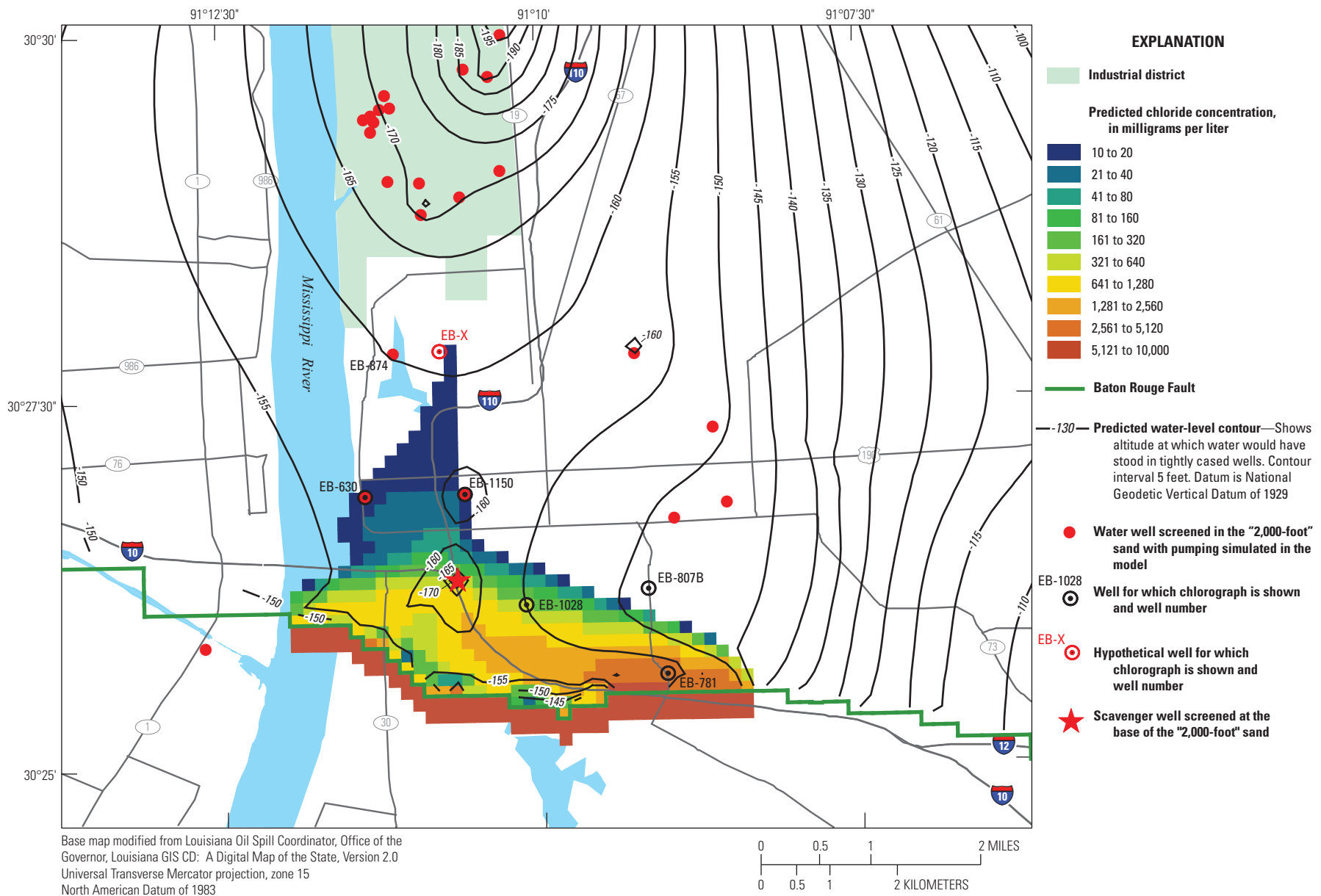
Figure 39. Predicted 2112 water levels and chloride concentrations at the base of the "2,000-foot" sand of the Baton Rouge area in the detailed model area in southeastern Louisiana after pumping is turned off at selected industrial and public-supply wells, a hypothetical public-supply well located north of the detailed model area in model row 22 and column 34 (see fig. 6) is turned on in 2015, and a scavenger well located in row 64 and column 29 pumps at 1.25 million gallons per day beginning in 2017 (scenario 7b).
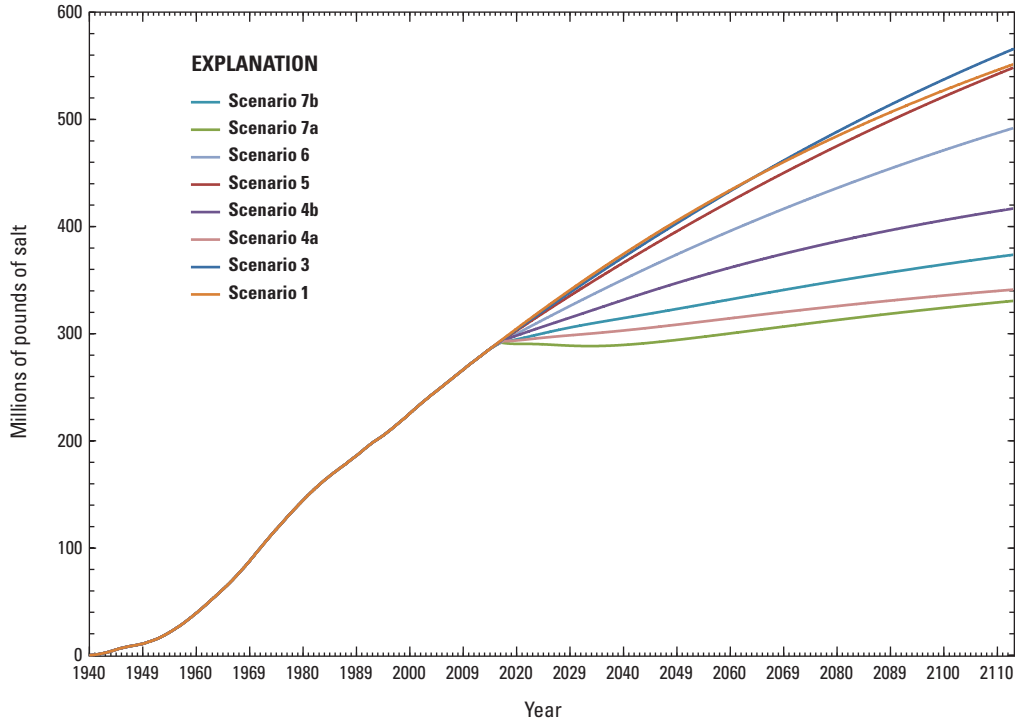
Figure 40. Simulated salt mass in the "2,000-foot" sand of the Baton Rouge area north of the Baton Rouge Fault, 1940–2012, and predicted salt mass during eight hypothetical pumping scenarios, 2013–2112.
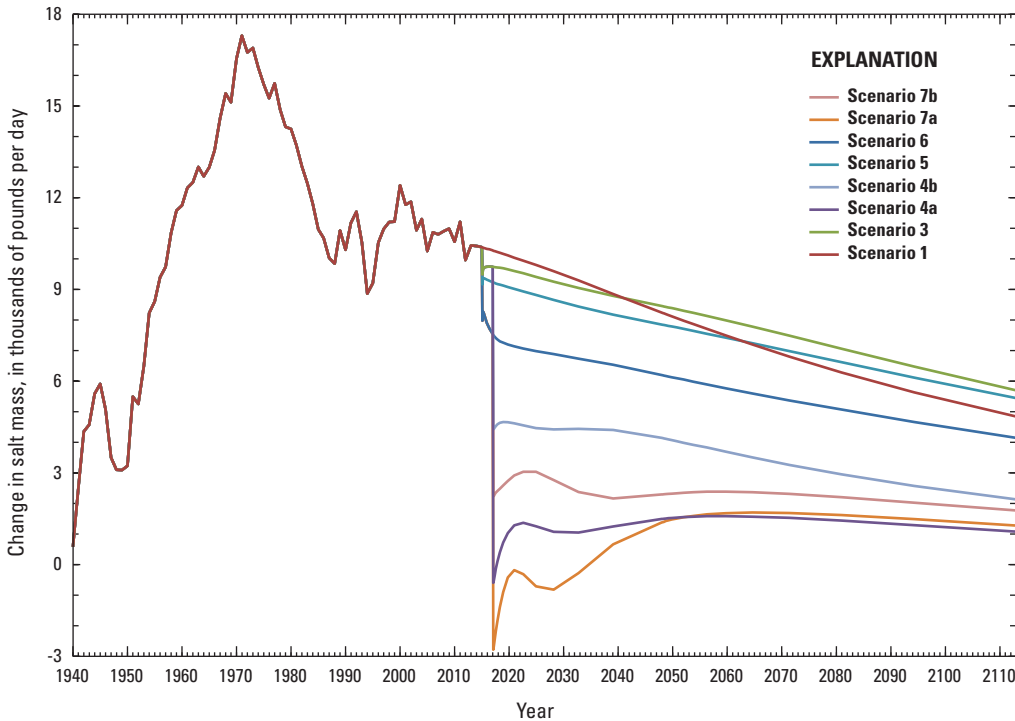
Figure 41. Predicted changes in salt mass in the "2,000-foot" sand of the Baton Rouge area north of the Baton Rouge Fault, 1940–2012, and predicted changes in salt mass during eight hypothetical pumping scenarios, 2013–2112.

Summary

Groundwater withdrawals in the Baton Rouge area since development in the 1940s have lowered water levels and altered groundwater-flow directions in the freshwater aquifers of the Southern Hills regional aquifer system. Generally, aquifers south of the Baton Rouge Fault contain saltwater, and aquifers north of the fault contain freshwater. The drawdown of groundwater levels has caused saltwater to encroach into previously freshwater areas in the Baton Rouge area. Saltwater encroachment has been detected north of the Baton Rouge Fault in East Baton Rouge Parish in 7 of the 10 Baton Rouge sands, including the "1,200-foot" sand and "2,000-foot" sand. The 10 aquifers that underlie the Baton Rouge area, which includes East and West Baton Rouge Parishes, Pointe Coupee Parish, and East and West Feliciana Parishes, provided about 184.3 million gallons per day (Mgal/d) for public supply and industrial use in 2012. Groundwater withdrawals from the "1,200-foot" sand, which totaled 23.33 Mgal/d during 2012, have resulted in measured water-level drawdowns as great as 177 feet (ft) and the potential for saltwater migration from south of the Baton Rouge Fault. Groundwater withdrawals from the "2,000-foot" sand, which totaled 28.5 Mgal/d during 2012, have resulted in measured water-level drawdowns as great as 356 ft and saltwater migration from south of the fault into the "2,000-foot" sand. This saltwater threatens industrial wells located about 3 miles (mi) north of the fault. A groundwater-flow and saltwater-transport model was constructed to assess the effects of groundwater withdrawals on the rate and pathways of saltwater migration in both the "1,200-foot" sand and the "2,000-foot" sand.

Because density differences between groundwater areas with contrasting saltwater concentrations may affect groundwater flow between those areas, both constant- and variable-density simulations of groundwater flow were utilized. The groundwater-flow simulation was initially constructed with the constant-density groundwater-flow simulation code MODFLOW and calibrated to observed water levels with the parameter-estimation code PEST. The calibrated groundwater-flow model parameters were subsequently utilized for the variable-density SEAWAT version of the model. Although much of the model input for SEAWAT is identical to MODFLOW input, withdrawal fluxes computed with the MODFLOW multinode well (MNW2) package were used to specify Well (WEL) package input for SEAWAT. Additional input was constructed to define transport boundary and initial conditions, transport properties, and specification of the equation of state relating solute concentration to groundwater density. The groundwater-flow and solute-transport equations are coupled because SEAWAT iteratively solves each equation for every transport time step, so computed concentrations affect groundwater density and influence groundwater velocities.

A three-dimensional hydrogeologic framework was constructed to define the extents and thicknesses of the aquifers and confining units in the study area. The framework consists of 24 layers that represent the entire sequence of sands and clays from land surface to the base of the "2,800-foot" sand. Layers 1, 3, 5, 7, 9, 11–20, 22, and 24 compose the aquifer layers. Layers 2, 4, 6, 8, 10, 21, and 23 compose the confining units that separate aquifer layers. Layer 1 represents the Mississippi River alluvial aquifer, shallow sands, Upland terrace aquifer, and the "400-foot" sand, "600-foot" sand, and "800-foot" sand. Layer 5 represents the "1,200-foot" sand. The "2,000-foot" sand is represented by 10 layers numbered 11 through 20.

The finite-difference grid with lateral cell dimensions of 500 by 500 ft in the Baton Rouge area incorporates increasing cell spacing toward the model-domain boundaries so that the entire 6,529-square-mile study area is contained within 95 rows and 120 columns of finite-difference cells. Vertical finite-difference discretization was defined such that model-cell layers correspond to the tops of hydrogeologic framework units north of the Baton Rouge Fault and are horizontal along columns from the fault southward. Because the Hydrogeologic-Unit Flow package was used to define the hydrogeologic framework geometry independently from finite-difference discretization, this discretization scheme facilitated simulation of flow between hydrogeologic units where they are juxtaposed at the Baton Rouge Fault. Additional resistance to flow across the Baton Rouge Fault was simulated with horizontal flow barriers. After an initial steady-state stress period that simulated predevelopment conditions prior to 1940, 73 annual transient stress periods simulated time from 1940 through 2012. The period from 2013 through 2014 was simulated with 2012 withdrawal rates. Three additional stress periods were used for scenarios that predict future conditions through 2112.

Boundary conditions utilized for the groundwater-flow simulation included no flow, specified head, and head-dependent flux types. Transient water levels within the top model layer, which represents the "400-foot" sand, "600-foot" sand, and "800-foot" sand, were specified by linear interpolation between levels constructed for 1944, 1980, 1990, 1998, 1999, and 2004. Water levels in the top model layer for simulated times before 1944 and after 2004 were specified at the 1944 and 2004 levels, respectively. A constant-head boundary was specified along row 95 in the bottom model layer, which corresponds to the southernmost extent of the "2,800-foot" sand. The water level for this boundary, which was estimated as a parameter during model calibration, enabled simulation of underflow to and from areas south of the simulated aquifer system. The remaining lateral and lower boundaries of the flow domain were simulated as no-flow boundaries. The layer-by-layer withdrawals simulated by MNW2 depend upon water levels simulated in the model layers in which wells have screens and are therefore head-dependent fluxes. The equivalent fluxes specified by using the WEL package in the SEAWAT simulation are the specified-flux type.

Average daily withdrawal rates were specified for 636 wells for each annual stress period from 1940 through 2012. After calibration of the MODFLOW model, the simulated layer-by-layer fluxes in and out of each well were specified as WEL package input for the SEAWAT simulation.

The area in which solute transport was simulated with SEAWAT is a subset of the groundwater-flow model domain and corresponds to the 60-row by 90-column portion of the grid with 500-ft by 500-ft finite-difference cells in the Baton Rouge area. Model cells within this area south of the Baton Rouge Fault are constant-concentration boundaries; cells north of the fault are variable-concentration cells for which a concentration was calculated for each transport time step. The sources of saltwater to the "1,200-foot" sand and "2,000-foot" sand are simulated as constant-concentration boundaries on the south side of the Baton Rouge Fault. For the "1,200-foot" sand, the constant-concentration boundary of 5,300 milligrams per liter (mg/L) is in model layer 5 and extends 8.6 mi east from the Mississippi River. For the "2,000-foot" sand, the concentration of the boundaries increases linearly with depth in model layers 10 through 20 (inclusive) from zero to a maximum concentration of 10,000 mg/L within a region that extends 3.6 mi east from the Mississippi River and is laterally connected to the 10 layers that simulate the "2,000-foot" sand north of the fault. All other portions of the solute-transport domain were assigned a zero initial concentration.

The groundwater-flow model was calibrated to 3,895 water levels measured between 1940 and 2011 with PEST. Additional water levels were used to evaluate the accuracy of the specified-head boundaries in the top model layer. The estimated values of hydraulic property parameters were all within the range considered reasonable.

Seven hypothetical scenarios predicted the effects of different groundwater-withdrawal options on groundwater levels and the transport of saltwater within the "1,200-foot" sand and the "2,000-foot" sand during 2015–2112. In all of the scenarios, 2012 groundwater-withdrawal rates are specified for the 2-year period from 2013 through 2014. Modifications to pumping rates are simulated to begin in 2015, except that withdrawals from a scavenger well are simulated to begin in 2017. Scenario 1 is the base case for comparison to the other scenarios and predicts the effects of 100 years (through 2112) of continued withdrawals at 2012 rates. Scenario 2 simulates increased withdrawals from industrial wells in the "1,200-foot" sand and predicts water levels 10–25 ft lower by 2047 and a negligible difference in chloride concentrations within the "1,200-foot" sand. Scenarios 3 through 7 predict the effects of various pumping schemes on future groundwater levels and chloride concentrations in the "2,000-foot" sand, and all incorporate a new hypothetical public-supply well within the industrial district withdrawing 1.9 Mgal/d. Scenario 3 simulates redistribution and a relatively modest 0.696-Mgal/d net decrease of withdrawals from the "2,000-foot" sand.

Scenario 4 simulates the same withdrawal modifications as those under scenario 3, with additional withdrawals from a scavenger well that withdraws salty water from the base of "2,000-foot" sand and presumably fresher water from the top of that aquifer at the same location. Two alternative pumping rates from the scavenger well, 2.5 Mgal/d and 1.25 Mgal/d, are simulated in each of scenarios 4 and 7. Scenario 5 is similar to scenario 3 but simulates additional withdrawal reductions from different wells than scenario 3, with the net reduction about four times greater (2.2 Mgal/d). Scenario 6 simulates the net largest reduction (7.3 Mgal/d) of groundwater withdrawals from the "2,000-foot" sand. Scenario 7 simulates the scenario 6 withdrawal modifications with the addition of scavenger-well withdrawals at the same rates and location as in scenario 4. The effects of all scenarios are illustrated by maps of predicted water levels and concentrations for the years 2047 and 2112 and chlorographs at observation wells within the "1,200-foot" sand and "2,000-foot" sand. For the "2,000-foot" sand scenarios, comparison of the predicted effects of the scenarios is facilitated by observation-well chlorographs, plots of salt mass in the aquifer through time, and a summary of the predicted plume area and average concentration. In all scenarios, water levels essentially equilibrate by 2047, after 31 years of simulated constant withdrawal rates. In scenario 2, water levels decline an additional 10–25 ft from 2012 levels in the "1,200-foot" sand, but the additional withdrawal stress does not substantially increase chloride concentrations north of the Baton Rouge Fault. In scenario 3, predicted water levels decline an additional 5–10 ft from 2012 levels in the "2,000-foot" sand despite the reduced withdrawal stress, and the chloride plume continues to migrate toward the industrial district but recedes from areas to the east where public-supply withdrawals were curtailed. In scenario 4, the additional scavenger-well withdrawals contribute to 15–25 ft of drawdown in the "2,000-foot" sand from 2012 levels, with greater drawdown near the scavenger well and reductions of chloride concentrations north of the scavenger well, which are more pronounced at the higher simulated scavenger-well withdrawal rate of 2.5 Mgal/d. In scenario 5, reductions in groundwater withdrawals cause about a 5-ft recovery from 2012 water levels in the "2,000-foot" sand and both lower concentrations and a slower rate of northward plume migration in comparison to scenario 1. In scenario 6, extensive reductions in groundwater withdrawals cause 35–50 ft of recovery from 2012 water levels and the smallest plume area and lowest median cell concentration among the scenarios that do not simulate a scavenger well. In scenario 7, the additional scavenger-well withdrawals dampen water-level recovery because of the scenario 6 reductions to the 20- to 45-ft range but enable marked decreases in the chloride plume area and concentration. Similar to scenario 4, the decreases in plume area and concentration are most pronounced at the higher simulated scavenger-well withdrawal rate of 2.5 Mgal/d.

References

Anderman, E.R., and Hill, M.C., 2000, MODFLOW-2000, the U.S. Geological Survey modular ground-water model—Documentation of the Hydrogeologic-Unit Flow (HUF) package: U.S. Geological Survey Open-File Report 00–342, 89 p.

Bates, R.L., and Jackson, J.A., eds., 1984, Dictionary of geological terms (3d ed.): New York, Doubleday, 571 p.

Boswell, E.H., and Arthur, J.K., 1988, Generalized potentiometric surface of shallow aquifers in southern Mississippi, 1982: U.S. Geological Survey Water-Resources Investigations Report 87–4257, 1 sheet.

Buono, Anthony, 1983, The Southern Hills regional aquifer system of southeastern Louisiana and southwestern Mississippi: U.S. Geological Survey Water-Resources Investigations Report 83–4189, 38 p.

Calhoun, Milburn, and Frois, Jeanne, eds., 1997, Louisiana almanac (1997–98 ed.): Gretna, La., Pelican Publishing Company, 695 p.

Dial, D.C., and Cardwell, G.T., 1999, A connector well to protect water-supply wells in the "1,500-ft" sand of the Baton Rouge, Louisiana, area from saltwater encroachment: Capital Area Ground Water Conservation Commission Bulletin no. 5, 17 p.

Doherty, John, 2004, PEST—Model-independent parameter estimation, user manual (5th ed.): Corinda, Australia, Watermark Numerical Computing, 336 p.

Durham, C.O., Jr., and Peeples, E.M., III, 1956, Pleistocene fault zone in southeastern Louisiana [abs.]: New Orleans, La., Transactions of the Gulf Coast Association of Geological Societies, v. 6, p. 65–66.

Griffith, J.M., 2003, Hydrogeologic framework of southeastern Louisiana: Louisiana Department of Transportation and Development Water Resources Technical Report no. 72, 21 p., 18 pl.

Griffith, J.M., 2006, Hydrogeologic maps and sections of the "400-foot," "600-foot," and "800-foot" sands of the Baton Rouge area and adjacent aquifers in East and West Baton Rouge, East and West Feliciana, and Pointe Coupee Parishes, Louisiana: U.S. Geological Survey Scientific Investigations Report 2006–5072, 15 p., 13 pls.

Halford, K.J., and Lovelace, J.K., 1994, Analysis of ground-water flow in the "1,200-foot" aquifer, Baton Rouge area, Louisiana: Louisiana Department of Transportation and Development Water Resources Technical Report no. 54, 68 p.

Hanor, J.S., 1982, Reactivation of fault movement, Tepetate fault zone, south central Louisiana, in Transactions of the Gulf Coast Association of Geological Societies: Gulf Coast Association of Geological Societies, v. 32, p. 237–245.

Harbaugh, A.W., 2005, MODFLOW-2005, the U.S. Geological Survey modular ground-water model—The ground-water flow process: U.S. Geological Survey Techniques and Methods 6–A16 [variously paged].

Harbaugh, A.W., Banta, E.R., Hill, M.C., and McDonald, M.G., 2000, MODFLOW-2000, the U.S. Geological Survey modular ground-water model—User guide to modularization concepts and the ground-water flow process: U.S. Geological Survey Open-File Report 00–92, 121 p.

Heywood, C.E., Griffith, J.M., and Lovelace, J.K., 2014, Simulation of groundwater flow in the "1,500-foot" sand and "2,000-foot" sand, with scenarios to mitigate saltwater migration in the "2,000-foot" sand of the Baton Rouge area, Louisiana (ver. 1.1, April 2014): U.S. Geological Survey Scientific Investigations Report 2013–5227, 63 p. [Also available at http://dx.doi.org/10.3133/sir20135227.]

Hill, M.C., and Tiedeman, C.R., 2007, Effective groundwater model calibration—With analysis of data, sensitivities, predictions, and uncertainty: Hoboken, N.J., Wiley, 455 p.

Hsieh, P.A., and Freckleton, J.R., 1993, Documentation of a computer program to simulate horizontal-flow barriers using the U.S. Geological Survey's modular three-dimensional finite-difference ground-water flow model: U.S. Geological Survey Open-File Report 92–477, 32 p.

Huntzinger, T.L., Whiteman, C.D., Jr., and Knochenmus, D.D., 1985, Simulation of ground-water movement in the "1,500- and 1,700-foot" aquifer of the Baton Rouge area, Louisiana: Louisiana Department of Transportation and Development, Office of Public Works Water Resources Technical Report no. 34, 52 p.

Kafri, U., and Yechieli, Y., 2010, Groundwater base level changes and adjoining hydrological systems: Berlin, Springer-Verlag, 171 p.

Kernodle, J.M., and Philip, R.D., 1988, Using a geographic information system to develop a ground-water flow model: American Water Resources Association Monograph, series no. 14, p. 191–202.

Konikow, L.F., Hornberger, G.Z., Halford, K.J., and Hanson, R.T., 2009, Revised multi-node well (MNW2) package for MODFLOW ground-water flow model: U.S. Geological Survey Techniques and Methods 6–A30, 67 p.

Kuniansky, E.L., 1989, Geohydrology and simulation of ground-water flow in the "400-foot," "600-foot," and adjacent aquifers, Baton Rouge area, Louisiana: Louisiana Department of Transportation and Development Water Resources Technical Report no. 49, 90 p.

Langevin, C.D., Shoemaker, W.B., and Guo, Weixing, 2003, MODFLOW-2000, the U.S. Geological Survey modular ground-water model—Documentation of the SEAWAT-2000 version with the variable-density flow process (VDF) and the integrated MT3DMS transport process (IMT): U.S. Geological Survey Open-File Report 03–426, 43 p.

Leake, S.A., and Lilly, M.R., 1997, Documentation of a computer program (FHB1) for assignment of transient specified-flow and specified-head boundaries in applications of the Modular Finite-Difference Ground-Water Flow Model (MODFLOW): U.S. Geological Survey Open-File Report 97–571, 56 p.

Lovelace, J.K., 2007, Chloride concentrations in ground water in East and West Baton Rouge Parishes, Louisiana, 2004–05: U.S. Geological Survey Scientific Investigations Report 2007–5069, 27 p.

Marsily, Ghislain de, 1986, Quantitative hydrogeology: San Diego, Calif., Academic Press, 440 p.

Martin, Angel, Jr., and Whiteman, C.D., Jr., 1985, Map showing generalized potentiometric surface of aquifers of Pleistocene age, southern Louisiana, 1980: U.S. Geological Survey Water-Resources Investigations Report 84–4331, 1 sheet.

Martin, Angel, Jr., and Whiteman, C.D., Jr., 1990, Calibration and sensitivity analysis of a ground-water flow model of the coastal lowlands aquifer system in parts of Louisiana, Mississippi, Alabama, and Florida: U.S. Geological Survey Water-Resources Investigations Report 89–4189, 54 p.

McCulloh, R.P., 1991, Surface faults in East Baton Rouge Parish: Baton Rouge, Louisiana Geological Survey Open-File series 91–02, 25 p.

Meyer, R.R., and Rollo, J.R., 1965, Saltwater encroachment, Baton Rouge area, Louisiana: Department of Conservation, Louisiana Geological Survey, and Louisiana Department of Public Works Water Resources Pamphlet 17, 9 p.

Meyer, R.R., and Turcan, A.N., Jr., 1955, Geology and ground-water resources of the Baton Rouge area, Louisiana: U.S. Geological Survey Water-Supply Paper 1296, 138 p.

Morgan, C.O., 1961, Ground-water conditions in the Baton Rouge area, 1954–59, with special reference to increased pumpage: Department of Conservation, Louisiana Geological Survey, and Louisiana Department of Public Works Water Resources Bulletin 2, 78 p.

Morgan, C.O., and Winner, M.D., Jr., 1964, Saltwater encroachment in aquifers of the Baton Rouge area—Preliminary report and proposal: Louisiana Department of Public Works, 37 p.

Murray, G.E., 1961, Geology of the Atlantic and Gulf Coastal Province of North America: New York, Harper Brothers, 692 p.

National Oceanic and Atmospheric Administration, 1995, Climatological data annual summary—Louisiana: Asheville, N.C., Environmental Data Service, 23 p.

Roland, H.L., Hill, T.F., Autin, Peggy, Durham, C.O., and Smith, C.G., 1981, The Baton Rouge and Denham Springs-Scotlandville faults (mapping and damage assessment): Baton Rouge, La., Report prepared for the Louisiana Department of Natural Resources, Geological Survey and Durham Geological Associates Consultants, contract no. 21576-80-01, 26 p.

Rollo, J.R., 1969, Saltwater encroachment in aquifers of the Baton Rouge area, Louisiana: Department of Conservation, Louisiana Geological Survey, and Louisiana Department of Public Works Water Resources Bulletin 13, 45 p.

Sargent, B.P., 2011, Water use in Louisiana, 2010: Louisiana Department of Transportation and Development Water Resources Special Report no. 17, 135 p.

Smith, C.G., 1979, A geohydrologic survey of the "1,200-foot" aquifer in the Capital Area Ground Water Conservation District: Capital Area Ground Water Conservation Commission Bulletin 3, 19 p.

Smith, C.G., and Kazmann, R.G., 1978, Subsidence in the Capital Area Ground Water Conservation District—An update: Baton Rouge, La., Capital Area Ground Water Conservation Commission Bulletin 2, 31 p.

Smoot, C.W., 1988, Louisiana hydrologic atlas map no. 3—Altitude of the base of freshwater in Louisiana: U.S. Geological Survey Water-Resources Investigations Report 86–4314, 1 sheet.

Stuart, C.G., Knochenmus, Darwin, and McGee, B.D., 1994, Guide to Louisiana's ground-water resources: U.S. Geological Survey Water-Resources Investigations Report 94–4085, 55 p.

Tomaszewski, D.J., 1996, Distribution and movement of saltwater in aquifers in the Baton Rouge area, Louisiana, 1990–92: Louisiana Department of Transportation and Development Water Resources Technical Report no. 59, 44 p.

Torak, L.J., and Whiteman, C.D., Jr., 1982, Applications of digital modeling for evaluating the ground-water resources of the "2,000-foot" sand of the Baton Rouge area, Louisiana: Louisiana Department of Transportation and Development, Office of Public Works Water Resources Technical Report no. 27, 87 p.

U.S. Census Bureau, 2010, Annual estimates of the population for counties of Louisiana—April 1, 2000, to July 1, 2004 (CO-EST2004-01-22): Accessed April 29, 2015, at http://www.census.gov/popest.

Viewlog Systems, 2004, VIEWLOG borehole data management system: Toronto, Ontario, Canada, Viewlog Systems, 465 p.

Whiteman, C.D., Jr., 1979, Saltwater encroachment in the "600-foot" and "1,500-foot" sands of the Baton Rouge area, Louisiana, 1966–78, including a discussion of saltwater in other sands: Louisiana Department of Transportation and Development, Office of Public Works Water Resources Technical Report no. 19, 49 p.

Winner, M.D., Jr.; Forbes, M.J., Jr.; and Broussard, W.L., 1968, Water resources of Pointe Coupee Parish, Louisiana: Department of Conservation, Louisiana Geological Survey, and Louisiana Department of Public Works Water Resources Bulletin 11, 110 p.

Zheng, Chunmiao, and Bennett, G.D., 1995, Applied contaminant transport modeling: New York, Van Nostrand Reinhold, 440 p.

Zheng, Chunmiao, and Wang, P.P., 1999, MT3DMS—A modular three-dimensional multispecies transport model for simulation of advection, dispersion and chemical reactions of contaminants in ground-water systems; documentation and user's guide: Jacksonville, Fla., U.S. Army Corps of Engineers Contract Report SERDP-99-1, 221 p.

≋USGS